AD_____

Award Number: DAMD17-01-1-0414

TITLE: Functional Interactions of Human Rad54 with the Rad51 Recombinase

PRINCIPAL INVESTIGATOR: Stephen J. Van Komen

CONTRACTING ORGANIZATION: The University of Texas Health Science Center at San Antonio
San Antonio, Texas 78229-3900

REPORT DATE: May 2003

TYPE OF REPORT: Annual Summary

PREPARED FOR: U.S. Army Medical Research and Materiel Command
Fort Detrick, Maryland 21702-5012

DISTRIBUTION STATEMENT: Approved for Public Release;
Distribution Unlimited

REPORT DOCUMENTATION PAGE

Form Approved
OMB No. 074-0188

1. AGENCY USE ONLY (Leave blank)	2. REPORT DATE	3. REPORT TYPE AND DATES COVERED
	May 2003	Annual Summary (1 May 01-30 Apr 03)

4. TITLE AND SUBTITLE
Functional Interactions of Human Rad54 with the Rad51 Recombinase

5. FUNDING NUMBERS
DAMD17-01-1-0414

6. AUTHOR(S)
Stephen J. Van Komen

7. PERFORMING ORGANIZATION NAME(S) AND ADDRESS(ES)
The University of Texas Health Science Center at San Antonio
San Antonio, Texas 78229-3900

E-Mail: stephen.vankomen@yale.edu

8. PERFORMING ORGANIZATION REPORT NUMBER

9. SPONSORING / MONITORING AGENCY NAME(S) AND ADDRESS(ES)
U.S. Army Medical Research and Materiel Command
Fort Detrick, Maryland 21702-5012

10. SPONSORING / MONITORING AGENCY REPORT NUMBER

11. SUPPLEMENTARY NOTES

12a. DISTRIBUTION / AVAILABILITY STATEMENT
Approved for Public Release; Distribution Unlimited

12b. DISTRIBUTION CODE

13. ABSTRACT (Maximum 200 Words)

Chromosomal DNA breaks occur in cells during normal metabolism and are induced by continual exposure to harmful radiation and other environmental insults. Homologous recombination represents a major pathway for the elimination of these chromosomal breaks. As such, homologous recombination is indispensable for the maintenance of genome stability in all organisms. Importantly, emerging evidence implicates the homologous recombination machinery in the suppression of cancer formation. In fact, defective homologous recombination represents one of the most prominent phenotypes of hereditary breast cancer patients mutated for BRCA1 and BRCA2, and mutations in key recombination factors have been found in various other tumor types as well. This research project will use a variety of mechanistic approaches to decipher the functions of human Rad51 and human Rad54, key protein factors that mediate homologous recombination, specifically focusing on the role of these factors in DNA remodeling and the formation of DNA joints which facilitated the genetic exchange between recombining homologous chromosomes during the break repair reaction.

14. SUBJECT TERMS	15. NUMBER OF PAGES
Breast Cancer	41
	16. PRICE CODE

17. SECURITY CLASSIFICATION OF REPORT	18. SECURITY CLASSIFICATION OF THIS PAGE	19. SECURITY CLASSIFICATION OF ABSTRACT	20. LIMITATION OF ABSTRACT
Unclassified	Unclassified	Unclassified	Unlimited

Table of Contents

Cover.....1

SF 298.....2

Table of contents.....3

Introduction.....4

Body.....5-9

Conclusions.....10

Key Research Accomplishments.....10

Reportable Outcomes.....11-12

References.....12-14

Appendices.....15-41

INTRODUCTION

Chromosomal DNA breaks occur in cells during normal metabolism and are induced by continual exposure to harmful radiation and other environmental insults (reviewed by Michel *et al.*, 2001; Rothstein *et al.*, 2000). Unrepaired or incorrectly repaired DSBs can lead to deletions or mutations in the coding sequence of a gene, translocations, inversions of chromosomes and cell death (reviewed in Paques and Haber, 1999).

Importantly, emerging evidence implicates the homologous recombination machinery in the suppression of cancer formation. In fact, defective homologous recombination represents one of the most prominent phenotypes of hereditary breast cancer patients mutated for BRCA1 and BRCA2, and mutations in key recombination factors have been found in various other tumor types as well.

Unlike single-strand DNA damage which can be repaired using information on the remaining undamaged DNA strand, double-strand breaks must either be repaired by joining and ligating the broken ends or by utilizing a homologous chromosome as a template to copy the lost or damaged DNA. In eukaryotes, DSBs are repaired either by joining the broken ends or by utilizing a homologous DNA molecule to direct repair by recombination. The former repair mechanism, termed nonhomologous end joining (NHEJ), involves nucleolytic processing and alignment of DNA ends, fill in DNA synthesis, and ligation. End-joining can occur between any two DNA ends and is therefore independent of DNA homology (reviewed in Paques and Haber, 1999). Repair by homologous recombination (homology-directed repair) utilizes DNA single-strands derived from the broken DNA to invade and displace a DNA strand from an intact homologous duplex to prime DNA synthesis to replace lost or damaged DNA, followed by resolution of DNA intermediates and ligation to restore the integrity of the injured chromosome. Although NHEJ often leads to the alteration of genetic information at the DNA junction, extensive genetic analyses indicate that homology-directed repair is mostly accurate.

In eukaryotic organisms homologous recombination is mediated by genes required for meiotic and mitotic recombination and for DSB repair collectively known as the *RAD52* epistasis group, consisting of *RAD50, RAD51, RAD52, RAD54, RAD55, RAD57, RAD59, RDH54/TID1, MRE11* and *XRS2*. Extensive studies have shown that the encoded proteins of these genes are conserved among eukaryotes from the baker's yeast *Saccharomyces cerevisiae* to humans in both primary sequence and biochemical functions (reviewed by Paques and Haber, 1999; Sung et al, 2000). The importance in the *RAD52* epistasis group in DSB repair, the maintenance of genomic stability, and the suppression of breast and other cancers has been manifest by several studies indicating that the encoded products of central human members of *RAD52* group genes interact with and are governed by the tumor suppressors BRCA1 and BRCA2 (reviewed in Dasika et al, 1999; Pierce et al, 2001). Notably, in response to DNA damage BRCA1 is hyperphosphorylated and effects the localization of the DNA end processing complex Rad50, Mre11 and Xrs2 to the ends of the DSBs. Genetic analysis indicated that BRCA1 is required for normal levels of homologous recombination and the repair of DSBs (reviewed in Moynahan et al, 1999; Pierce et al,

2001). Additionally, the human recombinase hRad51 interacts with BRCA2 though eight BRC repeats (Chen and al, 1998) and BRCA2 mutant cells are not only sensitive to DSB inducing agents but also show a marked reduction in recombination and DSB repair (Moynahan et al, 2001).

This research project will use a variety of mechanistic approaches to decipher the functions of key protein factors hRad51 and hRad54 that mediate homologous recombination, specifically focusing on the role of these factors in the formation of DNA joints and remodeling of chromatin during the break repair reaction.

BODY

A myriad of genetic analysis and biochemical studies on these *RAD52* epistasis genes and their encoded products have provided insights indicating the temporal order of events in homologous recombination (reviewed in Paques and Haber, 1999; Sung *et al.*, 2000). Consequently, members of the *RAD52* group genes have been divided into two categories. The first category includes members Rad50, Mre11, and Xrs2 function in the initial DNA end-processing of the double-strand break in the formation of 3' overhanging DNA while the second category members Rad51, Rad52, Rad54, Rad55, Rad57, Rad59, and Rdh54 nucleate onto the ssDNA tails generated from the break processing reaction and then mediate the promoting the key intermediate heteroduplex formation or D-loop with intact homologous duplex, either homologous chromosomes or heterochromatid.

hRad54 physically interacts with hRad51 - Human Rad51 (hRad51), structurally and functionally related to the yeast Rad51 and *E. coli* RecA DNA recombinases, is central in mediating DNA pairing and strand exchange. Like its homolog counterparts, hRad51 forms a highly extended right-handed nucleoprotein filament on ssDNA (reviewed in Yu et al, 2001). Once formed, the hRad51-ssDNA nucleoprotein filament has the ability to perform a search for homologous duplex, mediate the strand invasion and catalyze the formation of DNA joints by a process termed homologous pairing and strand exchange (Bauman et al, 1996; Gupta et al, 1997; Sigurdsson et al, 2001).

Although *in vitro* and yeast two-hybrid system analyses indicate that hRad54, a member of the Swi2/Ssnf2 protein family, can bind hRad51 via its amino-terminus (Golub et al, 1997), association of mRad51 and mRad54 in mouse ES cells has been shown requires prior treatment of cells with a DNA damaging agent (Tan et al, 1999). To examine whether purified hRad54 physically interacts with hRad51, hRad51 coupled hRad51 to Affi-gel beads was used as an affinity matrix for binding hRad54. As shown in Figure 1, purified hRad54 was efficiently retained on Affi-hRad51 beads but not on Affi-beads that contained bovine serum albumin. Furthermore, when less purified hRad54 (~25% hRad54) wsas used, hRad54, but not the contaminating protein species, bound to the Affi-hRad51 beads. The results thus indicate a direct and specific interaction between hRad51 and hRad54.

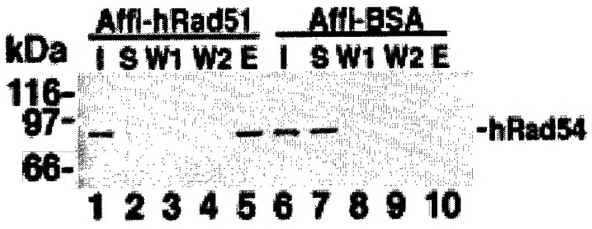

Figure 1. hRad54 interacts with hRad51. Purified hRad54 (1.2 μg) was mixed with Affi-beads containing either BSA (Affi-BSA) or hRad51 (Affi-Rad51) in 30 μl, washed twice with 50 μl buffer, followed by treatment of the beads with 30 μl SDS to elute bound hRad54. The starting material (I), supernatant (S), the two washes (W1 and W2), and the SDS eluate (E), 4 μl each, were subjected to immunoblotting to determine their hRad54 content.

DNA supercoiling and DNA strand opening by hRad54 - Purified hRad54 exhibits DNA-dependent ATPase and DNA supercoiling activities (Swagemakers et al, 1998; Tan et al, 1999; Ristic et al, 2001). Tan et al (1999) showed an ability of hRad54 to alter the DNA linking number of a nicked plasmid in the presence of DNA ligase. The induction of DNA linking number change was dependent on ATP hydrolysis by hRad54 (Tan et al, 1999). As in the schematic in Figure 2 depicting the basis for tracking-induced DNA supercoiling by hRad54, scanning force microscopy (SFM) was utilized by the same group to provide evidence that hRad54 tracks on DNA when ATP is hydrolyzed (Ristic et al, 2001).

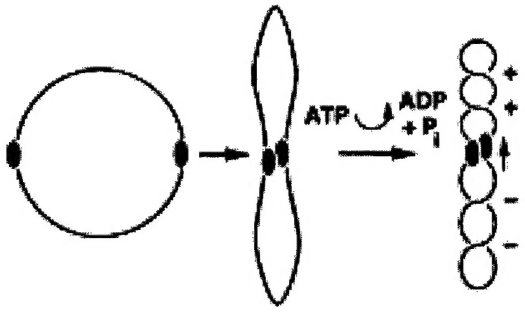

Figure 2. Basis for hRad54 induced supercoiling. The free energy from ATP hydrolysis fuels the tracking of a hRad54 oligomer on DNA, producing a positively supercoiled domain ahead of protein movement and a negatively supercoiled domain behind (Ristic et al, 2001; Van Komen et al, 2000.

My previous reluslts have shown that the yRad54 protein also tracks on DNA and, as a result, generates positive and negative supercoils in the DNA substrate. Removal of the negative supercoils by treatment with *E. coli* topoisomerase I leads to the accumulation of positive supercoils and the formation of an overwound DNA species called Form OW (Van Komen et al, 2000). Here the same strategy was utilized to examine the ability of hRad54 to supercoil DNA. As shown in Figure 3, in the presence of topoisomerase, purified hRad54 protein readily induces a linking number change in the DNA (Sigurdsson et al, 2002). A dependence on ATP hydrolysis in promoting a linking number change is evident by omission or substitution of ATP with a non-hydrolyzable analogue (ATP-γ-S or AMP-PNP) fails indicating a (Figure 3).

Figure 3. hRad54 supercoils DNA. Increasing amounts of hRad54 (200, 400, and 750 nM in lanes 3 to 5, respectively) was incubated with topologically relaxed DNA (20 μM nucleotides) and *E. coli* topoisomerase I in buffer that contained ATP. The highest amount of hRad54 (750 nM) was also incubated with the DNA substrate in the absence of topoisomerase (lane 6) and in the presence of topoisomerase but with the omission of ATP (lane 7) or the substitution of ATP by ATP-γ-S (γ-S; lane 8) and AMP-PNP (PNP; lane 9). DNA alone (lane 1) or DNA incubated with topoisomerase (lane 2) were also included. The reaction mixtures were run in a 1% agarose gel, which was treated with ethidium bromide to reveal the DNA species.

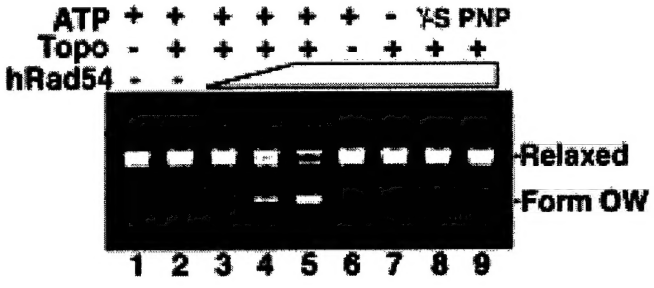

To address whether the negative supercoils generated as a result of hRad54 tracking on the DNA substrate (Ristic et al, 2001; Figure 2 and 3) leads to transient DNA strand opening, the sensitivity of a relaxed DNA template to the single-strand specific nuclease P1 was examined. As indicated by the accumulation of nicked circular and linear DNA forms, incubation of topologically relaxed DNA with hRad54 rendered the relaxed DNA substrate sensitive to P1 nuclease (Figure 4). Furthermore, the DNA strand opening reaction is completely dependent on ATP hydrolysis (Figure 4).

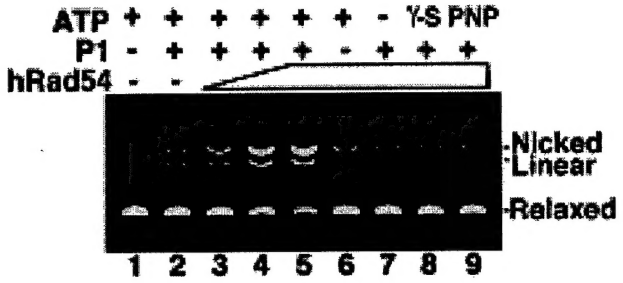

Figure 4. hRad54 promotes DNA strand opening. Increasing amounts of hRad54 (200, 400, and 750 nM in lanes 3 to 5, respectively) was incubated with topologically relaxed DNA (20 μM nucleotides) and P1 nuclease in buffer that contained ATP. The highest amount of hRad54 (750 nM) was also incubated with the DNA substrate in the absence of P1 (lane 6) and in the presence of P1 but with the omission of ATP (lane 7) or the substitution of ATP by ATP-γ-S (γ-S; lane 8) and AMP-PNP (PNP; lane 9). DNA alone (lane 1) and DNA incubated with P1 in the absence of hRad54 (lane 2) were also included. The reaction mixtures were run in a 1% agarose gel containing 10 μM ethidium bromide.

Activities of hRad54 are stimulated by hRad51 - Results presented here (Figure 1) and elsewhere (Golub et al, 1997) have established a specific interaction between hRad51 and hRad54 suggesting that this interaction may enhance the biological activities of these proteins. To test this, hRad54 ATPase activity was examined to see if it would be enhanced upon interaction with hRad51. As shown in Figure 5, when hRad54 was combined with hRad51 a much higher rate of ATP hydrolysis was seen. The fact that yRad51 was ineffective in this reaction (Figure 5) indicates that the action of hRad51 is specific. Even though hRad51 is known to have a weak ATPase activity (Benson et al, 1994), the fact that the hrad51 K133R mutant protein, which binds but does not hydrolyze ATP (Morrison et al, 1999), was just as effective in promoting ATP hydrolysis (data not shown) strongly indicated that the increase in ATP hydrolysis was due to enhancement of the hRad54 ATPase function.

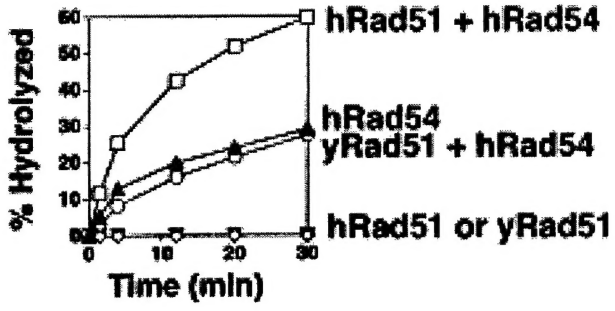

Figure 5. hRad54 ATPase activity is stimulated by hRad51. - hRad54 was incubated with ϕX replicative form I DNA (30 μM nucleotides) and 1.5 mM [γ-^{32}P] ATP for the indicated times, and the level of ATP hydrolysis was quantified by thin layer chromatography. ATPase activity was also measured for hRad51 alone, yRad51 alone, and the combinations of hRad54/hRad51 and hRad54/yRad51. The protein concentrations were: hRad54, 60 nM; hRad51, 400 nM; yRad51, 400 nM. In every case, negligible ATP hydrolysis was seen when DNA was omitted (data not shown).

We next asked whether the DNA supercoiling activity of hRad54 would also be upregulated by hRad51. As indicated by a much higher level of Form OW DNA (Figure 6A), the results showed that hRad51 stimulates the supercoiling reaction. Since negative supercoiling generated by hRad54 leads to DNA strand opening (Figure 4), we thought that hRad51 may also promote this activity. Indeed, the inclusion of hRad51 greatly elevated the nicking of the relaxed DNA substrate by P1 nuclease (Figure 6B). Even with the inclusion of hRad51, no Form OW DNA or nicking of DNA was seen when ATP was omitted or substituted by the non-hydrolyzable analogues ATP-γ-S and AMP-PNP (Figure 6 A & B). Thus, the results revealed that hRad51 markedly stimulates the ability of Rad54 to supercoil DNA and unwind DNA strands. The hrad51 K133R protein was just as effective as wild type hRad51 in enhancing the DNA supercoiling and strand opening activities of hRad54 (data not shown). Furthermore, yRad51 does not stimulate the hRad54 activities (data not shown), thus indicating a high degree of specificity in the hRad51 action.

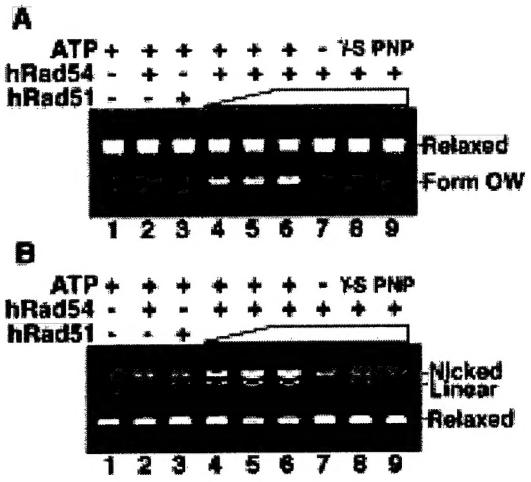

Figure 6. hRad51 stimulates hRad54 supercoiling and strand opening activities. *(A)* Relaxed DNA (20 μM nucleotides) was incubated with hRad54 (75 nM in lanes 2, and 4 to 9) and hRad51 (80, 160, and 240 nM in lanes 4 to 6, respectively) in the presence of ATP and *E. coli* topoisomerase I. The highest amount of hRad51 (240 nM) was incubated with substrate and topoisomerase I but without hRad54 (lane 3) and also with hRad54 (75 nM) but with the omission of ATP (lane 7) or its substitution with ATP-γ-S (γ-S; lane 8) or AMP-PNP (PNP; lane 9). DNA alone was analyzed in lane 1. After deproteinization, the reaction mixtures were run in a 1% agarose gel, which was treated with ethidium bromide to stain the DNA species.
(B) Relaxed DNA was incubated with hRad54 (75 nM in lanes 2 and 4 to 9) and hRad51 (80, 160, and 240 nM in lanes 4 to 6, respectively) in the presence of ATP and P1 nuclease. The highest amount of hRad51 (240 nM) was incubated with substrate and P1 but without hRad54 (lane 3) and also with hRad54 (75 nM) but with the omission of ATP (lane 7) or its substitution with ATP-γ-S (γ-S; lane 8) or AMP-PNP (PNP; lane 9). DNA alone was run in lane 1. Analysis was carried out in a 1% agarose gel that contained 10 μM ethidium bromide.

hRad51 and hRad54 co-operate in homologous DNA pairing

The RecA/Rad51 class of general recombinases is central to recombination processes by virtue of their ability to catalyze the homologous DNA pairing reaction that yields heteroduplex DNA joints (Bianco et al, 1998; Sung, 2000). Since hRad51 and hRad54 physically interact (Golub et al, 1997; Figure 1), and hRad51 enhances the various activities of hRad54 (Figure 5 and 6), it was of considerable interest to examine the influence of hRad54 on hRad51-mediated homologous DNA pairing.

The homologous pairing assay monitors the incorporation of a ^{32}P-labeled single-stranded oligonucleotide into a homologous supercoiled target (pBluescript) to give a D-loop structure (Figure 7A). As reported before (Mazin et al, 2000) and reiterated here (Figure 7B), hRad51 by itself is not particularly adept at forming D-loop. Importantly, inclusion of hRad54 rendered D-loop formation possible. D-loop formation by the combination of hRad51 and hRad54 requires ATP hydrolysis, as no D-loop was seen when ATP was omitted or when it was replaced by either ATP-γ-S or AMP-PNP (Figure 7B). Significantly, the time course revealed a cycle of rapid formation and disruption of D-loop, such that the D-loop level reached its maximum by 1 min but declined rapidly thereafter (Figure 7, B and D). In fact, by the reaction endpoint of 6 min, little or no D-loop remained (Figure 7, B and D). Such a cycle of D-loop synthesis and reversal has also been observed for *E. coli* RecA (Shibata et al, 1982). Since the RecA-ssDNA nucleoprotein filament disassembles upon ATP hydrolysis (Bianco et al, 1998), we considered the possibility that the dissociation of D-loop seen here (Figure 7B) could be related to ATP hydrolysis-mediated turnover of hRad51. To test this premise, we used the hrad51 K133R mutant protein, which binds but does not hydrolyze ATP (Morrison et al, 1999), with hRad54 in the D-loop assay. True to prediction, with hrad51 K133R, the D-loop amount increased with time, reaching a much higher final level than when hRad51 was used (Figure 7, B, C and D); by 5 min, 23% of the input ssDNA, or 55% of the pBluescript plasmid DNA, had been incorporated into the D-loop structure. As expected, with both hRad51/hRad54 and hrad51 K133R/hRad54, formation of D-loop required both the 90-mer substrate and pBluescript target, and substitution of the pBluescript DNA with the heterologous ϕX174 DNA completely abolished D-loop formation (data not shown).

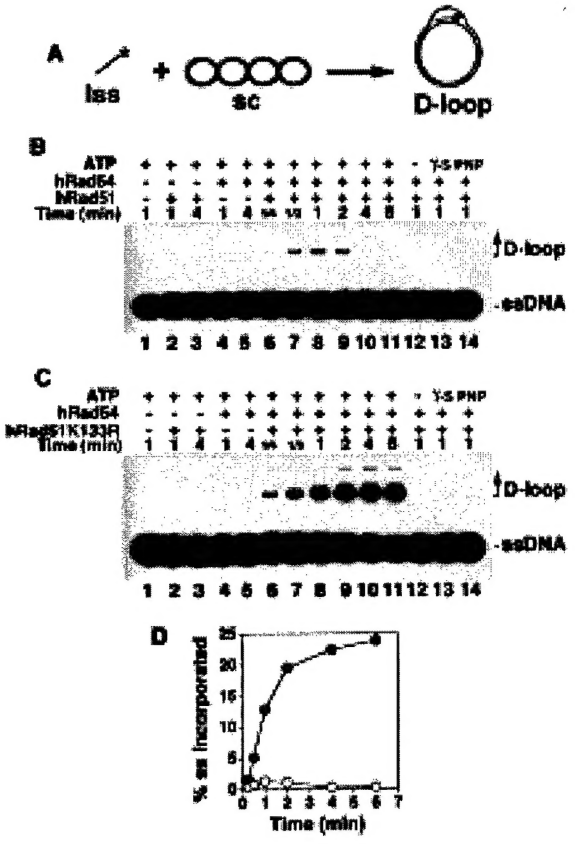

Figure 7. D-loop formation by hRad51 and hRad54. *(A)* Schematic of assay. A radiolabeled 90-mer DNA pairs with a homologous duplex target to yield a D-loop. *(B)* hRad51 alone (lanes 2 and 3), hRad54 alone (lanes 4 and 5), and the combination of hRad51 and hRad54 (lanes 6 to 14) were incubated at 30°C for the indicated times with the DNA substrates in the presence of ATP (lanes 2 to 11), ATP-γ-S (γS; lane 13), AMP-PNP (PNP; lane 14), or in the absence of nucleotide (lane 12). In lane 1, the DNA substrates were incubated in buffer without protein. The protein and DNA concentrations were: hRad51, 800 nM; hRad54, 120 nM; 90-mer oligonucleotide, 2.5 μM nucleotides or 27.7 nM oligonucleotide; pBluescript supercoiled DNA, 35 μM base pairs or 11.6 nM of plasmid. *(C)* The homologous pairing activity of hrad51 K133R was examined with hRad54 as described for hRad51 above. *(D)* The results in lanes 6 to 11 of B (open circles) and C (filled circles) were graphed.

CONCLUSIONS

In eukaryotes, the *RAD51* and *RAD54* genes are required for homologous recombination and DNA repair (Essers et al, 1997; Morita et al, 1993Like its bacterial homolog RecA, Rad51 protein has homologous DNA pairing activity that yields heteroduplex DNA joints in recombination processes (Sung, 1994; Baumann et al, 1996; Gupta et al, 1997). The Rad54 protein, a member of the Swi2/Snf2 protein family, is unique to eukaryotic organisms. Human Rad54 is shown in this study to have the ability to supercoil DNA and mediate transient opening of DNA strands in duplex DNA in a reaction that is driven by ATP hydrolysis. We show that hRad54 physically interacts with hRad51, and as a result of interaction, the supercoiling and strand opening activities of hRad54 are greatly stimulated. Importantly, we demonstrate that hRad51 and hRad54 functionally co-operate to make D-loop, the first DNA intermediate in recombination reactions in vivo. The results suggest a model in which hRad54 helps drive DNA joint formation via a highly specific interaction with hRad51 and an ability to utilize the free energy from ATP hydrolysis to promote the opening of the DNA double helix.

Our findings are of considerable general interest to a wide spectrum of investigators working on DNA repair, recombination, and cancer biology because **(i)** they elucidate the mechanism of action of human Rad54 protein, a recombination factor that is unique to eukaryotes, **(ii)** they provide a paradigm for dissecting the functions of the Rad54 homologs and counterparts in eukaryotic organisms, **(iii)** they provide an example of a Swi2/Snf2 protein family member whose function is to open the DNA double helix rather than to disrupt protein-nucleic acid complexes, and **(iv)** given the known role of the recombination machinery in tumor suppression, our findings have important implications as to cancer avoidance via the recombinational DNA repair mechanism.

APPENDED INFORMATION

(1) KEY RESEARCH ACCOMPLISHMENTS:

- **Demonstrate hRad51 and hRad54 directly interact using purified proteins.**
- **Demonstrate that in the presence of ATP hRad54 supercoils DNA and promotes a transient DNA strand opening.**
- **Demonstrate that hRad51 stimulates the ATPase activity of hRad54**
- **Demonstrate that hRad51 stimulates the DNA supercoiling and transient DNA strand opening activities of hRad54 in the presence of ATP.**
- **Demonstrate that hRad54 works in concert with hRad51 to promote homologous DNA joints or in D-loop formation.**

(2) REPORTABLE OUTCOMES

Presentations:

- Invited workshop speaker and poster presentation, Keystone Research Symposia on Molecular Mechanisms of DNA Replication and Recombination, Snowbird, UT. Title of Poster and Presentation " Functional interactions of Rad51 and Rad54 in Heteroduplex Joint Formation".

- Presentation at the Molecular Medicine Annual Retreat, Department of Molecular Medicine, University of Texas Health Science Center at San Antonio. Title of presentation "Functional Interactions Between Rad51 and Rad54 Provide Efficient Homologous DNA Pairing and Strand-Exchange".

- Poster presentation at the Era of Hope Department of Defense Breast Cancer Research Program Meeting, Orlando Florida, September 2002. Title of presentation "Rad51 and Rad54 cooperate in efficient Heteroduplex DNA Joint Formation".

- Ph.D. dissertation. Department of Molecular Medicine and Institute of Biotechnology, University of Texas Health Science Center at San Antonio. Title of dissertation "Functional interactions between Rad51 and Rad54 in Heteroduplex Joint Formation".

- Ph.D. defense. Department of Molecular Medicine Institute of Biotechnology,, University of Texas Health Science Center at San Antonio, October 2003. "Rad51 and Rad54 and their roles in promoting D-loop formation."

Publications:

Van Komen S., G. Petukhova, S. Sigurdsson, and P. Sung. (2002). Functional cross-talk among Rad51, Rad54, and replication protein A in heteroduplex DNA joint formation. ***J. Biol. Chem.***, 15;277(46):43578-87.

Sigurdsson S., **S. Van Komen**, G. Petukhova, and P. Sung. (2002). Homologous DNA pairing by human recombination factors Rad51 and Rad54. ***J. Biol. Chem.***, 8;277(45):42790-42794.

Jaskelioff M. *, **S. Van Komen***, J.E. Krebs, P. Sung, and C.L Peterson (2003). Rad54p is a chromatin remodeling enzyme required for heteroduplex DNA joint formation with chromatin. ***J. Biol. Chem.***, 14;278(11):9212-8.
<u>*These authors contributed equally to the work</u>

Krejci L.*, **S. Van Komen***, Y. Li, J. Villemain, M.S. Reddy, H. Klein, T. Ellenberger, and P. Sung. (2003). Attenuation of recombination by Srs2 helicase occurs via Rad51 presynaptic filament disruption. ***Nature***, 15;423(6937) 305-309.
***These authors contributed equally to the work**

Krejci L., L. Chen, **S. Van Komen**, P. Sung, and A. Tomkinson (2003). Mending the break: two repair machines in eukaryotes. ***Prog. Nucl. Acid Res. & Mol. Biol.***, *In press.*

Wolner B., **S. Van Komen**, P. Sung, and C.P. Peterson (2003). Recruitment of the recombinational repair machinery to a DNA double strand break in yeast. ***Molecular Cell***, *In press*

Personnel receiving pay from the research effort:

Stephen J. Van Komen

REFERENCES

Baumann, P., Benson, F.E., West, S.C. 1996. Human Rad51 protein promotes ATP-dependent homologous pairing and strand transfer reactions in vitro. Cell 15: 757-766.

Bianco PR, Tracy RB, Kowalczykowski SC. (1998). DNA strand exchange proteins: a biochemical and physical comparison. Front Biosci. 3:D570-603.

Chen PL, Chen CF, Chen Y, Xiao J, Sharp ZD, Lee WH. (1998). The BRC repeats in BRCA2 are critical for RAD51 binding and resistance to methyl methanesulfonate treatment. Proc Natl Acad Sci 95(9):5287-92.

Dasika GK, Lin SC, Zhao S, Sung P, Tomkinson A, Lee EY. (1999). DNA damage-induced cell cycle checkpoints and DNA strand break repair in development and tumorigenesis. Oncogene. 18(55):7883-99.

Essers, J., Hendriks, R.W., Swagemakers, S.M., Troelstra, C., de Wit, J., Bootsma, D., Hoeijmakers, J.H., and Kanaar, R. 1997. Disruption of mouse RAD54 reduces ionizing radiation resistance and homologous recombination. Cell 89: 195-204.

Golub, E.I., Kovalenko, O.V., Gupta, R.C., Ward, D.C., and Radding C.M. 1997. Interaction of human recombination proteins Rad51 and Rad54. Nucleic Acids Res. 25: 4106-4110.

Gupta, R.C., Bazemore, L.R., Golub, E.I., Radding, C.M. 1997. Activities of human recombination protein Rad51. Proc. Natl. Acad. Sci. U. S. A. 94: 463-468.

Havas, K., Flaus, A., Phelan, M., Kingston, R., Wade, P.A., Lilley, D.M., and Owen-Hughes, T. 2000. Generation of superhelical torsion by ATP-dependent chromatin remodeling activities. Cell 103: 1133-1142.

Kraus, E., Leung, W.Y., and Haber, J.E. 2001. Break-induced replication: a review and an example in budding yeast. Proc. Natl. Acad. Sci. U S A. 98: 8255-8262.

Krejci, L., Damborsky, J., Thomsen, B., Duno, M., and Bendixen, C. 2001. Molecular dissection of interactions between Rad51 and members of the recombination-repair group. Mol. Cell. Biol. 21: 966-976.

Mazin AV, Bornarth CJ, Solinger JA, Heyer WD, Kowalczykowski SC. (2000). Rad54 protein is targeted to pairing loci by the Rad51 nucleoprotein filament. Mol Cell. 6(3):583-92.

Michel B, Flores MJ, Viguera E, Grompone G, Seigneur M, Bidnenko V. (2001). Rescue of arrested replication forks by homologous recombination. Proc Natl Acad Sci. 98(15):8181-8.

Morrison, C., Shinohara, A., Sonoda, E., Yamaguchi-Iwai, Y., Takata, M., Weichselbaum, R.R., and Takeda, S. 1999. The essential functions of human Rad51 are independent of ATP hydrolysis. Mol. Cell. Biol. 19: 6891-6897.

Moynahan M. E, Cui T. Y. , Jasin M. (2001). Homology-directed dna repair, mitomycin-c resistance, and chromosome stability is restored with correction of a Brca1 mutation. Cancer Res. 15;61(12):4842-50.

Paques F., Haber J. E. (1999). Multiple pathways of recombination induced by double-strand breaks in Saccharomyces cerevisiae. Microbiol Mol Biol Rev. 63(2):349-404.

Pierce, A.J., Stark, J.M., Araujo, F.D., Moynahan, M.E., Berwick, M., and Jasin, M. 2001. Double-strand breaks and tumorigenesis. Trends Cell Biol. 11: S52-59.

Ristic, D., Wyman, C., Paulusma, C., and Kanaar, R. 2001. The architecture of the human Rad54-DNA complex provides evidence for protein translocation along DNA. Proc. Natl. Acad. Sci. U.S.A. 84: 8454-8460.

Rothstein R., Michel B., Gangloff S. (2000). Replication fork pausing and recombination or "gimme a break".Genes Dev. 1;14(1):1-10.

Sigurdsson, S., Trujillo, K., Song, B-W., Stratton, S., and Sung P. 2001. Basis for avid homologous DNA strand exchange by human Rad51 and RPA. J. Biol. Chem. 276: 8798-8806.

Shibata, T., Ohtani, T., Chang, P. K., and Ando, T. 1982. Role of superhelicity in homologous pairing of DNA molecules promoted by Escherichia coli recA protein.
J Biol Chem. 257:370-376.

Sung, P. 1994. Catalysis of ATP dependent homologous DNA pairing and strand exchange by the yeast RAD51 protein. Science 265:1241-1243.

Sung, P., and Robberson, D.L. 1995. DNA strand exchange mediated by RAD51-ssDNA nucleoprotein filament with polarity opposite to that of RecA. Cell. 82: 453-461.

Sung, P., Trujillo, K., and Van Komen, S. 2000. Recombination factors of Saccharomyces cerevisiae. Mutat. Res. 451: 257-275.

Swagemakers, S.M.A., Essers, J., de Wit, J., Hoeijmakers, J.H.J., and Kanaar, R. 1998. The human Rad54 recombinational DNA repair protein is a double-stranded DNA-dependent ATPase. J. Biol. Chem. 273: 28292-28297.

Tan TL, Essers J, Citterio E, Swagemakers SM, de Wit J, Benson FE, Hoeijmakers JH, Kanaar R. (1999). Mouse Rad54 affects DNA conformation and DNA-damage-induced Rad51 foci formation. Curr Biol. 25;9(6):325-8.

Trujillo KM, Yuan SS, Lee EY, Sung P. 1998. Nuclease activities in a complex of human recombination and DNA repair factors Rad50, Mre11, and p95. J. Biol. Chem. 273: 21447-21450.

Van Komen, S., Petukhova, G., Sigurdsson, S., Stratton, S., and Sung, P. 2000. Superhelicity-driven homologous DNA pairing by yeast recombination factors Rad51 and Rad54. Mol. Cell 6: 563-572.

Vignali, M., Hassan, A.H., Neely, K.E., and Workman, J.L. 2000. ATP-dependent chromatin-remodeling complexes. Mol. Cell. Biol. 20: 1899-1910.

Yu X, Jacobs SA, West SC, Ogawa T, Egelman EH. (2001). Domain structure and dynamics in the helical filaments formed by RecA and Rad51 on DNA. Proc Natl Acad Sci 98(15):8419-24.

THE JOURNAL OF BIOLOGICAL CHEMISTRY
Vol. 277, No. 46, Issue of November 15, pp. 43578–43587, 2002
Printed in U.S.A.

Functional Cross-talk among Rad51, Rad54, and Replication Protein A in Heteroduplex DNA Joint Formation*

Received for publication, June 12, 2002, and in revised form, September 3, 2002
Published, JBC Papers in Press, September 10, 2002, DOI 10.1074/jbc.M205864200

Stephen Van Komen‡, Galina Petukhova§, Stefan Sigurdsson¶, and Patrick Sung‖

From the Department of Molecular Medicine / Institute of Biotechnology, University of Texas Health Science Center at San Antonio, San Antonio, Texas 78245-3207

Saccharomyces cerevisiae **Rad51, Rad54, and replication protein A (RPA) proteins work in concert to make heteroduplex DNA joints during homologous recombination. With plasmid length DNA substrates, maximal DNA joint formation is observed with amounts of Rad51 substantially below what is needed to saturate the initiating single-stranded DNA template, and, relative to Rad51, Rad54 is needed in only catalytic quantities. RPA is still indispensable for optimal reaction efficiency, but its role in this instance is to sequester free single-stranded DNA, which otherwise inhibits Rad51 and Rad54 functions. We also demonstrate that Rad54 helps overcome various reaction constraints in DNA joint formation. These results thus shed light on the function of Rad54 in the Rad51-mediated homologous DNA pairing reaction and also reveal a novel role of RPA in the presynaptic stage of this reaction.**

Aside from contributing to the creation of genetic diversity, homologous recombination is indispensable for DNA double-stranded break repair, meiosis I, and for various aspects of telomere homeostasis. Genetic studies in *Saccharomyces cerevisiae* have been chiefly responsible for identifying the components of the recombination machinery. These recombination genes (*RAD50*, *RAD51*, *RAD52*, *RAD54*, *RAD55*, *RAD57*, *RAD59*, *RDH54/TID1*, *MRE11*, and *XRS2*) are collectively referred to as the *RAD52* epistasis group. Gene cloning, genetic analyses, and biochemical studies have revealed a remarkable degree of conservation of the *RAD52* group, from yeast to humans (1–4). In mammals, members of the *RAD52* group interact with the tumor suppressors BRCA1 and BRCA2, which in turn influence the activities of their partner recombination factors and the efficiency of recombination (5–8). The latter observations underscore the importance for deciphering the functions of individual recombination factors and the mechanism of the protein machine comprising these factors.

Results from combined genetic and biochemical studies have suggested the following sequence of events in recombination. Following the introduction of a DNA double-stranded break, the ends of the break are processed nucleolytically to generate long single-stranded tails that have a 3′ extremity. Mre11, working in conjunction with Rad50 and Xrs2, provides the nuclease function for the formation of the 3′ ssDNA[1] tails. Rad51, the eukaryotic equivalent of the *Escherichia coli* general recombinase RecA, nucleates onto the ssDNA tails to form a right-handed nucleoprotein filament. The Rad51-ssDNA nucleoprotein filament then conducts a search for a chromosomal homolog, either the sister chromatid or the homologous chromosome. Pairing between the initiating ssDNA tails and the complementary strand in the duplex partner yields heteroduplex DNA joints, followed by extension of the joints by branch migration. The biochemical reaction responsible for DNA homology search and the formation of heteroduplex DNA joints is commonly called "homologous DNA pairing and strand exchange" (1, 4, 9).

In the homologous DNA pairing and strand exchange reaction, the assembly of the Rad51-ssDNA nucleoprotein filament is referred to as the presynaptic phase. Rad52 and the Rad55-Rad57 complex are recombination mediators that promote the assembly of the Rad51-ssDNA presynaptic nucleoprotein filament (4, 10, 11). In the post-synaptic phase, the Rad51-ssDNA nucleoprotein filament cooperates with Rad54 and Rdh54 (also called Tid1) to form DNA joints (12, 13). Rad54 and Rdh54, both members of the Swi2/Snf2 protein family (4), utilize the free energy from ATP hydrolysis to produce compensatory negative and positive supercoils in duplex DNA, which probably result from a tracking motion of these proteins on DNA (13–15). The negative supercoils produced by Rad54 and Rdh54 lead to transient DNA strand opening, believed to be germane for the promotion of DNA joint formation (15). Interestingly, Rad51 enhances the DNA supercoiling and DNA strand opening activities of Rad54 (15, 16).

Whereas a good body of information concerning the biochemical properties of the *RAD52* group proteins has accumulated in recent years, the manner in which these recombination factors functionally interact with one another and with the DNA substrates to achieve the maximal efficiency of DNA joint formation has remained mysterious. Here we present results that shed light on the synergistic interactions among Rad51, Rad54, RPA, and the ssDNA substrate in the initial stages of recombination. The results also reveal a new role of RPA in the homologous DNA pairing reaction.

EXPERIMENTAL PROCEDURES

Recombination Proteins—Rad51 and Rad54 proteins were overexpressed in yeast cells and purified to near homogeneity as described

* This work was supported by United States Public Health Service Grants RO1ES07061 and RO1GM57814. The costs of publication of this article were defrayed in part by the payment of page charges. This article must therefore be hereby marked "*advertisement*" in accordance with 18 U.S.C. Section 1734 solely to indicate this fact.

‡ Supported in part by United States Army Predoctoral Fellowship DAMD17-01-1-0414.

§ Present Address: NIDDK, National Institutes of Health, Bldg. 10, Rm. 9D17, 9000 Rockville Pike, Bethesda, MD 20892.

¶ Supported in part by United States Army Training Grant DAMD17-99-1-9402 and Predoctoral Fellowship DAMD17-01-1-0412.

‖ To whom correspondence should be addressed: Dept. of Molecular Medicine/Institute of Biotechnology, University of Texas Health Science Center at San Antonio, 15355 Lambda Dr., San Antonio, TX 78245-3207. Tel.: 210-567-7216; Fax: 210-567-7277; E-mail: sung@uthscsa.edu.

[1] The abbreviations used are: ssDNA, single-stranded DNA; RPA, replication protein A.

previously (12, 17). RPA was overexpressed in yeast using three plasmids that code for the three subunits of RPA (18) and purified to near homogeneity as described (19). The concentrations of Rad51 and RPA were determined using extinction coefficients of 1.29×10^4 and 8.8×10^4 at 280 nm, respectively (20). The concentration of Rad54 was determined by densitometric scanning of SDS-PAGE gels of multiple loadings of purified Rad54 against known quantities of bovine serum albumin and ovalbumin.

DNA Substrates—The φX174 (+) strand and replicative form I DNA were purchased from New England Biolabs and Invitrogen, respectively. The replicative form DNA was linearized by treatment with *Apa*LI or *Stu*I to yield linear duplex substrates that have either 3′ 4-base overhangs or blunt ends, respectively. Linearization of the viral (+) strand was done by hybridizing a 26-mer oligonucleotide to create a *Pst*I site, followed by treatment with *Pst*I (12). The pBluescript (+) strand and replicative form DNA were prepared as described previously (21). The pBluescript dsDNA used in Fig. 4*B* was a 1712-bp fragment generated from the replicative form by treatment with *Apa*LI and *Bsa*I; it was purified from 0.9% agarose gels as above. The pBluescript dsDNA used in Fig. 5*C* was full-length replicative form DNA linearized with *Bsa*I. The 90-mer oligonucleotide (5′-AAATCAATCTAAAGTATATATGAGTAAACTTGGTCTGACAGTTACCAATGCTTAATCAGTGAGGCACCTATCTCAGCGATCTGTCTATTT-3′) used for D-loop formation in Fig. 8 is complementary to pBluescript SK DNA from position 1932 to 2022. The oligonucleotide was 5′-end-labeled with T4 polynucleotide kinase (Promega) and [γ-^{32}P]ATP (Amersham Biosciences) and then purified using the MERmaid Spin Kit (Bio 101). All of the DNA substrates were stored in TE (10 mM Tris-HCl, pH 7.0, 0.5 mM EDTA).

DNA Strand Exchange Reaction—Unless stated otherwise, the reactions containing Rad54 were carried out at 23 °C, and the reactions without Rad54 were carried out at 37 °C. In the standard reaction (12.5-μl final volume), circular φX (+)-strand (19.6 μM nucleotides) was incubated for 4 min in 10 μl of buffer R (35 mM Tris-HCl, pH 7.2, 60 mM KCl, 2.5 mM ATP, 3 mM $MgCl_2$, 1 mM dithiothreitol, and an ATP-regenerating system consisting of 20 mM creatine phosphate and 300 ng of creatine kinase) with the indicated amounts of Rad51 added in 0.5 μl of storage buffer. Following the incorporation of RPA in 0.5 μl of storage buffer and the indicated amounts of Rad54 in 0.3 μl of storage buffer and an additional 4-min incubation, *Apa*LI linearized dsDNA in 0.7 μl, and 1 μl of 50 mM spermidine hydrochloride (4 mM final concentration) was added to complete the reaction. For time course experiments, the reactions were scaled up accordingly, and unless stated otherwise, the same order of addition of reaction components was used. At the times indicated, 5-μl portions of the reaction mixtures were mixed with an equal volume of 1% SDS and then treated with proteinase K (0.5 mg/ml) for 10 min at 37 °C before being run in 0.9% agarose gels in TAE buffer (40 mM Tris acetate, pH 7.4, 0.5 mM EDTA) at 23 °C. The gels were stained with ethidium bromide and recorded in a Nucleotech gel documentation system. Quantitation of the data was done using the Gel Expert software.

L-loop Reactions with Plasmid Length ssDNA—The standard D-loop reaction was assembled by preincubating *Pst*I-linearized φX ssDNA with Rad51 for 3 min, followed by the incorporation of RPA and an additional 3-min incubation. Rad54 was then added, and, following a 2-min incubation, φX replicative form DNA was incorporated to complete the reaction. All of the incubations were carried out at 23 °C, and the reaction mixtures were processed for electrophoresis as described above. Other details are given in the figure legends.

D-loop Reactions with Oligonucleotide as Single-stranded Substrate—Unless stated otherwise, Rad51 (2 μM) and the indicated amounts of Rad54 were incubated with the 5′-end-labeled 90-mer oligonucleotide (6 μM nucleotides or 67 nM oligonucleotide) in 11.5 μl of buffer R. The protein/DNA mixture was incubated for 10 min at either 23 or 37 °C, and D-loop formation was initiated by the addition of pBluescript SK replicative form DNA (65 μM base pairs or 22 nM plasmid molecules) in 1 μl. The reaction mixtures were incubated for 5 min at 23 °C and arrested by the addition of an equal volume of 1% SDS. The reactions were deproteinized with proteinase K as above before being subjected to electrophoresis in 0.9% agarose gels in TAE buffer at 23 °C. The gels were dried, and the level of D-loop was quantified in a Personal FX phosphor imager with Quantity One software (Bio-Rad). The results were plotted as the percentage of oligonucleotide that had been incorporated into the D-loop. For the order of addition experiments in Fig. 8*D*, the reactions were scaled up accordingly with the indicated amounts of components.

Inhibition of DNA Pairing and Strand Exchange by ssDNA and Reversal by RPA—In Fig. 4*B*, *panels I* and *II*, the reaction mixtures (final volume of 14.5 μl) were assembled as described for the standard D-loop reaction, except that increasing concentrations of pBluescript circular ssDNA or linear duplex were added with the φX replicative form I DNA substrate in 3 μl of TE. In Fig. 4*B*, *panel III*, the reaction mixtures (final volume of 14.5 μl) were assembled as described for *panels I* and *II*, except that the pBluescript ssDNA competitor (150 μM nucleotides) had been preincubated with RPA (9 μM) at 37 °C for 3 min in buffer R. The RPA-coated ssDNA competitor was then diluted with buffer R to the desired concentrations and added in 2 μl with the replicative form I DNA in 1 μl to the D-loop reactions. In Fig. 5, *A* and *C*, the reaction mixtures (final volume of 14.5 μl) were assembled as described for the model DNA strand exchange reaction, except that increasing concentrations of pBluescript ssDNA (Fig. 5*A*, *lanes 3–6*) or pBluescript linear duplex (Fig. 5*C*, *lanes 3–6* and *9–12*) was added with the φX linear duplex in 3 μl of TE. In Fig. 5*A*, *lanes 7–10*, the pBluescript ssDNA competitor (150 μM nucleotides) had been preincubated with RPA (9 μM), as described above for Fig. 4*B*, and then added in 2 μl with the φX linear duplex in 1 μl of TE to the reaction.

ATPase Assay—In Fig. 1*A*, Rad54 (150 nM), in 8 μl of buffer A (30 mM Tris-HCl, pH 7.2, 1 mM dithiothreitol, 5 mM $MgCl_2$, 45 mM KCl, and 200 μg/ml bovine serum albumin), that had or had not been preincubated either at 37 or 23 °C was mixed with φX replicative form DNA (30 μM base pairs) and 1.5 mM [γ-^{32}P]ATP (Amersham Biosciences) in 2 μl. Where indicated, dsDNA or ATP was also present during the preincubation of Rad54 at 37 °C. The reactions (10 μl) were incubated at 23 °C, and at the indicated times a 1.5-μl aliquot was removed and mixed with an equal volume of 500 mM EDTA to halt the reaction. The amount of ATP hydrolysis was determined by thin layer chromatography, as described (12). To examine the effect of Rad51 on the thermal stability of Rad54 (Fig. 1*B*), the combination of Rad51 (2 μM) and Rad54 (75 nM), in 8 μl of buffer A, that had or had not been preincubated at 23 °C or 37 °C as above was mixed with φX replicative form DNA (30 μM base pairs) and 1.5 mM [γ-^{32}P] ATP in 2 μl.

In Fig. 5*D*, Rad54 (150 nM) was incubated for 15 min at 23 °C with 1.5 mM [γ-^{32}P]ATP and the indicated amounts of ssDNA (0.9, 3.6, 7.2, 14.4, or 28.7 μM nucleotides) in 10 μl of buffer A. Rad54 (150 nM) was also similarly incubated with φX replicative form DNA (30 μM base pairs) and the indicated amounts of pBluescript ssDNA (0.9, 3.6, 7.2, 14.4, and 28.7 μM nucleotides). To examine the effect of precoating the pBluescript ssDNA competitor with RPA, the ssDNA (150 μM nucleotides) was incubated with RPA (9 μM) at 37 °C for 5 min in buffer A, diluted with the appropriate volume of buffer A, before being incorporated with the φX replicative form DNA (30 μM base pairs) in 2 μl into the ATPase reactions. The completed reactions (10 μl) were incubated at 23 °C for 15 min.

In Fig. 3*A*, *panel III*, the ATPase assay was performed as described for the model D-loop reaction with 660 nM Rad54, 1.4 μM Rad51, 1.3 μM RPA, and [γ-^{32}P]ATP, either with or without the ATP-regenerating system consisting of 20 mM creatine phosphate and 300 ng of creatine kinase.

RESULTS

Rad54 Is Prone to Thermal Inactivation—The rate of dsDNA-activated ATP hydrolysis by Rad54 was linear with time for at least 12 min at 23 °C (Fig. 1*A*). Preincubation of Rad54 at 37 °C in the absence of ATP and dsDNA for brief periods caused a dramatic decrease in ATP hydrolysis in reactions conducted at 23 °C, whereas preincubation of Rad54 at 23 °C had no effect on the ATPase activity (Fig. 1*A*). These results indicate that the Rad54 ATPase function is prone to denaturation at 37 °C. Whereas ATP had only a very slight protective effect against thermal denaturation of Rad54 (Fig. 1*A*), dsDNA exhibited a modest protective effect (Fig. 1*A*). Although Rad51 physically interacts with Rad54 (12, 22, 23) and stimulates the Rad54 ATPase and DNA supercoiling activities (15, 16), it did not prevent thermal denaturation of Rad54 (Fig. 1*A*).

In the homologous DNA pairing reaction, preincubation of Rad54 or the combination of Rad51 and Rad54 at 37 °C for brief periods also greatly diminished the extent of the reaction (see below). By contrast, Rad51 is stable for at least 30 min at 37 °C, as gauged by its ATPase and homologous DNA pairing and strand exchange activities (data not shown). Thus, Rad54 is quite unstable at 37 °C, and because of this, all of the reactions involving Rad54 were routinely carried out at 23 °C, where it is

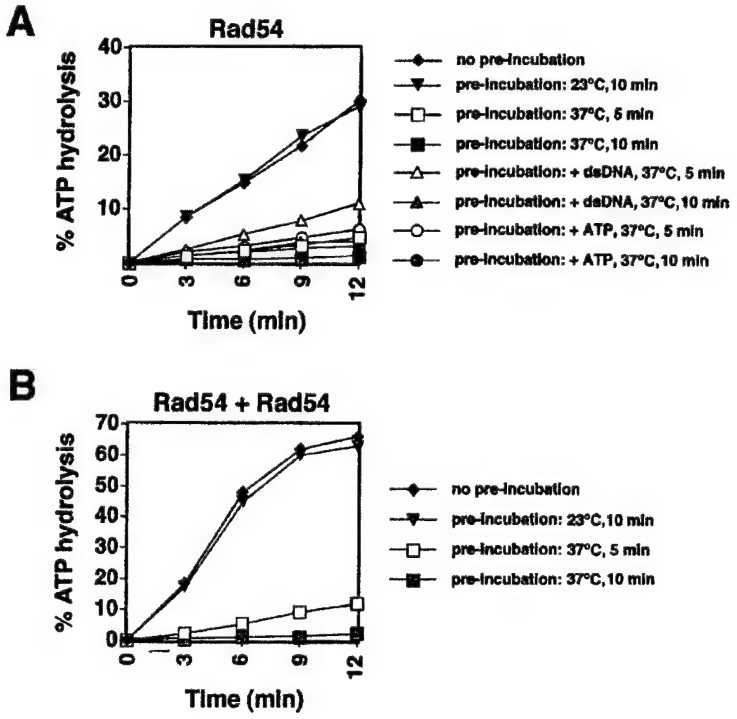

FIG. 1. **Thermal inactivation of Rad54 ATPase activity.** *A*, Rad54 (150 nM) was incubated with ϕX dsDNA (30 μM base pairs) and 1.5 mM [γ-^{32}P]ATP (*dark diamonds*) at 23 °C for the indicated times. Alternatively, the same amount of Rad54 was preincubated at 23 °C for 10 min (*gray inverted triangles*), at 37 °C for 5 min (*open squares*) or 10 min (*gray squares*), with the dsDNA at 37 °C for 5 min (*open triangles*) or 10 min (*gray triangles*), and with ATP at 37 °C for 5 min (*open circles*) or 10 min (*gray circles*), prior to mixing with the remaining reaction components and continuing the incubation at 23 °C for the indicated times. *B*, graphical representation of time courses of ATP hydrolysis by Rad54 (75 nM), Rad51 (2 μM), and ϕX dsDNA (30 μM base pairs) with no preincubation (*dark diamonds*) or preincubation at 23 °C for 10 min (*gray inverted triangles*) and at 37 °C for 5 min (*open squares*) or 10 min (*gray squares*), as done in *A*.

much more stable. Furthermore, since homologous pairing by Rad51 and Rad54 occurs efficiently, the use of a relatively low reaction temperature also allowed us to follow the reaction kinetics with greater ease.

With Rad54, a Contiguous Rad51-ssDNA Nucleoprotein Filament Is Not Needed for Homologous Pairing—In the model homologous DNA pairing and strand exchange reaction that employs circular ssDNA and linear duplex (see Fig. 2*A*, *panel I*, for schematic) but contains no Rad54, maximal reaction efficiency is observed at 3 nucleotides per Rad51 monomer (Fig. 2*B*, *panels I* and *III*) (20, 24). The optimal ratio of Rad51 to ssDNA in this model reaction corresponds to the ssDNA binding site size of Rad51 (25). Based on these observations, it has been generally assumed that a contiguous Rad51-ssDNA nucleoprotein filament is needed for achieving maximal homologous DNA pairing and strand exchange.

The stoichiometric relationship between Rad51 and the ssDNA substrate in the D-loop reaction (see Fig. 2*A*, *panel II*, for schematic) was examined here. Amounts of Rad51 varying from 30 to 3.2 nucleotides of ssDNA per protein monomer (0.66–6.1 μM Rad51 and 19.6 μM nucleotides of ssDNA) were used with a concentration of Rad54 (150 nM) sufficient to afford robust homologous DNA pairing. Surprisingly, maximal homologous pairing (see Fig. 2*B*, *panels II* and *III*) occurred over the range of 15 to 9 nucleotides/Rad51 monomer, which is substantially below the ratio of 3 nucleotides/Rad51 monomer needed for the formation of a contiguous Rad51 filament. In fact, increasing the Rad51 amount to 3 nucleotides/protein monomer consistently led to a greater than 3-fold decrease in the amount of D-loop (Fig. 2*B*, *panels II* and *III*). We note that whereas at 30 nucleotides/Rad51 monomer a substantial level of D-loop was obtained (Fig. 2*B*, *panel II*, *lane 2*), only a trace of reaction product was formed by an amount of Rad51 corresponding to 7.4 nucleotides/Rad51 monomer in the model reaction that did not contain Rad54 (Fig. 2*B*, *panel I*, *lane 2*). We have also examined the dependence of D-loop formation on the Rad51 amount with concentrations of Rad54 higher and lower than that used in the experiment above. Under those conditions, we again found that Rad51 amounts from ~15 to 9 nucleotides per protein monomer were optimal and that increasing the Rad51 level beyond this optimal range resulted in a similar degree of reduction of D-loop as in Fig. 2*B* (data not shown).

Turnover of RecA from the bound ssDNA occurs when the ssDNA is linear (9). If there had been sufficient Rad51 dissociating from the linear ssDNA substrate in the D-loop reaction, the free Rad51 pool could have sequestered the dsDNA from pairing with the ssDNA (24). To help eliminate this caveat, we examined the pairing between a circular ssDNA with linear duplex (Fig. 2*A*, *panel I*) in the presence of Rad54. In this case, the stoichiometric relationship between Rad51 and the ssDNA (Fig. 2*C*) closely resembled that seen in the D-loop experiment (Fig. 2*B*, *panel II*) (*i.e.* with the optimal concentration range of Rad51 at ~15 to 9 nucleotides per protein monomer and the reaction efficiency gradually decreasing with elevating Rad51 amounts).

In aggregate, the new data demonstrate that homologous pairing catalyzed by the combination of Rad51 and Rad54 does not require a contiguous Rad51 filament. In fact, suppression of DNA joint formation occurs when a full Rad51 filament is allowed to assemble.

Rad54 Is Required in Only Catalytic Amounts—Although a quantity of Rad54 substoichiometric to Rad51 affords a robust homologous pairing reaction (12, 15, 26) (see Fig. 2), we examined whether higher amounts of Rad54 would further enhance the reaction. Although an ATP-regenerating system was included in the pairing assays, to ensure that the increased amounts of Rad54 did not cause a depletion of the ATP pool, we also monitored the level of free ATP by thin layer chromatography. As shown in Fig. 3*A*, *panels I* and *II*, the optimal level of Rad54 was between 82.5 and 300 nM, substantially below that of Rad51 (1.4 μM) used. Importantly, increasing the amount of Rad54 to 660 nM in fact suppressed joint formation greatly. For example, after 2.5 min of incubation, whereas ~40% of the replicative form DNA had been converted to D loop at 82.5 nM of Rad54, a ratio of Rad51/Rad54 of 17 (Fig. 3*A*, *panel I*, *lane 3*; *panel II*), only ~4% of D-loop formation was observed at 660 nM

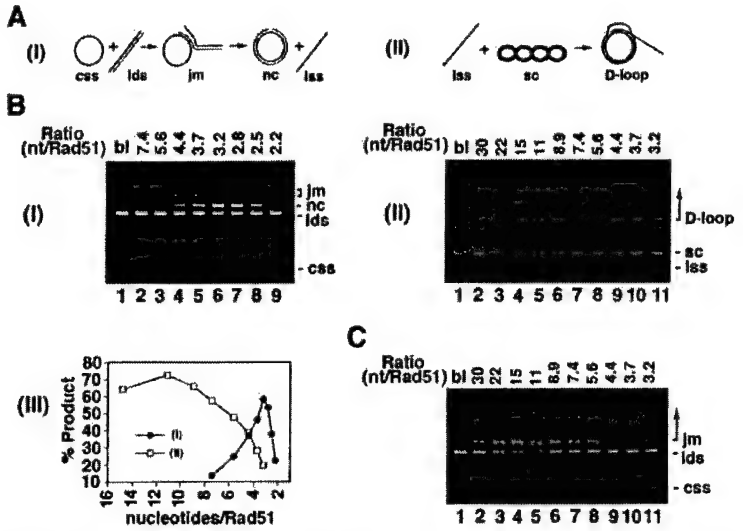

FIG. 2. **Subsaturating Rad51 amounts give maximal DNA pairing.** *A*, the pairing systems used. In *I*, pairing between the circular ssDNA and the linear duplex yields a joint molecule, which has the potential of generating a nicked circular duplex and a linear single strand as products, if branch migration of the DNA joint is successful over the 5.4 kb of ϕX ssDNA. *css*, circular single strand; *lds*, linear duplex; *jm*, joint molecules; *nc*, nicked circular duplex; *lss*, linear single strand. In *II*, pairing of linear ssDNA with the homologous replicative form I DNA gives a D-loop. *lss*, linear single-stranded DNA; *sc*, replicative form I DNA. *B*, stoichiometric relationship between Rad51 and ssDNA in homologous DNA pairing and strand exchange. In *panel I*, circular ϕX ssDNA (19.6 μM nucleotides) was first incubated with Rad51 (2.6, 3.5, 4.5, 5.3, 6.1, 7, 7.8, and 8.9 μM in *lanes 2–9*, respectively) and then with RPA (1.3 μM) at 37 °C, before the linear duplex (10 μM base pairs) was incorporated to complete the reaction, which was stopped after 50 min of incubation at 37 °C. In *panel II*, linear ϕX ssDNA (19.6 μM nucleotides) was incubated with Rad51 (0.66, 0.88, 1.3, 1.7, 2.2, 2.6, 3.5, 4.5, 5.3, and 6.1 μM in *lanes 2–11*, respectively) at 23 °C and then with RPA (1.3 μM) and Rad54 (150 nM) at 23 °C, before the ϕX replicative form I DNA (12.3 μM base pairs) was added to complete the reaction. The completed reaction mixtures were incubated at 23 °C for 5 min before electrophoresis. The efficiency of joint formation is plotted against the nucleotides (*nt*) to Rad51 monomer ratio in *panel III*. *Closed circles*, results from *panel I* of *B*; *open squares*, results from *panel II*. *C*, circular ϕX ssDNA (19.6 μM nucleotides) was incubated with Rad51 (0.66, 0.88, 1.3, 1.7, 2.2, 2.6, 3.5, 4.5, 5.3, and 6.1 μM in *lanes 2–11*, respectively) at 23 °C and then with RPA (1.3 μM) and Rad54 (150 nM) at 23 °C before the linear ϕX duplex (10 μM base pairs) was added. The completed reaction mixtures were incubated at 23 °C for 10 min before electrophoresis.

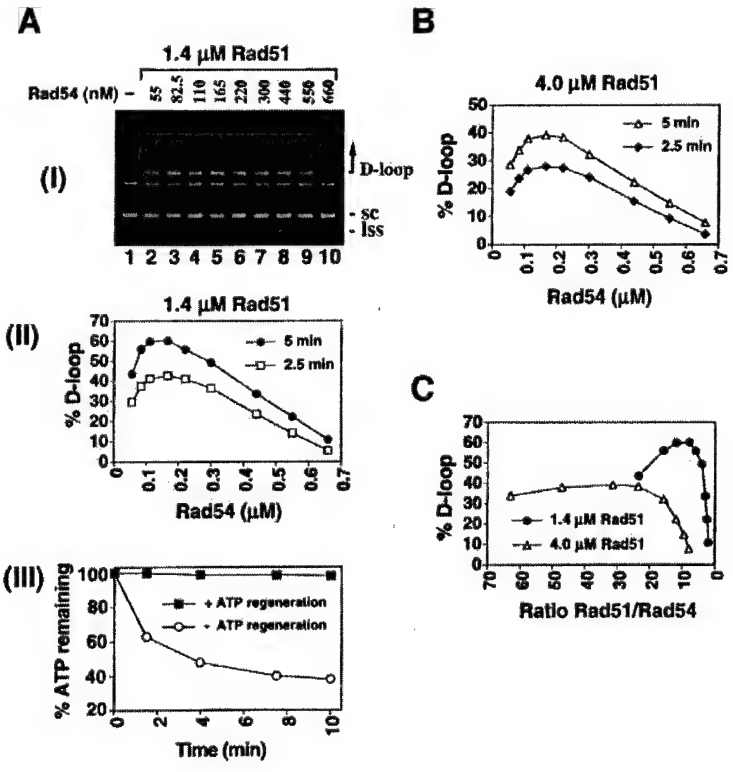

FIG. 3. **Catalytic amounts of Rad54 are sufficient for maximal DNA joint formation.** *A*, all of the steps were carried out at 23 °C. In *panel I*, linear ϕX ssDNA (19.6 μM nucleotides) was incubated with Rad51 (1.4 μM) and then with RPA (1.3 μM) and the indicated concentrations of Rad54 before the ϕX replicative form I DNA (12.3 μM base pairs) was incorporated. After 2.5 min and 5 min of incubation, a 5-μl aliquot was withdrawn and processed for electrophoresis. The agarose gel containing the samples from the 2.5-min time point is shown. *lss*, linear single-strand DNA; *sc*, replicative form DNA. The results are graphed in *panel II*. *Panel III* shows the level of ATP in D-loop reactions containing 660 nM Rad54 either with (*open squares*) or without (*closed circles*) the ATP-regenerating system. The reaction mixtures in *panel III* contained [γ-^{32}P]ATP and were assembled in the same manner as those in *panel I*. *B*, the results from another series of D-loop reactions that contained 4 μM Rad51, 1.3 μM RPA, and varying amounts of Rad54 are graphed. *C*, the results from the 5-min time point in *panel I* of *A* (*closed circles*) and in *B* (*open triangles*) are plotted as percentage of D-loop against the Rad51/Rad54 ratio.

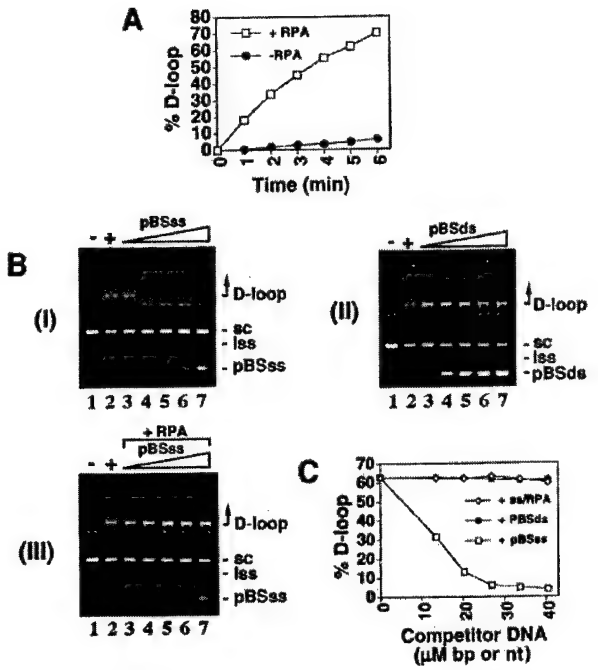

FIG. 4. **Role of RPA in DNA joint formation.** *A*, D-loop reactions containing Rad51 (1.4 μM) and Rad54 (150 nM) with (*open squares*) or without RPA (*closed circles*; 1.3 μM) were assembled and incubated as described under "D-loop Reactions with Plasmid Length ssDNA." The reaction mixtures had a final volume of 37.5 μl, and aliquots of 5 μl were withdrawn at the indicated times and analyzed. *B*, D-loop formation is specifically inhibited by free ssDNA. Reactions containing the same amounts of Rad51, Rad54, RPA, and φX DNA substrates as in *A* and also pBluescript ssDNA (in *panel I*, 13.5, 20, 27, 34, and 40.5 μM nucleotides in *lanes 3–7*, respectively) or pBluescript linear dsDNA (in *panel II*, 13.5, 20, 27, 34, and 40.5 μM base pairs in *lanes 3–7*, respectively) were assembled as described under "Experimental Procedures." In *panel III*, the pBluescript ssDNA competitor (13.5, 20, 27, 33.75, and 40.5 μM nucleotides) was precoated with RPA at a ratio of 17 nucleotides/RPA monomer before being added to the pairing reaction. The incubation time for these experiments was 5 min. *lss*, φX linear single-stranded DNA; *sc*, φX replicative form I DNA; *pBSss*, pBluescript ssDNA; *pBSds*, pBluescript linear duplex. *C*, graphical representation of the results in *panels I* (*open squares*), *II* (*closed circles*), and *III* (*open diamonds*) of *B*.

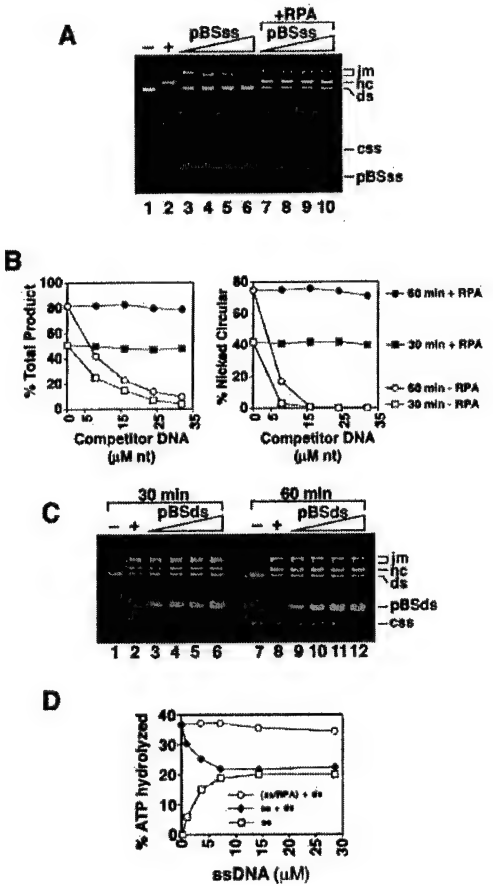

FIG. 5. **Effect of ssDNA on Rad51 and Rad54 functions.** *A*, all of the incubations were carried out at 37 °C. In *panel I*, φX circular ssDNA (19.6 μM nucleotides) was incubated first with Rad51 (6.5 μM) and then with RPA (1.3 μM). At the time of incorporation of the φX linear duplex (10 μM base pairs), increasing amounts of pBluescript circular ssDNA (8, 16, 24, and 32 μM nucleotides in *lanes 3–6*) or the same concentrations of pBluescript ssDNA precoated with RPA at a ratio of 17 nucleotides/RPA (*lanes 7–10*) was also added. Aliquots were withdrawn from the reactions after 30 and 60 min and subjected to electrophoresis. The agarose gel containing the samples from the 60-min time point is shown. *css*, circular φX ssDNA; *ds*, φX linear duplex; *jm*, φX DNA joint molecules; *nc*, φX nicked circular duplex; *pBSss*, pBluescript ssDNA. *B*, graphical representation of the results from the experiment in *A*. The total products (sum of joint molecules and nicked circular DNA; *left panel*) or percentage of nicked circular DNA (*right panel*) are plotted against increasing amounts of competitor pBluescript ssDNA. *Open circles*, results from *A* (*lanes 2–6*); *closed circles*, results from *A* (*lanes 2* and *7–10*); *open squares*, results from the 30-min time point with increasing amounts of competitor pBluescript ssDNA; *closed squares*, results from the 30-min time point with the pBluescript ssDNA competitor precoated with RPA. *C*, DNA strand exchange reactions were set up as described for *A*, except that linear pBluescript duplex DNA (12, 24, 36, and 48 μM base pairs in *lanes 3–6* and *lanes 9–12*, respectively) was added to the reaction mixtures at the time of incorporation of the φX linear duplex (10 μM base pairs). *Symbols* are as described for *A*; *pBSds*, pBluescript dsDNA. *D*, Rad54 (150 nM) was incubated with [γ-^{32}P]ATP, φX dsDNA (30 μM base pairs), and increasing concentrations of pBluescript ssDNA (0.9–28.7 μM nucleotides) with precoating of the ssDNA with RPA (*open circles*) or without (*closed diamonds*). ATPase activity (*open squares*) with 150 nM Rad54 was also determined for the same concentration range of pBluescript ssDNA (0.9–28.7 μM nucleotides). All of the reactions were incubated at 23 °C for 15 min.

Rad54, a ratio of Rad51/Rad54 of 2.1 (Fig. 3*A*, *panel I*, *lane 10*; *panel II*). Even at the highest concentration of Rad54, the ATP level never dropped below 98% of the nucleotide pool (Fig. 3*A*, *panel III*).

We also investigated whether maximal D-loop formation would require more Rad54 at a Rad51 concentration (4 μM) significantly higher than that used in Fig. 3*A* (1.4 μM). However, even with the increased Rad51 amount, the optimal concentration range of Rad54 (Fig. 3*B*) remained essentially the same as that observed before (Fig. 3*A*). Once again, elevating the Rad54 amount above the optimal range resulted in a precipitous decrease in DNA joint formation (Fig. 3*B*). It is important to note that in this particular instance (Fig. 3*B*), optimal D-loop formation was at ratios of Rad51/Rad54 of 48 to 16 (Fig. 3, *B* and *C*).

Taken together, we were able to conclude that only a catalytic quantity of Rad54 is needed for robust DNA joint formation and that there does not appear to be a formal stoichiometric relationship between Rad51 and Rad54 in order to achieve maximal reaction efficiency. We will discuss under "Discussion" why D-loop formation is suppressed by relatively high Rad54 concentrations.

RPA Shields the Presynaptic Complex from Free ssDNA—In the model reaction, RPA is indispensable for maximal reaction efficiency. By helping minimize secondary structure in the ssDNA template, RPA allows for the assembly of a contiguous Rad51-ssDNA nucleoprotein filament (20, 24). The results in Fig. 2 have shown that in the D-loop reaction, Rad51 amounts

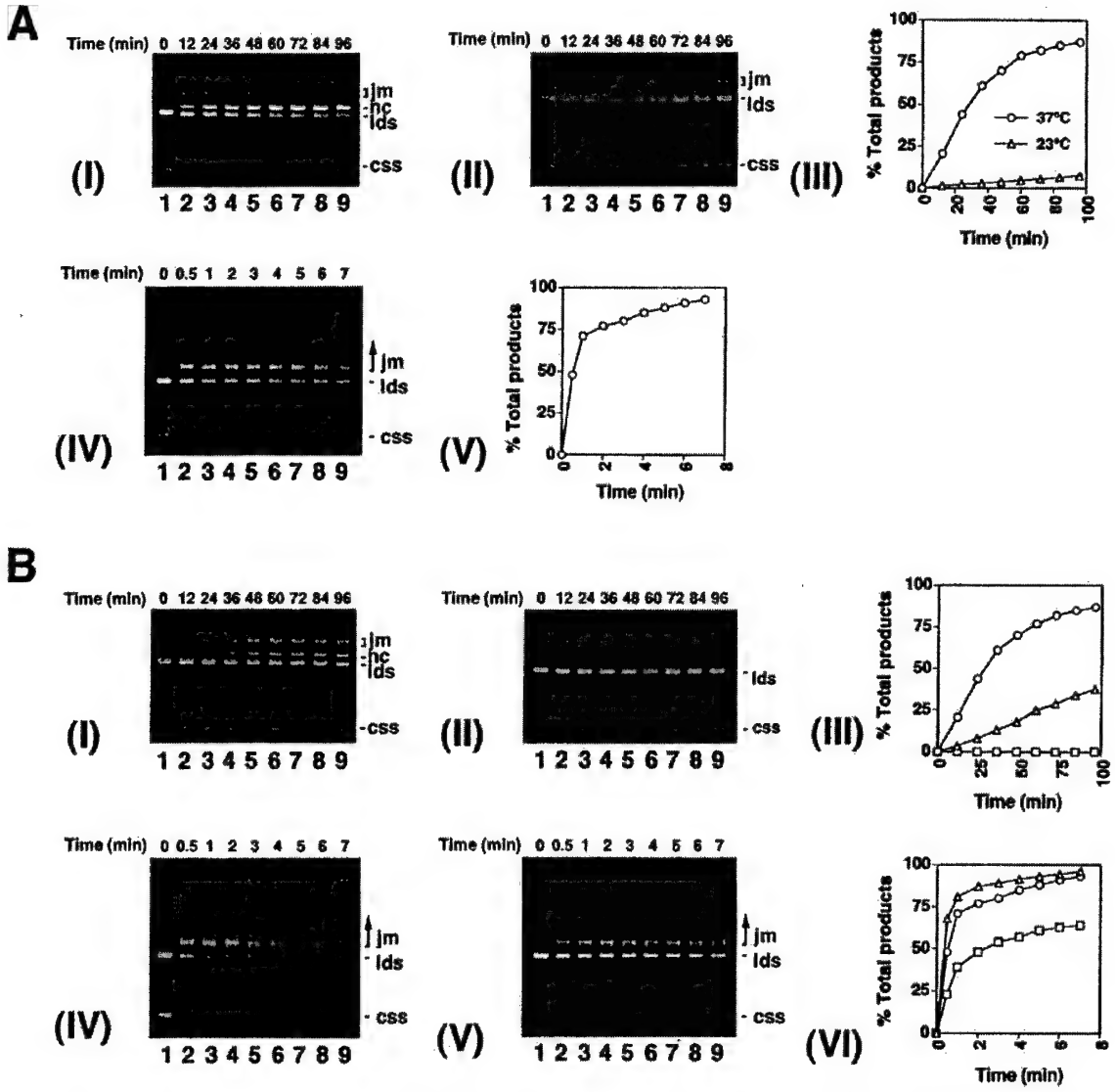

FIG. 6. **Rad54 overcomes various reaction impediments in Rad51-mediated DNA joint formation.** *A*, in *panels I* and *II*, circular ϕX ssDNA (19.6 μM nucleotides) was incubated for 4 min with Rad51 (6.1 μM) and then for an additional 4 min with RPA (1.3 μM) at 37 °C, followed by the addition of *Apa*LI-linearized ϕX duplex (10 μM base pairs) and 4 mM spermidine hydrochloride to complete the reaction mixture, which was further incubated either at 37 °C (*panel I*) or 23 °C (*panel II*) for the indicated times. *Panel III*, graphical representation of the reaction products (joint molecules and nicked circular duplex) in *panel I* (*open circles*) and *panel II* (*open triangles*). In *panel IV*, circular ϕX ssDNA (19.6 μM nucleotides) was incubated for 4 min with Rad51 (1.4 μM) and then for an additional 4 min with RPA (1.3 μM) and Rad54 (150 nM) at 23 °C, before *Apa*LI-linearized ϕX duplex (10 μM base pairs) and 4 mM spermidine hydrochloride were incorporated to complete the reaction mixture, which was incubated at 23 °C for the indicated times. *Panel V*, graphical representation of the reaction products (joint molecules and nicked circular duplex) in *panel IV*. *B*, the reactions in *panels I* and *II* were assembled in exactly the same manner as that in *panel I* of *A*, except that spermidine hydrochloride was substituted with either magnesium chloride (7.5 mM) in *panel I* or with water in *panel II*. *Panel III* is the graphical representation of the total reaction products (joint molecules and nicked circular duplex) in *panel I* (*open triangles*) and panel II (*open squares*); the results from *panel I* of *A* (*open circles*) are also included for comparison. The reactions in *panels IV* and *V* were assembled in exactly the same manner as that in *panel IV* of *A*, except that spermidine hydrochloride was substituted with either magnesium chloride (7.5 mM) in *panel IV* or with water in *panel V*. *Panel VI* is the graphical representation of the total reaction products (joint molecules and nicked circular duplex) in *panel IV* (*open triangles*) and *panel V* (*open squares*); the results from *panel IV* of *A* (*open circles*) are also included for comparison.

substantially below that required to saturate the ssDNA template in fact yield significantly more D-loop than when a saturating amount of Rad51 is used. As shown in Fig. 4*A*, at these low Rad51 concentrations, RPA was still needed for maximal DNA joint formation. Specifically, while greater than 60% of the input substrate had been converted into D-loop after 5 min, less than 5% of D-loop was seen with the omission of RPA.

In the optimized D-loop reaction there is insufficient Rad51 to make a contiguous nucleoprotein filament, yet RPA is still needed for optimal efficiency. Therefore, we concluded that RPA probably plays another role in this reaction. We considered the possibility that perhaps by sequestering free ssDNA left uncovered by Rad51, RPA might prevent the naked ssDNA from interfering with the homologous pairing reaction. To test this hypothesis directly, we carried out a reaction in which the ϕX ssDNA was incubated with Rad51, Rad54, and RPA as before (*e.g.* Fig. 2*B*, *panel II*), but an increasing amount of the unrelated pBluescript ssDNA was added with the ϕX replicative form. Severe inhibition of DNA loop formation by the pBluescript ssDNA was seen (Fig. 4, *B* (*panel I*) and *C*). For

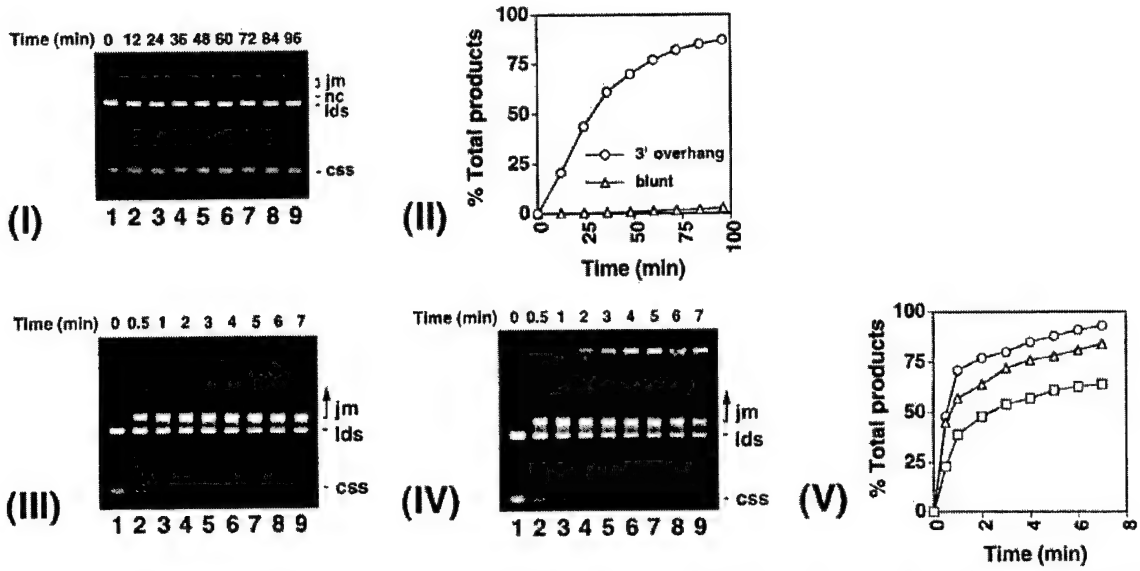

FIG. 7. **Rad51/Rad54 can utilize a blunt-ended substrate for homologous pairing.** The reaction in *panel I* contained Rad51 and RPA and was assembled in the same manner as that in *panel I* of Fig. 6*A*, except that *Stu*I-linearized blunt-ended dsDNA ϕX (10 μM base pairs) was used. *Panel II*, graphical representation of the reaction products (joint molecules and nicked circular duplex) in *panel I* (*open triangles*); the results in *panel I* of Fig. 6*A* (*open circles*) are also included for comparison. The reactions in *panels III* and *IV* contained Rad51, Rad54, and RPA and used *Stu*I-linearized blunt-ended DNA as substrate. Both of these reactions were assembled in the same manner as that in *panel IV* of Fig. 6*A*, except that in *panel IV*, magnesium chloride (7.5 mM) replaced spermidine hydrochloride. *Panel V* is the graphical representation of the total reaction products (joint molecules and nicked circular duplex) in *panel III* (*open squares*) and panel IV (*open triangles*); the results in *panel IV* of Fig. 6*A* (*open circles*) are also included for comparison.

instance, the level of D-loop was reduced from ~60% (Fig. 4*B*, *panel I*, *lane 2*) after 5 min of reaction to 11 and 4% by 20 and 34 μM of the pBluescript ssDNA, respectively (Fig. 4, *B* (*panel I*, *lanes 4* and *6*, respectively) and *C*). By contrast, the addition of equivalent amounts of pBluescript dsDNA did not cause inhibition of the D-loop reaction (Fig. 4, *B* (*panel II*) and *C*). Importantly, preincubation of the pBluescript ssDNA competitor with an amount of RPA sufficient to completely coat the ssDNA competitor proved to be highly effective in ablating the inhibitory effect of the DNA (Fig. 4, *B* (*panel III*) and *C*). Taken together, the results support the notion that free ssDNA left uncovered by Rad51/Rad54 constitutes a strong inhibitor of homologous pairing. The data also lent credence to the suggestion that the main role of RPA in the D-loop reaction is to sequester protein-free ssDNA and prevent inhibition of the pairing reaction by the DNA.

Single-stranded DNA Compromises Rad51 and Rad54 Functions—The results above indicated that naked ssDNA inhibits the D-loop reaction markedly but did not address whether the ssDNA inhibitor compromises the functional integrity of the Rad51 presynaptic filament and/or Rad54 function. To identify the target(s) of inhibition by ssDNA, we first tested the effect of ssDNA on the Rad51-mediated strand exchange reaction that used ϕX174 DNA substrates. As shown in Fig. 5, *A* (*lanes 3–6*) and *B*, the addition of free pBluescript ssDNA strongly inhibited strand exchange between the ϕX DNA substrates. By contrast, equivalent amounts of free pBluescript dsDNA had little or no effect on the reaction efficiency (Fig. 5*C*). Once again, preincubation of the ssDNA competitor with RPA (Fig. 5, *A* (*lanes 7–10*) and *B*) was sufficient to ablate its inhibitory effect.

Rad54 has a robust ATPase activity that is dependent on DNA for activation, and dsDNA is more effective than ssDNA in supporting ATP hydrolysis (12, 27). To assess whether ssDNA can also interfere with the binding of dsDNA by Rad54, we examined the effect of adding ssDNA on the Rad54 dsDNA-dependent ATPase activity. The results, as summarized in Fig. 5*D*, indicated that ATP hydrolysis by Rad54 was suppressed by concentrations of ssDNA (0.9–7.2 μM nucleotides) substantially below that of the duplex (30 μM base pairs). Here too, incubating the ssDNA with RPA can effectively reverse the suppression by ssDNA (Fig. 5*D*). In control experiments, the addition of extra dsDNA (45 μM base pairs) had no effect on the level of ATP hydrolysis (data not shown). Taken together, the results indicated that the Rad54 dsDNA-activated ATPase activity is strongly inhibited by ssDNA. Other experiments have found that Rad54 in fact has a higher affinity for ssDNA, which, when present, prevents Rad54 from binding to dsDNA (data not shown).

Rad54 Helps Overcome Various Reaction Constraints—The Rad51-mediated homologous DNA pairing and strand exchange reaction is normally conducted at 37 °C (Fig. 6*A*, *panel I*), since lowering the reaction temperature to 23 °C greatly diminishes product formation (Fig. 6*A*, *panels II* and *III*). As demonstrated before (15) and reiterated here (Figs. 6 and 7), homologous DNA pairing reactions that contain Rad54 proceed efficiently at 23 °C. In the reaction that does not contain Rad54, a low level of magnesium is present during the preincubation of Rad51 with ssDNA, but the addition of either spermidine or extra magnesium with the duplex substrate is critical for robust pairing and strand exchange (17, 19) (Fig. 6*B*, *panels I*, *II*, and *III*), with spermidine being more effective than magnesium in this regard (Fig. 6*B*, *panel III*). With the inclusion of Rad54, even in the absence of spermidine or additional magnesium, a highly significant amount of DNA joints is obtained (Fig. 6*B*, *panels V* and *VI*). Interestingly, with Rad54, higher rates of homologous pairing are seen with the addition of magnesium (Fig. 6*B*, *panels IV* and *VI*) than spermidine (Fig. 6*A*, *panel IV*). The duplex substrate used in the standard DNA strand exchange reaction has either 3′ or 5′ overhangs, since Rad51 has very limited capacity to utilize duplex DNA with blunt ends (28) (Fig. 7, *panel I*). By contrast, with Rad54 in the reaction, a blunt-ended DNA substrate is efficiently used for homologous pairing (Fig. 7, *panels III*, *IV*, and *V*).

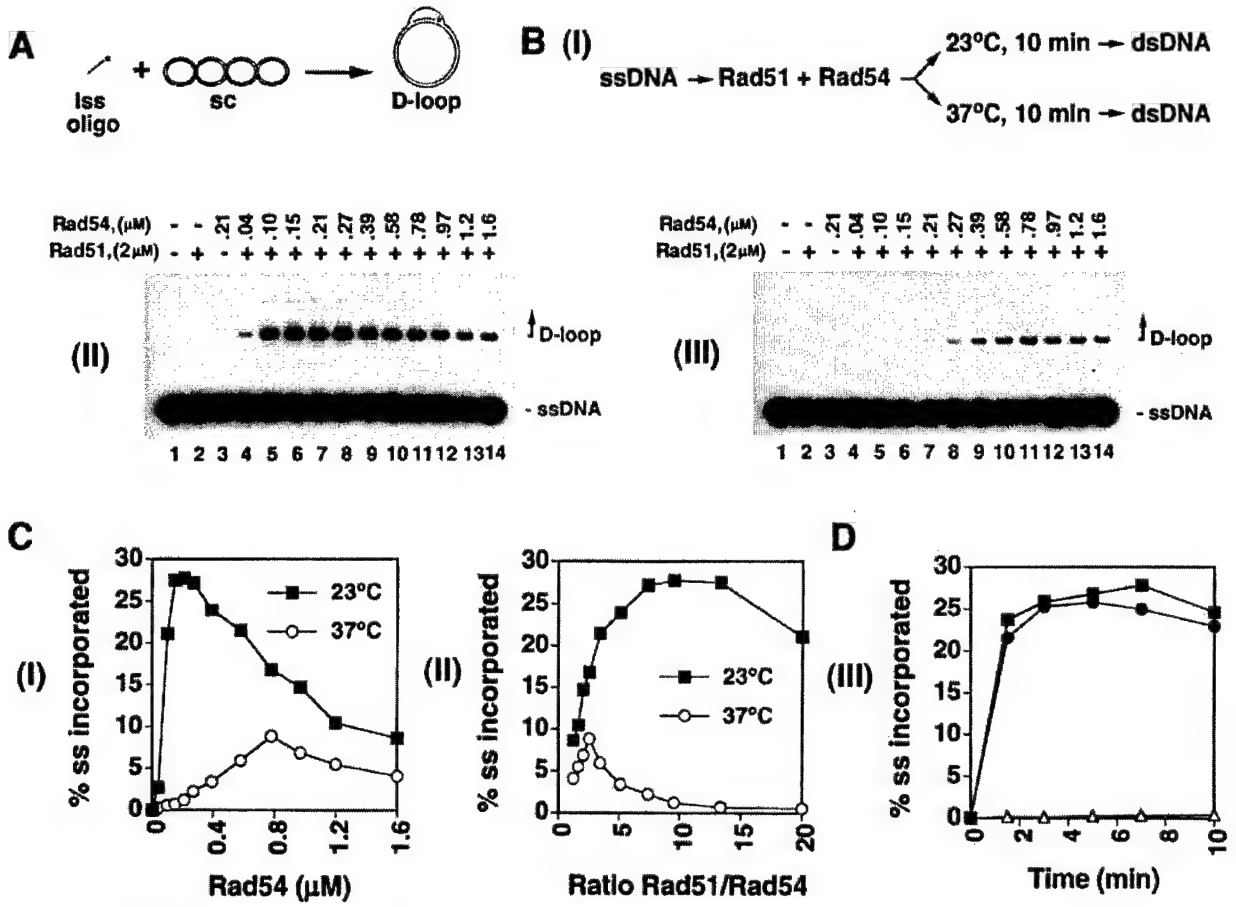

FIG. 8. **Characteristics of the D-loop reaction with an oligonucleotide as initiating substrate.** *A*, schematic of assay. A 90-mer ^{32}P-labeled oligonucleotide (*lss oligo*) is paired with its homologous supercoiled DNA target (*sc*) to yield a D-loop. *B*, *panel I*, reaction schematic. The combination of Rad51 (2 μM) and Rad54 (0.04–1.6 μM) was mixed with the 90-mer oligonucleotide (6 μM nucleotides) in the presence of ATP. The reactions were preincubated for 10 min at either 23 or 37 °C prior to the addition of target duplex. The completed reaction mixtures were incubated at 23 °C for 5 min and processed for electrophoresis in 0.9% agarose gels. *Panel II* displays the reactions in which Rad51 and Rad54 were preincubated with the 90-mer oligonucleotide at 23 °C, whereas *panel III* shows the reaction with the preincubation step done at 37 °C. *C*, the results in *panels II* (*lanes 5–14*) and *III* (*lanes 5–14*) of *B* are graphed as a function of Rad54 concentration and against the Rad51/Rad54 ratio, as shown. The level of reaction product is expressed as the percentage of the input single-stranded oligonucleotide incorporated into the D-loop structure. *D*, in one reaction (*shaded squares*), Rad51 was incubated with the 90-mer oligonucleotide for 8 min at 23 °C, followed by the addition of Rad54 and a 2-min incubation at 23 °C, before the pBluescript DNA was incorporated to complete the reaction mixture. In another reaction (*closed circle*), Rad51 and Rad54 were coincubated with the oligonucleotide for 10 min at 23 °C, and then the pBluescript DNA was incorporated to complete the reaction. In the third reaction (*open triangles*), Rad51 and Rad54 were coincubated with the oligonucleotide for 10 min at 37 °C, and then the pBluescript DNA was incorporated to complete the reaction. In all three cases, the completed reaction mixture was incubated at 23 °C, and aliquots were withdrawn at the indicated times and analyzed as described for *B*. The concentrations of reaction components were as follows: Rad51, 2 μM; Rad54, 150 nM; 90-mer oligonucleotide, 6 μM nucleotides or 67 nM oligonucleotides; pBluescript DNA, 65 μM base pairs or 22 nM plasmid molecules.

D-loop Reaction with an Oligonucleotide as Initiating Substrate—Recently, Mazin *et al.* (16) reported that maximal D-loop formation required an amount of Rad54 equivalent to that of Rad51. In this work, the D-loop reaction was carried out with an oligonucleotide as the initiating substrate (see Fig. 8*A* for schematic). In addition, a fusion of Rad54 to glutathione *S*-transferase (GST-Rad54) and a reaction temperature of 37 °C were employed (16). With our histidine-tagged Rad54 and 23 °C as the reaction temperature, even when an oligonucleotide was used (Fig. 8), optimal D-loop formation occurred at a Rad51/Rad54 ratio of ≥10 (Fig. 8, *B* (*panel II*) and *C* (*panel II*)), which is congruent with results obtained with plasmid length ssDNA (see Fig. 3). As with the plasmid length ssDNA substrate (see Fig. 3), when an oligonucleotide was used, elevating Rad54 beyond the optimal range resulted in suppression of the D-loop reaction (Fig. 8, *B* (*panel II*) and *C* (*panel I*)).

Mazin *et al.* (16) also suggested that GST-Rad54 was targeted to the site of homologous pairing by the Rad51-ssDNA nucleoprotein filament. This conclusion was drawn from experiments in which the order of addition of GST-Rad54, Rad51, and ssDNA was varied. Specifically, preincubation of GST-Rad54 with the ssDNA substrate at 37 °C for 10 min, regardless of whether Rad51 was present, resulted in a substantial drop in reaction efficiency, as compared with the addition of GST-Rad54 after the formation of the Rad51 presynaptic complex (16). We wished to reexamine this issue, since we know that Rad54 is quite unstable at 37 °C (Fig. 1), which was the reaction temperature used in the work of Mazin *et al.* (16). Importantly, when all the reaction steps were carried out at 23 °C, preincubation of Rad51, Rad54, and the oligonucleotide resulted in nearly identical levels of D-loop as when Rad54 was added to a preassembled Rad51-ssDNA nucleoprotein complex (Fig. 8*D*). In sharp contrast, preincubation of Rad51, Rad54, and the oligonucleotide at 37 °C resulted in almost complete

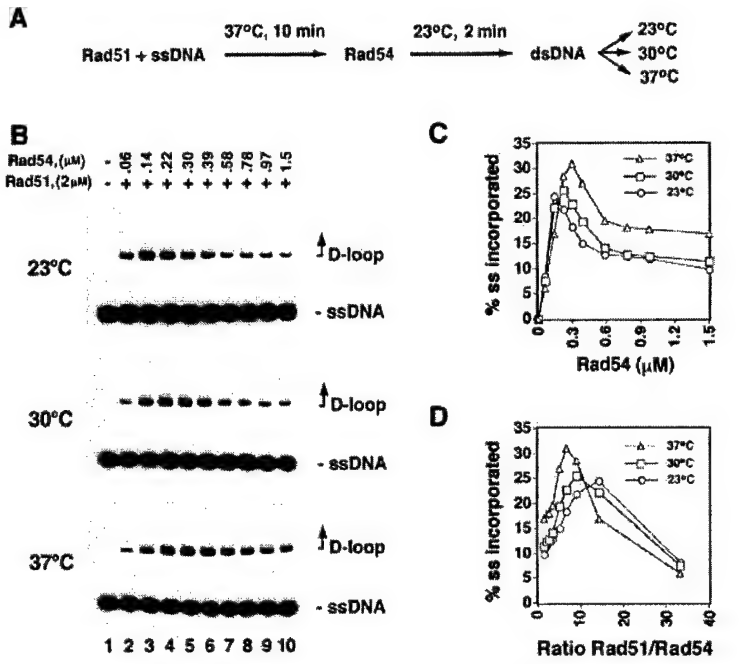

FIG. 9. **Stoichiometric relationship of Rad51/Rad54 at different reaction temperatures.** A series of D-loop reactions were set up in which Rad51 (2 μM) was incubated with the 90-mer oligonucleotide (6 μM nucleotides) for 10 min at 37 °C in the presence of ATP, followed by mixing with Rad54 (0.06–1.5 μM) and a 2-min incubation at 23 °C. At this stage, the reaction mixtures were divided into three equal portions, with each being mixed with the supercoiled DNA substrate and then continuing the incubation at 23, 30, or 37 °C for 5 min, respectively. The reaction mixtures (6 μl each) were processed for electrophoresis in 0.9% agarose gels. The reaction scheme is summarized in *A*, and the autoradiograms containing the reaction mixtures are presented in *B*. The results in *B* are shown graphically as percentage of ssDNA (*ss*) incorporated into D-loop as a function of the Rad54 concentration (*C*) and as a function of the Rad51/Rad54 molar ratio (*D*).

ablation of D-loop formation (Fig. 8, B (*panel III, lane 6*) and *D*). The lack of D-loop formation in this instance was due to thermal inactivation of Rad54, since incubating Rad51 with the ssDNA at 37 °C for 20 min before adding Rad54 and then continuing the incubation at 23 °C did not result in inhibition of the D-loop reaction (data not shown).

We have also investigated whether increasing amounts of Rad54 would at least partially compensate for the thermal denaturation of Rad54. Although some D-loop was seen with higher concentrations of Rad54 preincubated at 37 °C (Fig. 8, *B* (*panel III*) and *C* (*panel I*)), its final level was substantially lower than what was attained when the preincubation step was done at 23 °C (Fig. 8, *B* (*panel II*) and *C* (*panel I*)). Importantly, with plasmid length ssDNA, preincubation of Rad51 and Rad54 with the ssDNA at 23 °C also did not diminish the efficiency of the D-loop reaction, whereas when 37 °C was used as the preincubation temperature, a dramatic decrease in the level of D-loop was again seen (data not shown).

To further delineate the stoichiometric relationship between Rad51 and Rad54 as a function of the reaction temperature, we carried out another series of experiments in which the Rad51 presynaptic filament was preassembled at 37 °C and then mixed with Rad54 that had not previously been exposed to 37 °C, with the actual D-loop reactions being carried out at 23, 30, and 37 °C, respectively (Fig. 9). At all three reaction temperatures, maximal D-loop formation occurred at amounts of Rad54 substoichiometric to that of Rad51. Interestingly, significantly more Rad54 was needed to achieve maximal D-loop formation at 37 °C than at 23 °C; this could be due to rapid thermal denaturation of Rad54 that was offset by increasing amounts of this protein.

Taken together, the results clearly indicate that Rad54 is equally effective in homologous pairing whether it is added with Rad51 to the ssDNA or to a preformed Rad51-ssDNA nucleoprotein complex. Our results also provide evidence that the decrease in D-loop formation seen with preincubation of Rad54 with Rad51 and the ssDNA substrate as reported by Mazin *et al.* (16) was probably due to thermal inactivation of Rad54.

DISCUSSION

Stoichiometric Relationship among Rad51, Rad54, and the ssDNA Substrate—We have demonstrated that in the Rad51/Rad54/RPA-mediated homologous DNA pairing reaction that utilizes plasmid length DNA substrates, a contiguous Rad51-ssDNA filament is not needed for maximal DNA joint formation. In fact, the reaction efficiency decreases significantly when an amount of Rad51 sufficient to yield a contiguous filament is used. Equally important, our results indicate that amounts of Rad54 substantially below that of Rad51 can achieve highly robust DNA joint formation and that increasing the Rad54 concentration beyond the optimal level results in a lower reaction efficiency.

Our observation that catalytic amounts of Rad54 are sufficient for attaining the maximal rate of homologous pairing is seemingly at odds with the work of Mazin *et al.* (16), who suggested that the assembly of a 1:1 complex of Rad51 and Rad54 was required for maximal efficiency of DNA joint formation. We do not yet have a definitive answer to this discrepancy between the two studies, but it is possible that the GST-Rad54 used in the work of Mazin *et al.* behaves differently than the six histidine-tagged Rad54 employed in our work. In addition, the different purification protocols used in the two studies could have resulted in Rad54 preparations with different specific activities. Last, it remains possible that the GST-Rad54 protein is even more prone to thermal denaturation than our histidine-tagged Rad54, such that higher amounts of the GST-Rad54 fusion protein could be needed for achieving optimal homologous pairing at the reaction temperature of 37 °C. Regardless of the reason(s) for the discrepancy between the two studies, we note that in the work of Mazin *et al.* (16), significant D-loop formation was seen at levels of Rad54 severalfold below that of Rad51 (16). Together with our results reported here and elsewhere (12, 15), it seems clear that efficient homologous pairing is not contingent upon the assembly of an equimolar complex of Rad51 and Rad54.

Mazin *et al.* (16) also reported that incubation of Rad54 with the ssDNA led to a greatly diminished reaction efficiency. By contrast, we find that with both plasmid length ssDNA and an

oligonucleotide, Rad54 is just as active in the D-loop reaction whether it is added to the ssDNA or to a preassembled Rad51-ssDNA nucleoprotein complex. Furthermore, our results have provided compelling evidence that the diminished ability of Rad54 to promote homologous pairing when used in conjunction with the ssDNA substrate (16) was probably due to thermal inactivation of this protein.

Modulation of Homologous DNA Pairing Efficiency by ssDNA and RPA—RPA is known to promote Rad51 presynaptic filament assembly by effecting the removal of secondary structure in the DNA (20, 24). We have found that free ssDNA greatly diminishes the ability of a preassembled Rad51-ssDNA nucleoprotein filament to conduct the homologous DNA pairing and strand exchange reaction. Our data have shown that this strong suppressive effect of free ssDNA can be ablated by RPA. Based on the paradigm established with RecA (1, 29), we propose that free ssDNA exerts its inhibitory effect by occupying the "secondary" DNA binding site in the Rad51-ssDNA presynaptic filament and thereby excluding the homologous duplex molecule from being recognized by the presynaptic filament. Our results thus reveal a novel role of RPA, not in the removal of secondary DNA structure in the ssDNA template, but in sequestering ssDNA and preventing it from occupying the secondary DNA binding site in the Rad51-ssDNA nucleoprotein filament. In addition, RPA could effect the sequestering of Rad51 molecules at the end of the linear single strand, which would enhance the probability for the formation of a stable DNA joint with the homologous duplex.

We have also asked whether ssDNA affects Rad54 functions. At the expense of ATP hydrolysis, Rad54 tracks on duplex DNA and generates negatively and positively supercoiled domains in the DNA (14, 15). Furthermore, as a result of negative superhelical stress, the DNA strands in the duplex molecule undergo transient separation, resulting in a marked sensitivity to the single-stranded specific nuclease P1 (15). Regretfully, we have been unable to ascertain whether free ssDNA inhibits Rad54-mediated DNA supercoiling and DNA strand opening, because the *E. coli* topoisomerase I used in monitoring DNA supercoiling is completely inhibited by ssDNA, and the P1 nuclease employed in the detection of DNA strand opening digests the ssDNA competitor rapidly. However, since both DNA supercoiling and DNA strand opening by Rad54 are strictly coupled to the hydrolysis of ATP, it seems reasonable to suggest that free ssDNA would also adversely affect the ability of Rad54 to supercoil and transiently unwind duplex DNA.

A Model for DNA Strand Invasion—The available results indicate that Rad54 tracks on the incoming duplex, producing compensatory negative and positive supercoils (14, 15). The tracking motion probably enhances the rate at which the incoming duplex molecule can be sampled for homology by the presynaptic complex. The negative supercoils produced lead to transient opening of the DNA strands that is thought to facilitate the formation of the nascent DNA joint upon locating DNA homology (14, 15).

Although it can be expected that long heteroduplex joints may only occur with a contiguous Rad51 filament, our results strongly suggest that a nascent DNA joint can be made before a contiguous filament of Rad51 is assembled on the initiating ssDNA substrate. In fact, as indicated from our biochemical experiments, the assembly of a contiguous Rad51 nucleoprotein filament at the very initial stage of the recombination reaction may compromise the formation of the nascent DNA joint. We speculate that extensive interactions between the incoming duplex and the "secondary" DNA binding site within the presynaptic Rad51 filament may actually impede scanning of the duplex molecule for DNA homology and DNA supercoiling by Rad54. We envision that at a later stage of the recombination reaction, the branch migration of the nascent DNA joint to extend the region of heteroduplex DNA will probably require the assembly of a contiguous Rad51 nucleoprotein filament. The assembly of a contiguous Rad51 nucleoprotein filament is expected to depend on the mediator function of Rad52 and the Rad55-Rad57 heterodimer (4).

Our results have shown that an excess of Rad54 is inhibitory to DNA joint formation, suggesting that uncoordinated movement of the incoming duplex molecule relative to the presynaptic nucleoprotein complex may diminish the ability of the nucleoprotein complex to conduct DNA homology search and joint formation. Alternatively, or in addition, the ssDNA that results from extensive unwinding of the DNA duplex by Rad54 may inhibit DNA joint formation by compromising the functional integrity of the presynaptic protein complex through inhibition of Rad51 and Rad54 functions.

Acknowledgments—We are grateful to Lumir Krejci and Kelly Trujillo for reading the manuscript.

REFERENCES

1. Bianco, P. R., Tracy, R. B., and Kowalczykowski, S. C. (1998) *Front. Biosci.* **3,** 570–603
2. Cromie, G. A., Connelly, J. C., and Leach, D. R. (2001) *Mol. Cell* **8,** 1163–1174
3. Paques, F., and Haber, J. E. (1999) *Microbiol. Mol. Biol. Rev.* **63,** 349–404
4. Sung, P., Trujillo, K. M., and Van Komen, S. (2000) *Mutat. Res.* **451,** 257–275
5. Dasika, G. K., Lin, S. C., Zhao, S., Sung, P., Tomkinson, A., and Lee, E. Y. (1999) *Oncogene* **18,** 7883–7899
6. Moynahan, M. E., Chiu, J. W., Koller, B. H., and Jasin, M. (1999) *Mol. Cell* **4,** 511–518
7. Moynahan, M. E., Pierce, A. J., and Jasin, M. (2001) *Mol. Cell* **7,** 263–272
8. Pierce, A. J., Stark, J. M., Araujo, F. D., Moynahan, M. E., Berwick, M. B., and Jasin M. (2001) *Trends Cell Biol.* **11,** 52–59
9. Roca, A. I., and Cox, M. M. (1997) *Prog. Nucleic Acids Res. Mol. Biol.* **56,** 129–223
10. Beernink, H. T., and Morrical, S. W. (1999) *Trends Biochem. Sci.* **24,** 385–389
11. Kanaar, R., Hoeijmakers, J. H., and van Gent, D. C. (1998) *Trends Cell Biol.* **8,** 483–489
12. Petukhova, G., Stratton, S., and Sung, P. (1998) *Nature* **393,** 91–94
13. Petukhova, G., Sung, P., and Klein, H. (2000) *Genes Dev.* **14,** 2206–2215
14. Ristic, D., Wyman, C., Paulusma, C., and Kanaar, R. (2001) *Proc. Natl. Acad. Sci. U. S. A.* **98,** 8454–8460
15. Van Komen, S., Petukhova, G., Sigurdsson, S., Stratton, S., and Sung, P. (2000) *Mol. Cell* **6,** 563–572
16. Mazin, A. V., Bornarth, C. J., Solinger, J. A., Heyer, W. D., and Kowalczykowski, S. C. (2000) *Mol. Cell* **6,** 583–592
17. Sung, P. (1994) *Science* **265,** 1241–1243
18. Nakagawa, T., Flores-Rozas, H., and Kolodner, R. D. (2001) *J. Biol. Chem.* **276,** 31487–31493
19. Sung, P. (1997) *Genes Dev.* **11,** 1111–1121
20. Sugiyama, T., Zaitseva, E. M., and Kowalczykowski, S. C. (1997) *J. Biol. Chem.* **272,** 7940–7945
21. Petukhova, G., Stratton, S. A., and Sung, P. (1999) *J. Biol. Chem.* **274,** 33839–33842
22. Jiang, H., Xie, Y., Houston, P., Stemke-Hale, K., Mortensen, U. H., Rothstein, R., and Kodadek, T. (1996) *J. Biol. Chem.* **271,** 33181–33186
23. Clever, B., Interthal, H., Schmuckli-Maurer, J., King, J., Sigrist, M., and Heyer, W. D. (1997) *EMBO J.* **16,** 2535–2544
24. Sung, P., and Robberson, D. L. (1995) *Cell* **82,** 453–461
25. Zaitseva, E. M., Zaitsev, E. N., and Kowalczykowski, S. C. (1999) *J. Biol. Chem.* **274,** 2907–2915
26. Petukhova, G., Van Komen, S., Vergano, S., Klein, H., and Sung, P. (1999) *J. Biol. Chem.* **274,** 29453–29462
27. Swagemakers, S. M., Essers, J., de Wit, J., Hoeijmakers, J. H., and Kanaar, R. (1998) *J. Biol. Chem.* **273,** 28292–28297
28. Namsaraev, E. A., and Berg, P. (1997) *Mol. Cell Biol.* **17,** 5359–5368
29. Mazin, A. V., and Kowalczykowski, S. C. (1998) *EMBO J.* **17,** 1161–1168

THE JOURNAL OF BIOLOGICAL CHEMISTRY
Vol. 277, No. 45, Issue of November 8, pp. 42790–42794, 2002
Printed in U.S.A.

Homologous DNA Pairing by Human Recombination Factors Rad51 and Rad54*

Received for publication, August 6, 2002
Published, JBC Papers in Press, August 29, 2002, DOI 10.1074/jbc.M208004200

Stefan Sigurdsson‡, Stephen Van Komen§, Galina Petukhova¶, and Patrick Sung‖

From the Department of Molecular Medicine and Institute of Biotechnology, University of Texas Health Science Center, San Antonio, Texas 78254-3207

Human Rad51 (hRad51) and Rad54 proteins are key members of the *RAD52* group required for homologous recombination. We show an ability of hRad54 to promote transient separation of the strands in duplex DNA via its ATP hydrolysis-driven DNA supercoiling function. The ATPase, DNA supercoiling, and DNA strand opening activities of hRad54 are greatly stimulated through an interaction with hRad51. Importantly, we demonstrate that hRad51 and hRad54 functionally cooperate in the homologous DNA pairing reaction that forms recombination DNA intermediates. Our results should provide a biochemical model for dissecting the role of hRad51 and hRad54 in recombination reactions in human cells.

In eukaryotic organisms, the repair of DNA double-stranded breaks by homologous recombination is mediated by a group of evolutionarily conserved genes known as the *RAD52* epistasis group. Members of the *RAD52* group (*RAD51*, *RAD52*, *RAD54*, *RAD55*, *RAD57*, *RAD59*, and *RDH54/TID1*) were first uncovered in genetic screens in the budding yeast *Saccharomyces cerevisiae* (1, 2). In mammals, the efficiency of homology-directed recombinational DNA repair is modulated by the tumor suppressors BRCA1 and BRCA2 (3), providing a compelling link between this DNA repair pathway and the suppression of tumor formation. The involvement of the homologous recombination machinery in the maintenance of genome stability and tumor suppression underscores the need for deciphering the action mechanism of this machinery.

During the recombinational repair of DNA double-stranded breaks, a single-stranded DNA intermediate is utilized by the recombination machinery to invade a DNA homolog, most often the sister chromatid, to form a DNA joint molecule referred to as a D-loop (2). D-Loop formation is critical for subsequent steps in the recombination reaction, which include repair DNA synthesis and resolution of recombination intermediates (1, 2), that lead to the restoration of the integrity of the injured chromosome.

In the past several years, biochemical studies have begun to shed light on the functions of the human *RAD52* group proteins in DNA joint formation. Much of the published work has centered on the human Rad51 (hRad51)[1] protein, which is structurally related to the *Escherichia coli* recombinase enzyme RecA (4). Like RecA, hRad51 assembles into a right-handed filament on single-stranded (ss) DNA in a reaction that is dependent on ATP binding (reviewed in Ref. 5). Importantly, hRad51 protein has been shown to have DNA pairing and strand exchange activities that yield DNA joints between homologous ssDNA and double-stranded DNA substrates (6–8). The homologous pairing and strand exchange function of hRad51 is augmented by replication protein A (RPA), a heterotrimeric single-stranded DNA binding factor (6, 8), by hRad52 protein (9), and by the Rad51B-Rad51C heterodimeric complex (10), which is the functional equivalent of the yeast Rad55-Rad57 complex (11).

The *RAD54* encoded product belongs to the Swi2/Snf2 protein family (12). Purified hRad54 exhibits DNA-dependent ATPase and DNA supercoiling activities (13–15). However, the manner in which hRad54 influences the hRad51-mediated recombination reaction has remained mysterious. Here we report our biochemical studies that show functional interactions between hRad51 and hRad54 in DNA supercoiling and homologous DNA pairing reactions. We discuss how hRad51 and hRad54 cooperate to make DNA joints during recombination processes.

EXPERIMENTAL PROCEDURES

Anti-Rad54 Antibodies—The first 238 amino acid residues of the human Rad54 protein were fused to glutathione *S*-transferase in the vector pGEX-3X. The fusion protein was expressed in *E. coli* strain BL21 (DE3) and purified from inclusion bodies by preparative denaturing polyacrylamide gel electrophoresis and used as antigen for raising polyclonal antibodies in rabbits. The same antigen was covalently conjugated to cyanogen bromide-activated Sepharose 4B and used as affinity matrix to purify the antibodies from rabbit antisera, as described (16).

Rad54 Expression and Purification—A recombinant baculovirus containing the cloned *hRad54* cDNA with an added FLAG epitope at the C terminus was generated. HighFive insect cells were infected with the recombinant baculovirus at a multiplicity of infection of 10 and harvested after 48 h of incubation. An extract was prepared from 500 ml of insect cell culture (5×10^8 cells) using a French Press in 60 ml of cell breakage buffer (50 mM Tris-HCl, pH 7.5, 2 mM EDTA, 10% sucrose, 200 mM KCl, 1 mM dithiothreitol, 1 mM phenylmethylsulfonyl fluoride, and the following protease inhibitors at 3 μg/ml each: aprotinin, chymostatin, leupeptin, and pepstatin). After centrifugation (100,000 × *g* for 60 min), the clarified extract was loaded onto a Q-Sepharose column (10-ml matrix). The flow-through fraction from the Q column was fractionated in a sulfopropyl-Sepharose column (10-ml matrix) with a 50-ml, 0–700

* This work was supported in part by National Institutes of Health Grants GM57814 and CA81020. The costs of publication of this article were defrayed in part by the payment of page charges. This article must therefore be hereby marked "*advertisement*" in accordance with 18 U.S.C. Section 1734 solely to indicate this fact.

‡ Supported in part by United States Army Predoctoral Fellowship DAMD17-01-1-0412.

§ Supported in part by United States Army Predoctoral Fellowship DAMD17-01-1-0414.

¶ Supported in part by National Institutes of Health Training Grant T32AG00165. Present address: NIDDK, National Institutes of Health, Bldg. 10, Rm. 9D17, 9000 Rockville Pike, Bethesda, MD 20892.

‖ To whom correspondence should be addressed. Tel.: 210-567-7216; Fax: 210-567-7277; E-mail: sung@uthscsa.edu.

[1] The abbreviations used are: hRad51, human Rad51; yRad51, yeast Rad51; ss, single-stranded; BSA, bovine serum albumin; AMP-PNP, adenosine 5′-(β,γ-imino)triphosphate; ATPγS, adenosine 5′-3-*O*-(thio)-triphosphate.

mM KCl gradient in K buffer (20 mM KH_2PO_4 at pH 7.4, 0.5 mM EDTA, 1 mM dithiothreitol, and 10% glycerol). Fractions containing the peak of hRad54 were pooled and loaded onto a 1-ml Macro-hydroxyapatite (Bio-Rad) column, which was eluted with 30 ml of 0–300 mM KH_2PO_4 in K buffer. The peak fractions were pooled and mixed with 1.5 ml of Anti-FLAG M2 agarose (Sigma) and rocked for 3 h at 4 °C. The FLAG agarose was washed three times with 3 ml of 150 mM KCl in buffer K before eluting hRad54 using the same buffer containing 1 mg/ml of the FLAG peptide (Sigma). hRad54 (~1 mg) eluted from the FLAG matrix was concentrated in a Centricon-30 microconcentrator to 5 mg/ml and stored in small aliquots at −70 °C.

Rad51 and hrad51 K133R Proteins—The hRad51 protein was expressed in the *E. coli* RecA-deficient strain BLR (DE3) and purified to near homogeneity using our previously described procedure (8). The hrad51 K133R mutant was expressed and purified to near homogeneity in exactly the same way.

Topoisomerase I—*E. coli* topoisomerase I was purified to near homogeneity from the *E. coli* strain JM101 with plasmid pJW312-sal containing the *topA* gene under the Lac promoter, as described (17).

Binding of hRad54 to Affi-hRad51 Beads—Purified hRad51 and bovine serum albumin (BSA) were coupled to Affi-Gel 15 beads at 4 °C following the instructions of the manufacturer (Bio-Rad). The resulting matrices contained 4 and 12 mg/ml hRad51 and BSA, respectively. Purified hRad54 (1.2 μg) was mixed with 5 μl of Affi-Rad51 or Affi-BSA at 4 °C for 30 min in 30 μl of buffer containing 100 mM KCl and 0.1% Triton X-100 by constant tapping. The beads were washed twice with 50 μl of the same buffer before being treated with 30 μl of 2% SDS at 37 °C for 5 min to elute the bound hRad54. The various fractions (4 μl each) were analyzed by immunoblotting to determine their content of hRad54.

DNA Substrates—Topologically relaxed φX174 DNA was prepared as described (18), and pBluescript SK DNA was made in *E. coli* DH5α and purified as described (19). The oligonucleotide used in the D-loop reaction is complementary to positions 1932–2022 of the pBluescript SK DNA and had the sequence 5′-AAATCAATCTAAAGTATATATGAGTAAACTTGGTCTGACAGTTACCAATGCTTAATCAGTGAGGCACCTATCTCAGCGATCTGTCTATTT-3′. This oligonucleotide was 5′ end-labeled with [γ-^{32}P]ATP and T4 polynucleotide kinase.

ATPase Assay—The hRad54 protein (60 nM) was incubated with replicative form I φX174 DNA (30 μM base pairs) and 1.5 mM [γ-^{32}P]ATP with or without 400 nM hRad51 or yRad51 in 10 μl of reaction buffer (20 mM Tris-HCl, pH 7.4, 25 mM KCl, 1 mM dithiothreitol, 4 mM $MgCl_2$, 100 μg/ml BSA) at 30 °C for the indicated times. The level of ATP hydrolysis was determined by thin layer chromatography, as described (19).

DNA Supercoiling and DNA Strand-opening Reactions—Increasing amounts of hRad54 were incubated with 80 ng of relaxed φX174 DNA (12 μM nucleotides) for 2 min at 23 °C in 12 μl of reaction buffer (20 mM Tris-HCl, pH 7.4, 5 mM $MgCl_2$, 1 mM dithiothreitol, 100 μM ATP, and an ATP-regenerating system consisting of 10 mM creatine phosphatase and 28 μg/ml creatine kinase). Following the addition of 100 ng of *E. coli* topoisomerase I in 0.5 μl, the reactions were incubated for 10 min at 23 °C and then deproteinized by treatment with 0.5% SDS and proteinase K (0.5 mg/ml) for 10 min at 37 °C. Samples were run on 1% agarose gels in TAE buffer (35 mM Tris acetate, pH 7.4, 0.5 mM EDTA) at 23 °C and then stained with ethidium bromide. In the experiment in Fig. 4*B*, the relaxed DNA was incubated with the indicated amounts of hRad51 and hRad54 for 2 min at 23 °C, followed by the addition of topoisomerase and a 10-min incubation at 23 °C. For the P1 sensitivity experiments in Figs. 3*C* and 4*C*, the reactions were assembled in the same manner except that 0.4 unit of P1 nuclease (Roche) was used instead of topoisomerase. The DNA species were resolved in a 1% agarose gel containing 10 μM ethidium bromide in TAE buffer.

D-Loop Reaction—For the time course reactions (25 μl, final volume) in Fig. 5, hRad51 or hrad51 K133R (800 nM) was incubated with the 5′-labeled ss oligonucleotide (2.5 μM nucleotides) for 3 min at 37 °C in 22 μl of reaction buffer (20 mM Tris-HCl, pH 7.4, 100 μg/ml BSA, 1.5 mM $MgCl_2$, 2 mM ATP, and the ATP-generating system described above). This was followed by the addition of hRad54 (120 nM) in 1 μl and incubation at 23 °C for 2 min. The reaction was completed by adding the pBluescript SK replicative form DNA (35 μM base pairs) in 2 μl. The reaction mixture was incubated at 30 °C, and 3.8-μl aliquots were withdrawn at the indicated times, deproteinized, and run in 1% agarose gels in TAE buffer. The gels were dried and the levels of D-loop were quantified by phosphorimage analysis. The reactions in which ATP, hRad51, or hRad54 was omitted or ATP was replaced by ATPγS or AMP-PNP were scaled down 2-fold to a 12.5-μl final volume, but they were otherwise assembled and processed in exactly the same manner.

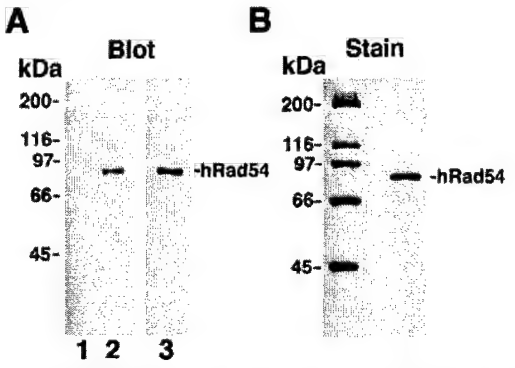

FIG. 1. **Purification of hRad54.** *A*, expression of hRad54 in insect cells. Extracts from uninfected insect cells (*lane 1*) and from insect cells infected with the recombinant hRad54 baculovirus (*lane 2*) were probed with affinity-purified anti-hRad54 antibodies. In *lane 3*, 100 ng of purified hRad54 was also subjected to immunoblotting. *B*, purified hRad54 protein (1 μg) was run in an 8% denaturing polyacrylamide gel and stained with Coomassie Blue.

RESULTS

Human Recombination Factors—Human Rad51 was expressed in a recA-*E. coli* strain and purified to near homogeneity as described previously (8). The hrad51 K133R mutant, which harbors the change of the conserved lysine residue in the Walker type A nucleotide binding motif to arginine, was also similarly expressed and purified. In agreement with previously published results (20), hrad51 K133R has negligible ATPase activity compared with wild type hRad51 (data not shown). We cloned the human *RAD54* cDNA from a testis cDNA library using the polymerase chain reaction. The entire cloned *hRAD54* cDNA was sequenced to ensure that it agreed with the published sequence (21). We tagged hRad54 protein with a FLAG epitope at the carboxyl terminus and expressed it in insect cells by the use of a recombinant baculovirus (Fig. 1*A*). We obtained ~1 mg of nearly homogeneous hRad54 (Fig. 1*B*) from 500 ml of insect cell culture by a combination of conventional column chromatography and affinity binding to an antibody specific for the FLAG epitope. The purified hRad54 has a level of DNA-dependent ATPase very similar to that described in the literature (13) (see later).

hRad54 Physically Interacts with hRad51—Golub *et al.* (22) found that the amino terminus of hRad54 can bind hRad51 in *in vitro* analyses and also in the yeast two-hybrid system. However, in mouse embryonic stem cells, association of mRad51 and mRad54 requires prior treatment of cells with a DNA damaging agent (14). To examine whether purified hRad54 physically interacts with hRad51, we coupled hRad51 to Affi-Gel beads to use as affinity matrix for binding hRad54. As shown in Fig. 2, purified hRad54 was efficiently retained on Affi-hRad51 beads but not on Affi-beads that contained BSA. When a less purified hRad54 fraction (~25% hRad54) was used, hRad54, but not the contaminating protein species, bound to the Affi-hRad51 beads (data not shown). The results thus indicate a direct and specific interaction between hRad51 and hRad54.

DNA Supercoiling and DNA Strand Opening by hRad54—Tan *et al.* (14) showed an ability of hRad54 to alter the DNA linking number of a nicked plasmid in the presence of DNA ligase. The induction of DNA linking number change was dependent on ATP hydrolysis by hRad54 (14). The same group also used scanning force microscopy to provide evidence that hRad54 tracks on DNA when ATP is hydrolyzed (15). A schematic depicting the basis for tracking-induced DNA supercoiling by hRad54 is given in Fig. 3*A*.

The yRad54 protein also tracks on DNA and, as a result,

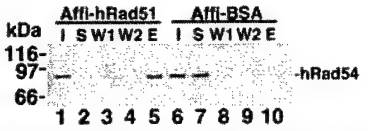

FIG. 2. **hRad54 interacts with hRad51.** Purified hRad54 (1.2 μg) was mixed with Affi-beads containing either BSA (Affi-BSA) or hRad51 (Affi-Rad51) in 30 μl and washed twice with 50 μl buffer, followed by treatment of the beads with 30 μl of SDS to elute bound hRad54. The starting material (*I*), supernatant (*S*), the two washes (*W1* and *W2*), and the SDS eluate (*E*), 4 μl each, were subjected to immunoblotting to determine their hRad54 content.

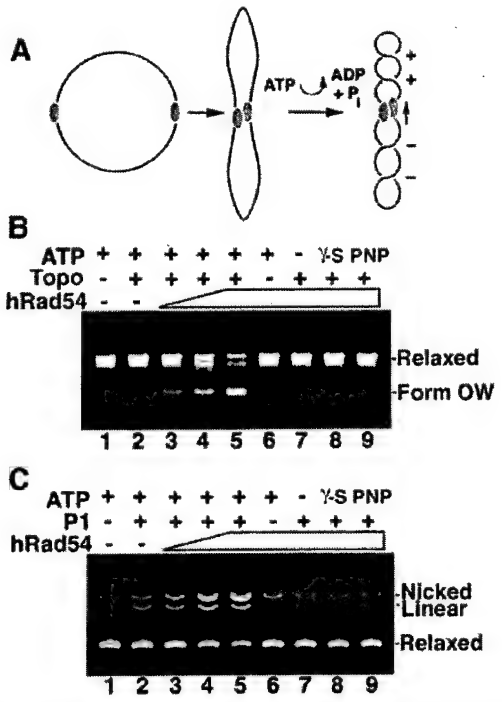

FIG. 3. **hRad54 supercoils DNA and promotes DNA strand opening.** *A*, basis for hRad54-induced supercoiling, as per Ristic *et al.* (15) and Van Komen *et al.* (18). The free energy from ATP hydrolysis fuels the tracking of a hRad54 oligomer on DNA, producing a positively supercoiled domain ahead of protein movement and a negatively supercoiled domain behind. *B*, increasing amounts of hRad54 (200, 400, and 750 nM in *lanes 3–5*, respectively) were incubated with topologically relaxed DNA (20 μM nucleotides) and *E. coli* topoisomerase I in buffer that contained ATP. The highest amount of hRad54 (750 nM) was also incubated with the DNA substrate in the absence of topoisomerase (*lane 6*) and in the presence of topoisomerase but with the omission of ATP (*lane 7*) or the substitution of ATP by ATPγS (γ-*S*; *lane 8*) and AMP-PNP (*PNP*; *lane 9*). DNA alone (*lane 1*) or DNA incubated with topoisomerase (*lane 2*) was also included. The reaction mixtures were run in a 1% agarose gel, which was treated with ethidium bromide to reveal the DNA species. *C*, increasing amounts of hRad54 (200, 400, and 750 nM in *lanes 3–5*, respectively) were incubated with topologically relaxed DNA (20 μM nucleotides) and P1 nuclease in buffer that contained ATP. The highest amount of hRad54 (750 nM) was also incubated with the DNA substrate in the absence of P1 (*lane 6*) and in the presence of P1 but with the omission of ATP (*lane 7*) or the substitution of ATP by ATPγS (γ-*S*; *lane 8*) and AMP-PNP (*PNP*; *lane 9*). DNA alone (*lane 1*) and DNA incubated with P1 in the absence of hRad54 (*lane 2*) were also included. The reaction mixtures were run in a 1% agarose gel containing 10 μM ethidium bromide.

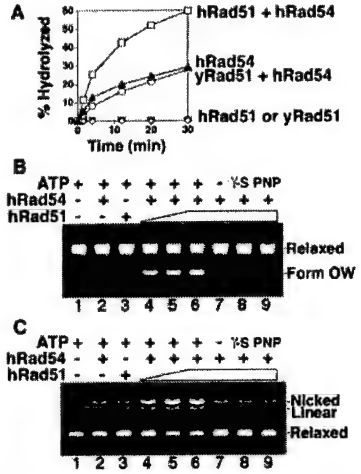

FIG. 4. **The hRad54 activities are stimulated by hRad51.** *A*, hRad54 was incubated with ϕX replicative form I DNA (30 μM nucleotides) and 1.5 mM [γ-^{32}P]ATP for the indicated times, and the level of ATP hydrolysis was quantified by thin layer chromatography. ATPase activity was also measured for hRad51 alone, yRad51 alone, and the combinations of hRad54/hRad51 and hRad54/yRad51. The protein concentrations were as follows: hRad54, 60 nM; hRad51, 400 nM; yRad51, 400 nM. In every case, negligible ATP hydrolysis was seen when DNA was omitted (data not shown). *B*, relaxed DNA (20 μM nucleotides) was incubated with hRad54 (75 nM in *lanes 2* and *4–9*) and hRad51 (80, 160, and 240 nM in *lanes 4–6*, respectively) in the presence of ATP and *E. coli* topoisomerase I. The highest amount of hRad51 (240 nM) was incubated with substrate and topoisomerase I but without hRad54 (*lane 3*) and also with hRad54 (75 nM) but with the omission of ATP (*lane 7*) or its substitution with ATPγS (γ-*S*; *lane 8*) or AMP-PNP (*PNP*; *lane 9*). DNA alone was analyzed in *lane 1*. After deproteinization, the reaction mixtures were run in a 1% agarose gel, which was treated with ethidium bromide to stain the DNA species. *C*, relaxed DNA was incubated with hRad54 (75 nM in *lanes 2* and *4–9*) and hRad51 (80, 160, and 240 nM in *lanes 4–6*, respectively) in the presence of ATP and P1 nuclease. The highest amount of hRad51 (240 nM) was incubated with substrate and P1 but without hRad54 (*lane 3*) and also with hRad54 (75 nM) but with the omission of ATP (*lane 7*) or its substitution with ATPγS (γ-*S*; *lane 8*) or AMP-PNP (*PNP*; *lane 9*). DNA alone was run in *lane 1*. Analysis was carried out in a 1% agarose gel that contained 10 μM ethidium bromide.

generates positive and negative supercoils in the DNA substrate. Removal of the negative supercoils by treatment with *E. coli* topoisomerase I leads to the accumulation of positive supercoils and the formation of an overwound DNA species called Form OW (18). Here we used the same strategy to examine the ability of hRad54 to supercoil DNA. As shown in Fig. 3*B*, in the presence of topoisomerase, purified hRad54 protein readily induces a linking number change in the DNA (18). The DNA supercoiling reaction is dependent on ATP hydrolysis, as revealed by its omission or substitution with a nonhydrolyzable analogue (ATPγS or AMP-PNP) (Fig. 3*B*).

We asked whether the negative supercoils generated as a result of hRad54 tracking on the DNA substrate (15) (Fig. 3, *A* and *B*) leads to transient DNA strand opening by examining the sensitivity of a relaxed DNA template to the single-strand specific nuclease P1, as per Van Komen *et al.* (18). Fig. 3*C* shows that incubation of topologically relaxed DNA with hRad54 rendered the relaxed DNA substrate sensitive to P1 nuclease, as indicated by the accumulation of nicked circular and linear DNA forms. The DNA strand opening reaction is also completely dependent on ATP hydrolysis (Fig. 3*C*).

Activities of hRad54 Are Stimulated by hRad51—The results presented here (Fig. 2) and elsewhere (22) have unveiled a specific interaction between hRad51 and hRad54. We examined whether the hRad54 ATPase would be enhanced upon interaction with hRad51. As shown in Fig. 4*A*, a much higher rate of ATP hydrolysis was seen when hRad54 was combined with hRad51. The fact that yRad51 was ineffective in this reaction (Fig. 4*A*) indicates that the action of hRad51 is specific. Although hRad51 is known to have a weak ATPase activity (23), the fact that the hrad51 K133R mutant protein, which binds but does not hydrolyze ATP (20), was just as effective in

promoting ATP hydrolysis (data not shown) strongly indicated that the increase in ATP hydrolysis was because of enhancement of the hRad54 ATPase function.

We next asked whether the DNA supercoiling activity of hRad54 would also be up-regulated by hRad51. The results showed that hRad51 stimulates the supercoiling reaction, as indicated by a much higher level of Form OW DNA (Fig. 4*B*). Because negative supercoiling generated by hRad54 leads to DNA strand opening (Fig. 3*C*), we thought that hRad51 might also promote this activity. Indeed, the inclusion of hRad51 greatly elevated the nicking of the relaxed DNA substrate by P1 nuclease (Fig. 4*C*). Even with the inclusion of hRad51, no Form OW DNA or nicking of DNA was seen when ATP was omitted or substituted by the nonhydrolyzable analogues ATPγS and AMP-PNP (Fig. 4, *B* and *C*). Thus, the results revealed that hRad51 markedly stimulates the ability of Rad54 to supercoil DNA and unwind DNA strands. The hrad51 K133R protein was just as effective as wild type hRad51 in enhancing the DNA supercoiling and strand opening activities of hRad54 (data not shown). Furthermore, we found that yRad51 does not stimulate the hRad54 activities (data not shown), thus indicating a high degree of specificity in the hRad51 action.

hRad51 and hRad54 Cooperate in Homologous DNA Pairing—The RecA/Rad51 class of general recombinases is central to recombination processes by virtue of their ability to catalyze the homologous DNA pairing reaction that yields heteroduplex DNA joints (2, 24). Because hRad51 and hRad54 physically interact (22) (Fig. 2) and hRad51 enhances the various activities of hRad54 (Fig. 4), it was of considerable interest to examine the influence of hRad54 on hRad51-mediated homologous DNA pairing.

The homologous pairing assay monitors the incorporation of a ^{32}P-labeled single-stranded oligonucleotide into a homologous supercoiled target (pBluescript) to give a D-loop structure (Fig. 5*A*). As reported before (25) and reiterated here (Fig. 5*B*), hRad51 by itself is not particularly adept at forming D-loop. Importantly, the inclusion of hRad54 rendered D-loop formation possible. D-Loop formation by the combination of hRad51 and hRad54 requires ATP hydrolysis, because no D-loop was seen when ATP was omitted or when it was replaced by either ATPγS or AMP-PNP (Fig. 5*B*). Significantly, the time course revealed a cycle of rapid formation and disruption of D-loop, such that the D-loop level reached its maximum by 1 min but declined rapidly thereafter (Fig. 5, *B* and *D*). In fact, by the reaction end point of 6 min, little or no D-loop remained (Fig. 5, *B* and *D*). Such a cycle of D-loop synthesis and reversal seems to be a general characteristic for the RecA/Rad51 class of recombinases (26, 27). Because the RecA-ssDNA nucleoprotein filament disassembles upon ATP hydrolysis (24), we considered the possibility that the dissociation of D-loop seen here (Fig. 5*B*) could be related to ATP hydrolysis-mediated turnover of hRad51. To test this premise, we used the hrad51 K133R mutant protein, which binds but does not hydrolyze ATP (20), with hRad54 in the D-loop assay. True to prediction, with hrad51 K133R, the D-loop amount increased with time, reaching a much higher final level than when hRad51 was used (Fig. 5, *B–D*); by 4 min, 23% of the input ssDNA or 55% of the pBluescript plasmid DNA had been incorporated into the D-loop structure. As expected, with both hRad51/hRad54 and hrad51 K133R/hRad54, formation of D-loop required both the 90-mer substrate and the pBluescript target, and substitution of the pBluescript DNA with the heterologous ϕX174 DNA completely abolished D-loop formation (data not shown).

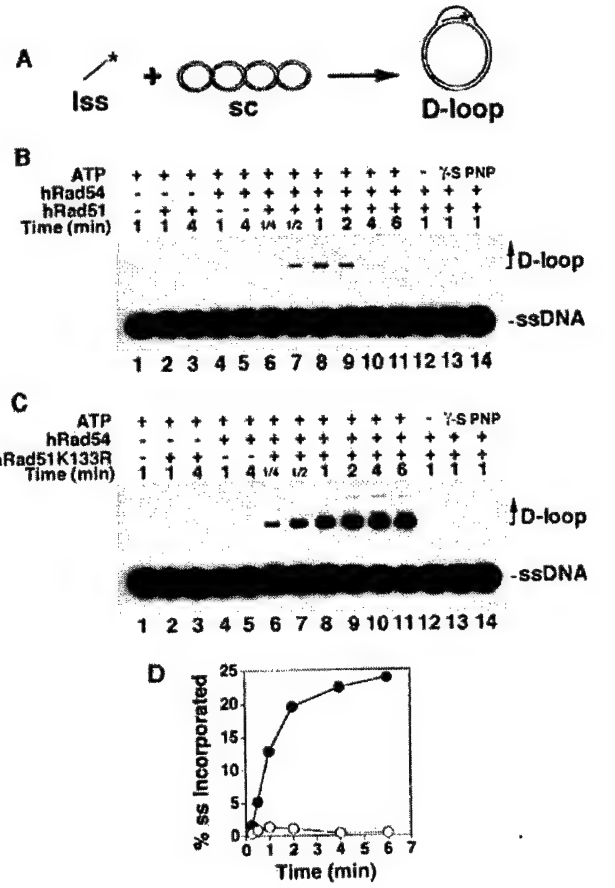

FIG. 5. **D-Loop formation by hRad51 and hRad54.** *A*, schematic of assay. A radiolabeled 90-mer DNA pairs with a homologous duplex target to yield a D-loop. *B*, hRad51 alone (*lanes 2* and *3*), hRad54 alone (*lanes 4* and *5*), and the combination of hRad51 and hRad54 (*lanes 6–14*) were incubated at 30 °C for the indicated times with the DNA substrates in the presence of ATP (*lanes 2–11*), ATPγS (*γS*; *lane 13*), or AMP-PNP (*PNP*; *lane 14*) or in the absence of nucleotide (*lane 12*). In *lane 1*, the DNA substrates were incubated in buffer without protein. The protein and DNA concentrations were as follows: hRad51, 800 nM; hRad54, 120 nM; 90-mer oligonucleotide, 2.5 μM nucleotides or 27.7 nM oligonucleotide; pBluescript supercoiled DNA, 35 μM base pairs or 11.6 nM plasmid. *C*, the homologous pairing activity of hrad51 K133R was examined with hRad54 as described for hRad51 above. *D*, the results in *lanes 6–11* of *B* (○) and *C* (●) were graphed.

DISCUSSION

It has been deduced from biochemical and scanning force microscopy analyses that Rad54 tracks on DNA, producing positive supercoils ahead of the protein movement and negative supercoils tailing it (15, 18). As a result of interaction with hRad51, the ATPase, DNA supercoiling, and DNA strand opening activities of Rad54 are greatly enhanced (this work). Petukhova *et al.* (19) first reported that yRad54 enhances homologous DNA pairing by yRad51. Here we have presented biochemical evidence that hRad51 and hRad54 also work in concert to make DNA joints. Interestingly, the hRad51/hRad54-mediated D-loop reaction undergoes a rapid cycle of joint formation and dissociation. We have speculated that ATP hydrolysis by hRad51 could have resulted in its turnover from the bound ssDNA. This might have led to the transfer of hRad51/hRad54 to the displaced strand in the D-loop to initiate a second round of homologous pairing with the newly formed DNA joint. The presumed secondary pairing reaction could have accounted for the dissociation of the initial D-loop. Consistent with this hypothesis, the ATP hydrolysis-defective hrad51 K133R mutant is much more adept at forming D-loop than the wild type protein. Previously, studies in yeast and chicken DT40 cells with the same Rad51 ATPase mutant have

shown that it is biologically active but that an increased level of this mutant is needed for full complementation of the various phenotypes of Rad51-deficient cells (20, 28). The fact that the hrad51 K133R mutant is even more effective than the wild type protein in the D-loop reaction strongly suggests that the slighted biological efficacy (20, 28) and observed dominance (29) of this protein are because of a reason other than a diminished ability to mediate homologous pairing. The hrad51 K133R mutant may form a highly stable complex with DNA, thus reducing the effective concentration of free protein available for recombination reactions. Importantly, our biochemical results predict that other members of the *RAD52* group may function to prevent reversal of the D-loop reaction catalyzed by hRad51/hRad54.

Inactivation of the hRad54 ATPase activity impairs the ability to carry out recombination *in vivo* (14), consistent with the premise that the ATP hydrolysis-dependent DNA supercoiling and DNA strand opening activities of hRad54 are germane for recombination. As discussed here and elsewhere (15, 18, 30), it is likely that the DNA strand opening activity of hRad54 promotes the acquisition of an unwound DNA structure conducive for the formation of the nascent DNA joint that links recombining chromosomes. The ability of hRad54 to pull the incoming duplex molecule through its fold (*i.e.* tracking) is also expected to enhance the rate at which the duplex can be sampled by the hRad51-ssDNA nucleoprotein filament for homology. Finally, it remains a distinct possibility that the dynamic DNA topological changes induced by the combination of hRad51 and hRad54 are critical for the remodeling of chromatin during recombination.

Acknowledgment—We thank Toshiyuki Habu for helping with plasmid constructions.

REFERENCES

1. Paques, F., and Haber, J. E. (1999) *Microbiol. Mol. Biol. Rev.* **63,** 349–404
2. Sung, P., Trujillo, K., and Van Komen, S. (2000) *Mutat. Res.* **451,** 257–275
3. Pierce, A. J., Stark, J. M., Araujo, F. D., Moynahan, M. E., Berwick, M., and Jasin, M. (2001) *Trends Cell Biol.* **11,** S52–59
4. Shinohara, A., Ogawa, H., Matsuda, Y., Ushio, N., Ikeo, K., and Ogawa, T. (1993) *Nat. Genet.* **4,** 239–243
5. Yu, X., Jacobs, S. A., West, S. C., Ogawa, T., and Egelman, E. H. (2001) *Proc. Natl. Acad. Sci. U. S. A.* **17,** 8419–8424
6. Baumann, P., Benson, F. E., and West, S. C. (1996) *Cell* **87,** 757–766
7. Gupta, R. C., Bazemore, L. R., Golub, E. I., and Radding, C. M. (1997) *Proc. Natl. Acad. Sci. U. S. A.* **94,** 463–468
8. Sigurdsson, S., Trujillo, K., Song, B.-W., Stratton, S., and Sung P. (2001) *J. Biol. Chem.* **276,** 8798–8806
9. Benson, F. E., Baumann, P., and West, S. C. (1998) *Nature* **391,** 401–404
10. Sigurdsson, S., Van Komen, S., Bussen, W., Schild, D., Albala, J. S., and Sung, P. (2001) *Genes Dev.* **15,** 3308–3318
11. Sung, P. (1997) *Genes Dev.* **11,** 1111–1121
12. Eisen, J. A., Sweder, K. S., and Hanawalt, P. C. (1995) *Nucleic Acids Res.* **23,** 2715–2723
13. Swagemakers, S. M. A., Essers, J., de Wit, J., Hoeijmakers, J. H. J., and Kanaar, R. (1998) *J. Biol. Chem.* **273,** 28292–28297
14. Tan, T. L., Essers, J., Citterio, E., Swagemakers, S. M., de Wit, J., Benson, F. E., Hoeijmakers, J. H., and Kanaar, R. (1999) *Curr. Biol.* **9,** 325–328
15. Ristic, D., Wyman, C., Paulusma, C., and Kanaar, R. (2001) *Proc. Natl. Acad. Sci. U. S. A.* **84,** 8454–8460
16. Sung, P., Prakash, L., Matson, S. W., and Prakash, S. (1987) *Proc. Natl. Acad. Sci. U. S. A.* **84,** 8951–8955
17. Lynn, R. M., and Wang, J. C. (1989) *Proteins* **6,** 231–239
18. Van Komen, S., Petukhova, G., Sigurdsson, S., Stratton, S., and Sung, P. (2000) *Mol. Cell* **6,** 563–572
19. Petukhova, G., Stratton, S., and Sung, P. (1998) *Nature* **393,** 91–94
20. Morrison, C., Shinohara, A., Sonoda, E., Yamaguchi-Iwai, Y., Takata, M., Weichselbaum, R. R., and Takeda, S. (1999) *Mol. Cell. Biol.* **19,** 6891–6897
21. Kanaar, R., Troelstra, C., Swagemakers, S. M., Essers, J., Smit, B., Franssen, J. H., Pastink, A., Bezzubova, O. Y., Buerstedde, J. M., Clever, B., Heyer, W. D., and Hoeijmakers, J. H. (1996) *Curr. Biol.* **6,** 828–838
22. Golub, E. I., Kovalenko, O. V., Gupta, R. C., Ward, D. C., and Radding, C. M. (1997) *Nucleic Acids Res.* **25,** 4106–4110
23. Benson, F. E., Stasiak, A., and West, S. C. (1994) *EMBO J.* **13,** 5764–5771
24. Bianco, P. R., Tracy, R. B., and Kowalczykowski, S. C. (1998) *Front. Biosci.* **3,** D580–603
25. Mazin, A. V., Zaitseva, E., Sung, P., and Kowalczykowski, S. C. (2000) *EMBO J.* **19,** 1148–1156
26. Shibata, T., Ohtani, T., Iwabuchi, M., and Ando, T. (1982) *J. Biol. Chem.* **10,** 13981–13986
27. Mcllwraith, M. J., Van Dyck, E., Masson, J. Y., Stasiak, A. Z., Stasiak, A., and West, S. C. (2000) *J. Mol. Biol.* **304,** 151–164
28. Sung, P., and Stratton, S. A. (1996) *J. Biol. Chem.* **271,** 27983–27986
29. Stark, J. M., Hu, P., Pierce, A. J., Moynahan, M. E., Ellis, N., and Jasin, M. (2002) *J. Biol. Chem.* **277,** 20185–20194
30. Mazin, A. V., Bornarth, C. J., Solinger, J. A., Heyer, W. D., and Kowalczykowski, S. C. (2000) *Mol. Cell* **6,** 583–592

THE JOURNAL OF BIOLOGICAL CHEMISTRY
Vol. 278, No. 11, Issue of March 14, pp. 9212–9218, 2003
Printed in U.S.A.

Rad54p Is a Chromatin Remodeling Enzyme Required for Heteroduplex DNA Joint Formation with Chromatin*

Received for publication, November 12, 2002, and in revised form, January 2, 2003
Published, JBC Papers in Press, January 3, 2003, DOI 10.1074/jbc.M211545200

Mariela Jaskelioff‡§¶, Stephen Van Komen§‖, Jocelyn E. Krebs‡ ‡‡, Patrick Sung‖, and Craig L. Peterson‡§§**

From the ‡Interdisciplinary Graduate Program and Program in Molecular Medicine, University of Massachusetts Medical School, Worcester, Massachusetts 01605, and ‖Department of Molecular Medicine and Institute of Biotechnology, University of Texas Health Science Center at San Antonio, San Antonio, Texas 78245-3207

In eukaryotic cells, the repair of DNA double-strand breaks by homologous recombination requires a RecA-like recombinase, Rad51p, and a Swi2p/Snf2p-like ATPase, Rad54p. Here we find that yeast Rad51p and Rad54p support robust homologous pairing between single-stranded DNA and a chromatin donor. In contrast, bacterial RecA is incapable of catalyzing homologous pairing with a chromatin donor. We also show that Rad54p possesses many of the biochemical properties of *bona fide* ATP-dependent chromatin-remodeling enzymes, such as ySWI/SNF. Rad54p can enhance the accessibility of DNA within nucleosomal arrays, but it does not seem to disrupt nucleosome positioning. Taken together, our results indicate that Rad54p is a chromatin-remodeling enzyme that promotes homologous DNA pairing events within the context of chromatin.

Chromosomal DNA double-strand breaks (DSBs)[1] arise through exposure of cells to harmful environmental agents such as ionizing radiation or mutagenic chemicals (radiomimetics, alkylating agents, etc.). DSBs can also be caused by endogenously produced oxygen radicals, by errors in DNA replication, or as obligatory intermediates during programmed cellular processes, such as meiosis or V(D)J recombination (1–3). Cell survival and maintenance of genome integrity depend on efficient repair of DSBs, because unrepaired or misrepaired DSBs may lead to mutations, gene translocations, gross chromosomal rearrangements, or cellular lethality.

Several pathways for repairing DSBs have evolved and are highly conserved throughout eukaryotes. Homologous recombination (HR) is a major pathway of DSB repair in all eukaryotes and has a distinct advantage over other mechanisms in that it is mostly error-free. In organisms ranging from yeast to human, HR is mediated by members of the *RAD52* epistasis group (*RAD50*, *RAD51*, *RAD52*, *RAD54*, *RAD55*, *RAD57*, *RAD59*, *MRE11*, and *XRS2*). Accordingly, mutations in any one of these genes result in sensitivity to ionizing radiation and other DSB-inducing agents (2). The importance of the HR pathway in maintaining genome integrity is underscored by the fact that mutations in each one of its critical factors have been correlated with chromosomal instability-related ailments, including ataxia telangiectasia-like disease, Nijmegen breakage syndrome, Li Fraumeni syndrome, as well as various forms of cancer (4).

In vivo and *in vitro* studies have suggested the following sequence of molecular events that lead to the recombinational repair of a DSB. First, the 5′ ends of DNA that flank the break are resected by an exonuclease to create ssDNA tails (5). Next, Rad51p polymerizes onto these DNA tails to form a nucleoprotein filament that has the capability to search for a homologous duplex DNA molecule. After DNA homology has been located, the Rad51-ssDNA nucleoprotein filament catalyzes the formation of a heteroduplex DNA joint with the homolog. The process of DNA homology search and DNA joint molecule formation is called "homologous DNA pairing and strand exchange." Subsequent steps entail DNA synthesis to replace the missing information followed by resolution of DNA intermediates to yield two intact duplex DNA molecules (6).

The homologous DNA pairing activity of Rad51p is enhanced by Rad54p (7). Rad54p is a member of the Swi2p/Snf2p protein family (8) that has DNA-stimulated ATPase activity and physically interacts with Rad51p (7, 9, 10). Because of its relatedness to the Swi2p/Snf2p family of ATPases, Rad54p may have chromatin remodeling activities in addition to its established role in facilitating Rad51p-mediated homologous pairing reactions. In this study we show that Rad51p and Rad54p mediate robust D-loop formation with a chromatin donor, whereas the bacterial recombinase, RecA, can only function with naked DNA. Furthermore, we find that the ATPase activity of Rad54p is essential for D-loop formation on chromatin and that Rad54p can use the free energy from ATP hydrolysis to enhance the accessibility of nucleosomal DNA. Experiments are also presented to suggest that chromatin remodeling by Rad54p and yeast SWI/SNF involves DNA translocation.

EXPERIMENTAL PROCEDURES

DNA—All DNA manipulations were carried out using standard methods (11). Oligonucleotides were obtained from Operon Technologies (Alameda, CA). Plasmid pXG540 and T4 EndonucleaseVII used in the cruciform extrusion experiments were a kind gift of Dr. T. Owen-Hughes.

The oligonucleotide used for triplex formation was TFO (triplex-forming oligonucleotide) (5′-TTCTTTTCTTTCTTCTTTCTTT-3′). To

* This work was supported by grants from the National Institutes of Health to C. L. P. (GM49650) and P. S. (GM57814). The costs of publication of this article were defrayed in part by the payment of page charges. This article must therefore be hereby marked "*advertisement*" in accordance with 18 U.S.C. Section 1734 solely to indicate this fact.

§ Both authors contributed equally to this work.

¶ Supported by a U. S. Department of Defense Predoctoral Fellowship (DAMD17-02-1-0471).

** Supported by a U. S. Department of Defense Predoctoral Fellowship (DAMD17-01-1-0414).

‡‡ Current Address: Dept. of Biological Sciences, University of Alaska, 3211 Providence Dr., Anchorage, AK 99508.

§§ To whom correspondence should be addressed. Tel.: 508-856-5858; Fax: 508-856-5011; E-mail: Craig.Peterson@umassmed.edu.

[1] The abbreviations used are: DSB, double-strand break; HR, homologous recombination; ssDNA, single-stranded DNA; dsDNA, double-stranded DNA; TFO, triplex-forming oligonucleotide; DTT, dithiothreitol; BSA, bovine serum albumin; ATPγS, adenosine 5′-*O*-(thiotriphosphate); AMP-PNP, adenosine 5′-(β,γ-imino)triphosphate; Mnase, micrococcal nuclease.

generate pMJ5, the annealed oligonucleotides TFOB5 (5′-TCGAGAAGAAAAGAAAGAAAGAAAC-3′) and TFOB3 (5′-TCGAGT TTCTTTCTTTCTTTTCTTC-3′) were ligated to the product of a *Xho*I digestion carried out on pCL7c (12). This yielded a pBluescript SKII (−) plasmid containing 5 head-to-tail repeats of the 208-bp *Lytechinus variegatus* 5S rDNA nucleosome positioning element flanked by a TFO-binding site. The DNA template (208–11) for reconstituting nucleosomal arrays for the ATPase, remodeling, and Mnase assays consists a *Not*I-*Hin*dIII fragment derived from pCL7b (12), containing 11 head-to-tail repeats of a 5S rRNA gene from *L. variegatus*, each one possessing a nucleosome positioning sequence. The sixth nucleosome is tagged by a unique *Sal*I restriction site.

Reagent Preparation—Recombinant yeast Rad51p, Rad54p, rad54K341Ap, and rad54K341Rp were overexpressed in yeast and purified as previously described (7). SWI/SNF purification was as described (13). Histone octamers were purified from chicken erythrocytes as described by Hansen *et al.* (14). Octamer concentrations were determined by measurements of A_{230} (15). Nucleosomal array DNA templates (pXG540, pMJ5, or 208–11) were labeled by the Klenow polymerase fill-in reaction using [α-^{32}P]dCTP (3000 μCi/mmol, Amersham Biosciences). Nucleosomal arrays were reconstituted by salt dialysis as previously described (13), and the nucleosome saturation was determined to be 60–80% by digestion analysis.

D-loop Reactions—Oligonucleotide D1 (90-mer) used in the D-loop experiments has the sequence: 5′-AAATCAATCTAAAGTATATATGAGTAAACTTGGTCTGACAGTTACCAATGCTTAATCAGTGAGGCACCTATCTCAGCGATCTGTCTATTT-3′, being complementary to positions 1932–2022 of pBluescript SK(−) replicative form I DNA. Oligonucleotide D1 was 5′ end-labeled with ^{32}P using [γ-^{32}P]dATP and polynucleotide kinase, as described (7). Buffer R (35 mM Tris-HCl, pH 7.4, 2.0 mM ATP, 2.5 mM $MgCl_2$, 30 mM KCl, 1 mM DTT, and an ATP-regenerating system consisting of 20 mM creatine phosphate and 30 μg/ml creatine kinase) was used for the reactions; all of the incubation steps were carried out at 30 °C. Rad51 (0.8 μM) and Rad54 (120 nM) were incubated with radiolabeled oligonucleotide D1 (2.4 μM nucleotides) for 5 min to assemble the presynaptic filament, which was then mixed with naked pBluescript replicative form I DNA (38 μM base pairs) or the same DNA assembled into chromatin (38 μM base pairs). Chromatin assembly was monitored by following topological changes as well as measuring the degree of occlusion of a unique *Eco*RI restriction site close to the D1 sequence. Substrates were estimated to be ~80% saturated with nucleosomes. The reactions containing RecA protein (0.8 μM) were assembled in the same manner, except that they were supplemented with an additional 12.5 mM $MgCl_2$ at the time of incorporation of the duplex substrates. At the indicated times, 4-μl portions of the reactions were withdrawn and mixed with an equal volume of 1% SDS containing 1 mg/ml proteinase K. After incubation at 37 °C for 5 min, the deproteinized samples were run in 1% agarose gels in TAE buffer (40 mM Tris-HCl, pH 7.4, 0.5 mM EDTA) at 4 °C. The gels were dried, and the radiolabeled DNA species were visualized and quantified by PhosphorImager analysis (Personal Molecular Imager FX, Bio-Rad).

ATPase Assay—Recombinant yeast Rad54p (1 nM) was incubated at 30 °C or 37 °C with 5 nM of either naked 208–11 dsDNA or reconstituted nucleosomal arrays in the presence of 100 μM ATP, 2.5μCi [γ-^{32}P]dATP (6000 μCi/mmol, Amersham Biosciences), 2.5% glycerol, 0.1% Tween 20, 20 mM Tris-HCl, pH 8.0, 200 μM DTT, 5 mM $MgCl_2$, 100 μg/ml BSA. For the DNA length-dependence assays, 5 nM Rad54p, 5 nM Rad51p, or 10 nM SWI/SNF were used. Oligonucleotides (random N-mers ranging from 10–100 nucleotides in length) were PAGE-purified to ensure length homogeneity (Integrated DNA Technologies, Inc., Coralville, IA). Samples were taken after 2, 5, 15, and 30 min and resolved by TLC. The proportion of liberated ^{32}P-pyrophosphate was determined using the Molecular Dynamics PhosphorImager and ImageQuant Software. ATPase assays were independently repeated 3 times, yielding very similar results.

Cruciform Formation Assay—Cruciform formation assays were performed as previously described (16). Briefly, 8 ng of *Ava*I-linearized pXG540 (either naked, N, or nucleosomal, C) were incubated with various concentrations of Rad54, Rad51, or rad54 K341A and 0.15 mg/ml EndoVII (except where noted), in the presence of 10 mM Hepes, pH 7.9, 50 mM NaCl, 3 mM $MgCl_2$, 5% glycerol, 0.1 mM DTT, 1 mM ATP (except where noted), 3 mM phosphoenolpyruvate, and 20 units/ml pyruvate kinase for 30 min at 30 °C. The products were resolved in 1.2% agarose gels and visualized with Sybr Gold staining (Molecular Probes, Eugene, OR) followed by analysis with ImageQuant software.

Chromatin-remodeling Reaction—For the coupled SWI/SNF-or Rad54-*Sal*I reactions, reconstituted 208–11 nucleosomal arrays (~1 nM final concentration) were preincubated at 37 °C for 20 min with 2.5units/μl *Sal*I in a buffer containing (final concentrations) 50 mM NaCl, 5 mM $MgCl_2$, 1 mM ATP, 3 mM phosphoenolpyruvate, 10 units/ml pyruvate kinase, 1 mM DTT, 10 mM Tris-HCl, pH 8.0, 100 μg/ml BSA, and 3% glycerol. Nucleosomal arrays were ~80% saturated with nucleosomes. Buffer, 2 nM SWI/SNF complex, or various concentrations of recombinant Rad51p and Rad54p were added and samples were taken at the indicated time points, vigorously mixed for 10s with 25 μl TE and 50 μl 1:1 solution of phenol/chloroform. The purified DNA fragments were resolved by electrophoresis in 1.2% agarose gels in the presence of 50 μg/ml ethidium bromide. The gels were then dried on 3MM Whatman paper. The fraction of cut and uncut DNA was determined by PhosphorImager analysis using a Molecular Dynamics PhosphorImager and ImageQuant software. Experiments were repeated independently at least 3 times, which yielded very similar results.

Micrococcal Nuclease Digestion—15 nM reconstituted 208–11 nucleosomal arrays were incubated at 37 °C with 2 nM SWI/SNF, 100 nM Rad54p, or buffer, in the presence of 2 mM ATP, 5 mM NaCl, 2.5 mM Tris-HCl, pH 8.0, 0.25 mM $MgCl_2$, 0.3 mM $CaCl_2$, 3 mM phosphoenolpyruvate, 10 units/ml pyruvate kinase, 1 mM DTT, 10 μg/ml BSA, 0.5% glycerol. After 20 min, 0.0005 units of Micrococcal Nuclease (Worthington) was added to the reaction, and aliquots were taken at the indicated time points and then treated for 20 min with 2 μg/μl proteinase K and extracted twice with a 1:1 solution of phenol:chloroform. The resulting digestion products were resolved by electrophoresis in 2% agarose gels, run at 2.5 volts/cm for 12 h. The gels were fixed, dried, and analyzed using a Molecular Dynamics PhosphorImager and ImageQuant Software.

Triple-helix Displacement Assay—Triple-helix formation was performed as described (17). Briefly, equimolar concentrations (100 nM) of *Ssp*I-linearized pMJ5 and ^{32}P-labeled TFO were mixed in buffer MM (25 mM MES, pH 5.5, 10 mM $MgCl_2$) at 57 °C for 15 min and left to cool to room temperature overnight. The resulting triplex was either used directly or reconstituted into nucleosomal arrays. To introduce nicks into the DNA, pMJ5 was exposed to various concentrations of DNaseI (Promega, Madison, WI) for 2 min at 37 °C, the reactions were stopped with 5 mM EDTA, vigorously mixed for 10 s with a 1:1 solution of phenol/chloroform, ethanol-precipitated, and resuspended in water. The degree of nicking introduced by DNaseI treatment was assessed by electrophoretic analysis of native and heat-denatured samples (in the presence of 15% formamide) on denaturing 1.3% agarose gels, followed by Sybr Gold Stain (Molecular Probes, Eugene, OR).

The triplex-containing substrates (5 nM) were incubated at 30 °C with 5 nM recombinant Rad54 protein or SWI/SNF complex, in a buffer containing 35 mM Tris-HCl, pH 7.2, 3 mM $MgCl_2$, 100 μg/ml BSA, 50 mM KCl, 1 mM DTT, 3 mM phosphocreatine, 28 μg/ml creatine phosphokinase, and where noted, 3 mM ATP. Samples were taken at the indicated time points, the reactions were quenched with GSMB buffer (15% (w/v) glucose, 3% (w/v) SDS, 250 mM 4-morpholinepropanesulfonic acid, pH 5.5, 0.4 mg/ml bromphenol blue), and analyzed in 1.2% agarose gels (40 mM Tris acetate, 5 mM sodium acetate, 1 mM $MgCl_2$, pH 5.5) at 10 volts/cm for 1.5 h at 4 °C. Gels were fixed in 5% acetic acid, 50% methanol for 1 h, and dried. The proportion of bound and free TFO was determined using a Molecular Dynamics PhosphorImager and ImageQuant Software.

RESULTS

Rad51p and Rad54p Promote DNA Pairing with a Chromatin Donor—Repair of a DSB by homologous recombination begins with the invasion of a double-stranded, homologous donor by a Rad51-ssDNA nucleoprotein filament, also referred to as the presynaptic filament. This strand invasion reaction is typically monitored *in vitro* by following the Rad51p-dependent formation of a D-loop between a radiolabeled oligonucleotide and a homologous double-stranded DNA donor (Fig. 1*A*). In this case, efficient D-loop formation also requires the ATPase activity of Rad54p. *In vivo*, however, the search for homology and strand invasion involves a homologous donor that is assembled into chromatin. Given that the Rad54p ATPase shows sequence relatedness to known chromatin remodeling enzymes, it was of considerable interest to examine the ability of Rad54p to promote Rad51p-dependent D-loop formation with a nucleosomal donor.

Fig. 1 shows the results of D-loop assays that use either a circular, naked DNA donor or this same circular DNA assembled into nucleosomes. Consistent with previous studies, the

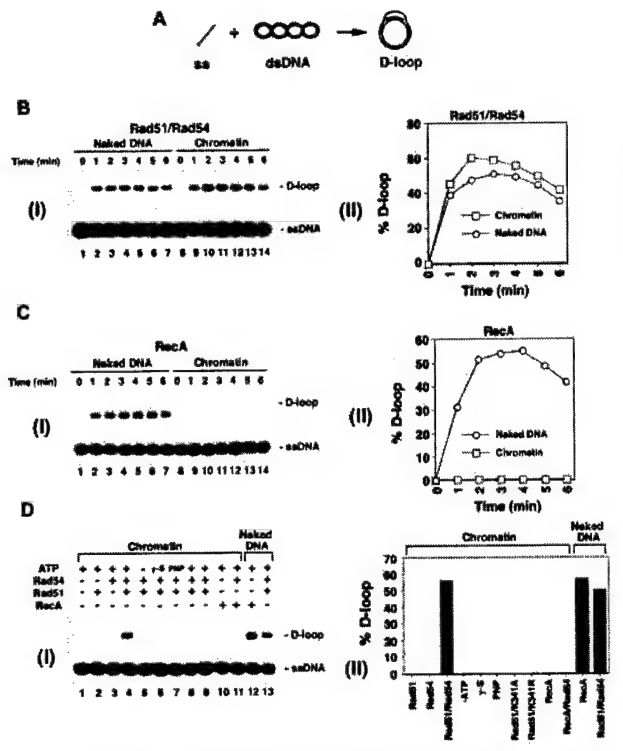

FIG. 1. **Rad51p and Rad54p promote efficient DNA strand invasion with chromatin.** *A*, schematic of the D-loop reaction. A radiolabeled oligonucleotide (*ss*) pairs with a homologous duplex target (*dsDNA*) to yield a D-loop, which, after separation from the free oligonucleotide on an agarose gel, is visualized and quantified by PhosphorImager analysis of the dried gel. *B*, *panel I* shows D-loop reactions mediated by Rad51p and Rad54p with the naked homologous duplex (*Naked DNA*) and the homologous duplex assembled into chromatin (*Chromatin*). The results from the experiments in *panel I* are graphed in *panel II*. The *ordinate* refers to the proportion of the homologous duplex converted into D-loop. *C*, *panel I* shows D-loop reactions mediated by RecA with the naked homologous duplex (*Naked DNA*) and the homologous duplex assembled into chromatin (*Chromatin*). The results from the experiments in *panel I* are graphed in *panel II*. *D*, *panel I* shows D-loop reactions in which Rad51p and RecA were used either alone or in conjunction with Rad54p or rad54 mutant variants with the naked homologous duplex (*Naked DNA*) and the homologous duplex assembled into chromatin (*Chromatin*), as indicated. ATP was omitted from the reaction in *lane 5*, and ATPγS (γ*S*) and AMP-PNP (*PNP*) replaced ATP in *lanes 6* and *7*, respectively. The reactions in *lanes 8* and *9* contained ATP, but Rad54p was replaced with the ATPase-defective variants rad54 K341A (*KA*) and rad54 K341R (*KR*), respectively. The results from the experiments in *panel I* are summarized in the bar graph in *panel II*.

combination of yeast Rad51p and Rad54p led to rapid and highly efficient D-loop formation on the naked DNA donor (Fig. 1*B*). A similar level of D-loop formation was also obtained when the bacterial recombinase RecA was used in these assays with naked DNA (Fig. 1*C*). Surprisingly, assembly of the circular donor into chromatin had no effect on the efficiency of D-loop formation by Rad51p and Rad54p (Fig. 1*B*). D-loop formation on the chromatin donor required ATP hydrolysis by Rad54p, because nonhydrolyzable ATP analogs (ATPγS and AMP-PNP) were unable to substitute for ATP (Fig. 1*C*, *panel I*, *lanes 6* and *7*), and two ATPase-defective mutant variants of Rad54p, rad54K341Ap and rad54K341Rp (18), were inactive (Fig. 1*D*). In contrast to reactions that contained Rad51p/Rad54p, the activity of RecA was completely eliminated when the donor was assembled into nucleosomes (Fig. 1*C*). Furthermore, addition of Rad54p to the RecA reaction did not rescue D-loop formation on chromatin (Fig. 1*D*, *panel I*, *lane 11*). Thus, the eukaryotic recombination proteins have the unique capability of performing the DNA strand invasion reaction with a chromatin donor.

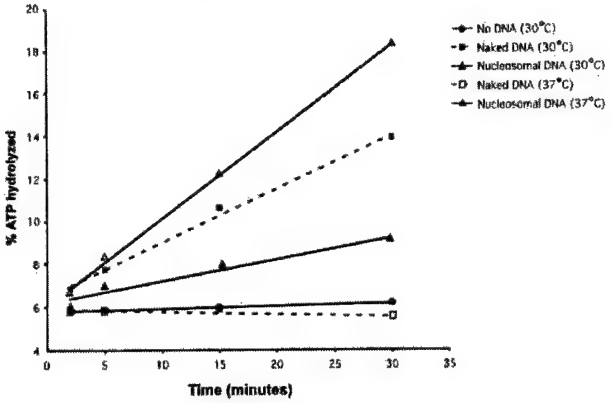

FIG. 2. **Nucleosomal DNA protects Rad54p from thermal inactivation.** ATPase assays. 1 nM Rad54p was incubated at 30 °C with no DNA (*circles*), 5 nM naked (*closed squares*) or nucleosomal dsDNA (*closed triangles*), or at 37 °C with 5 nM naked (*open squares*) or nucleosomal dsDNA (*open triangles*). Samples were taken after 2, 5, 15, and 30 min.

Nucleosomal DNA Protects Rad54p from Thermal Denaturation—The ATPase activity of Rad54p is required for many of its biological functions *in vivo* and for enhancing Rad51p-mediated homologous DNA pairing reactions *in vitro*, both on naked DNA (18) and on chromatin (Fig. 1*D*). Given the latter finding, we were interested in determining whether chromatin influences the ATPase activity of Rad54p.

As shown in Fig. 2, both naked DNA (*solid squares*) and chromatin (*solid triangles*) stimulated the ATPase activity of Rad54p at 30 °C, with naked DNA being somewhat more effective. At the low protein concentrations at which these assays were performed (1 nM), purified Rad54p is extremely temperature-labile and is rapidly inactivated at 37 °C (Fig. 2; Ref. 36). Thus, as expected, the ATPase activity of Rad54p was not detectable in the presence of naked DNA when the reactions were performed at 37 °C (Fig. 2, *open squares*). Importantly, when the reaction was carried out in the presence of chromatin (*open triangles*), the rate of ATP hydrolysis at 37 °C was even greater than the rate obtained in reactions conducted at 30 °C. Importantly, there was no measurable ATPase activity associated with the nucleosomal arrays in the absence of Rad54p, and BSA, free histones, and replication protein A were unable to stimulate the DNA-stimulated ATPase activity of Rad54p at 37 °C. These results indicate that nucleosomal DNA is uniquely able to protect Rad54p from thermal inactivation, and these data suggest that Rad54p may physically interact with nucleosomes.

Rad54 Generates Unconstrained Superhelical Torsion in Nucleosomal DNA—A number of chromatin remodeling complexes that contain Swi2/Snf2-related ATPases have been shown to alter chromatin structure by generating superhelical torsion in DNA and nucleosomal arrays (16). Indeed, the ability to introduce superhelical stress may represent a primary biomechanical activity of all Swi2/Snf2-like ATP-dependent DNA motors, and this activity is likely to be crucial for catalyzing alterations in chromatin structure. Previous studies have shown that Rad54p can also generate both negative and positive supercoiled domains in dsDNA, and it has been suggested that this activity reflects the tracking of Rad54p along DNA (19, 20).

We investigated whether Rad54p is able to introduce superhelical torsion on nucleosomal substrates, using a cruciform extrusion test that has been used for examining other chromatin remodeling enzymes (Fig. 3*A*). In this assay, superhelical

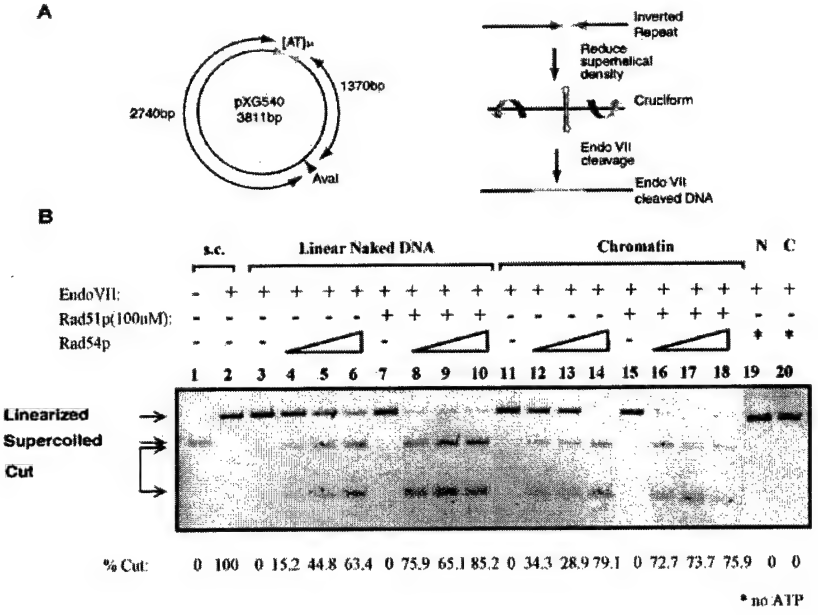

FIG. 3. **Rad54 generates superhelical torsion on nucleosomal DNA.** *A*, schematic illustration of the cruciform extrusion assay. A linearized plasmid (*pXG540*) containing an inverted repeat sequence is incubated with T4 Endonuclease VII, a highly selective junction resolving enzyme, and Rad54p, in the presence of ATP. Rad54p increases the local unconstrained superhelical density, resulting in the extrusion of a cruciform structure, which is recognized and cut by Endo VII. Adapted from Havas *et al.* (16). *B*, results of a typical cruciform formation assay. Supercoiled (*lanes 1, 2*), *Ava*I-linearized pXG540 DNA (*lanes 3–10, 19*), or nucleosomal pXG540 (*lanes 11–18, 20*) was incubated with 12.5, 25, or 50 nM Rad54p as indicated, in the presence or absence of 100 nM Rad51p. EndoVII was omitted in *lane 1*. ATP was omitted in *lanes 19* and *20*. The numbers below each lane (*% cut*) represent the percentage of pXG540 molecules cleaved by EndoVII. *s.c.*, supercoiled substrate; *C*, chromatin substrate; *N*, naked linear DNA substrate.

torsion leads to extrusion of a cruciform that is then recognized and cleaved by bacteriophage T4 endonuclease VII that has high specificity for this DNA structure (16). Consistent with previous studies (19), Rad54p action generates torsional stress on a linear, dsDNA substrate (*N*) which leads to cruciform extrusion (Fig. 3*B*, *lanes 4–6*). Importantly, Rad54p was able to generate torsional stress on the nucleosomal substrate (*C*) with comparable efficiency (*lanes 12–14*). The addition of 100 nM Rad51p greatly stimulated the ability of Rad54p to promote the formation of cruciform structures on both naked and nucleosomal substrates (compare *lanes 4* and *8*, and *12* and *16*, respectively. Also note the decreased levels of linear template in *lanes 16–18*). Importantly, Rad51p fails to support cruciform formation by itself (*lanes 7* and *15*). As expected, the generation of torsional stress required ATP (*lanes 19* and *20*). Furthermore, the ATP hydrolysis mutant variant rad54 K341A was inactive in these assays (data not shown). These data indicate that Rad54p, like other Swi2/Snf2 family members, uses the free energy from ATP hydrolysis to alter DNA topology and that nucleosomal arrays constitute excellent substrates for this activity.

Rad54p Can Disrupt a DNA Triple Helix—How Rad54p introduces topological stress in nucleosomal DNA is unclear. Previously, we suggested that superhelical torsion might result from translocation of Rad54p along the DNA double helix (19). Recently, chromatin remodeling by the yeast RSC complex (which contains the Swi2/Snf2-related ATPase, Sth1p) has been shown to involve ATP-dependent DNA translocation (21). To further evaluate the ability of Rad54p to translocate on DNA, we used a DNA triple-helix-displacement assay that was originally developed to follow the translocation of a type I restriction endonuclease along DNA (17). The substrate used (see Fig. 4*A*) consists of a radioactively labeled oligonucleotide (TFO*) bound via Hoogsteen hydrogen bonds to the major groove of a 2.5-kb linear dsDNA. Translocation of a protein along the DNA displaces the triplex, which can be detected as dissociation of the radioactive TFO* from the DNA triplex. Fig. 4*B* shows typical levels of triplex displacement in the absence or presence of Rad54p or yeast SWI/SNF. Both Rad54p and ySWI/SNF were able to efficiently displace a preformed triplex from both naked (*squares*) and nucleosomal (*triangles*) substrates in an ATP-dependent manner. Similar results were

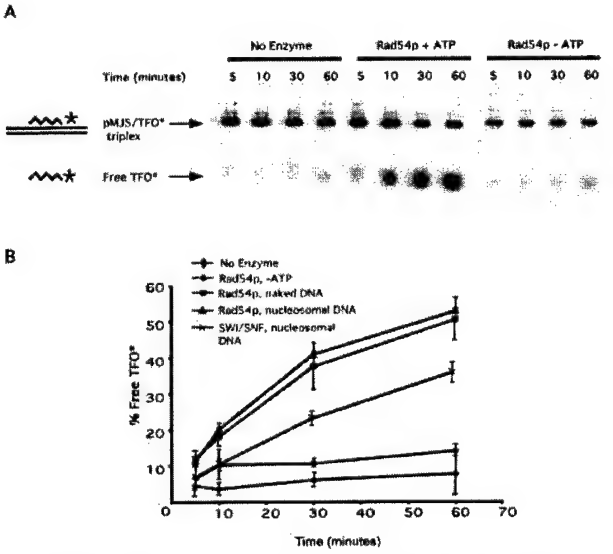

FIG. 4. **Rad54p action displaces a preformed triplex.** *A*, typical results obtained with naked triplex-containing substrate. The upper band corresponds to the duplex-bound TFO*; the lower band corresponds to free TFO*. Reactions contained 5 nM triplex substrate and 5 nM Rad54p. *B*, percentage of free TFO* in four or more experiments were averaged and plotted as a function of time. Note that triplex displacement from the nucleosomal template occurs at equal efficiency to that of naked DNA.

obtained when the TFO*-bound substrate contained single-strand nicks (data not shown), strongly suggesting that the displacement of the TFO* reflects translocation of Rad54p and ySWI/SNF and that it is not due simply to the generation of torsional stress. Thus, yeast RSC (21), ySWI/SNF, and Rad54p (Fig. 4) all share the ability to use the free energy from ATP hydrolysis to disrupt triplex DNA.

Rad54p Has ATPase Kinetics Diagnostic of a DNA-translocating Enzyme—The "inch-worm" model for DNA translocation, originally envisioned (22) for DNA helicases and later modified by Velankar *et al.* (23), proposes that the translocating enzyme progresses along the contour of the DNA in steps of

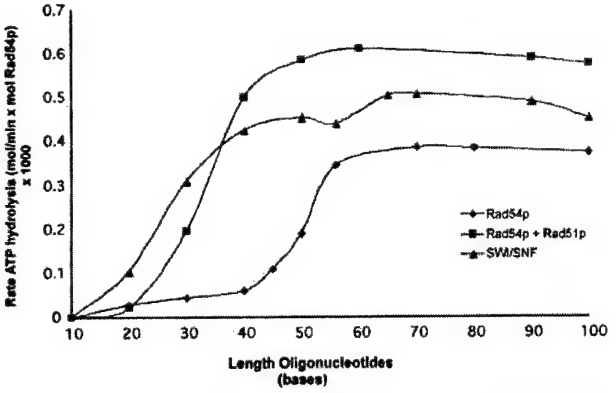

FIG. 5. **Rad54 has ATPase kinetics typical of a unidirectional DNA translocating enzyme.** The rate of ATP hydrolysis by 5 nM Rad54p (*diamonds*), 5 nM Rad54p + 5 nM Rad51p (*squares*), or 10 nM SWI/SNF (*triangles*) was measured in the presence of 50 μM ssDNA (n-mers) oligonucleotides of different lengths. The average values from 3 independent experiments were plotted. Rates were determined from experiments with at least four time points.

a single base, and each step requires the hydrolysis of one ATP molecule. This model predicts that the rate of ATP hydrolysis of a unidirectional DNA translocating enzyme will depend on the length of the DNA (24).

To investigate whether Rad54p has ATPase properties characteristic of a unidirectional DNA translocating enzyme, the rate of ATP hydrolysis was measured in the presence of saturating amounts of single-stranded oligonucleotides ranging from 10 to 100 nucleotides in length (Fig. 5). For comparison, we also monitored the ATPase activity of yeast SWI/SNF (*triangles*). In the case of Rad54p, oligonucleotides shorter than 40 bases failed to stimulate the ATPase activity of Rad54p (*diamonds*), whereas oligonucleotides between 40 and 70 bases led to a stimulation of ATPase activity that was proportional to DNA length. For oligonucleotides longer than 70 bases, the ATPase activity no longer increased with the DNA length. When Rad51p was added to these reactions (*squares*), shorter oligonucleotides became more effective in promoting ATP hydrolysis, and the overall activity was enhanced. Likewise, the ATPase activity of ySWI/SNF (*triangles*) was also proportional to the DNA length, with a plateau reached at 60 bases.

These results are fully consistent with both Rad54p and ySWI/SNF coupling ATP hydrolysis to unidirectional translocation, in which the rate of DNA binding is slower than the rate of DNA translocation (21). In this case, no ATP hydrolysis is observed with very short substrates, presumably because a minimum DNA length is required for Rad54p or ySWI/SNF to bind and to translocate before reaching an end and releasing the DNA. When the substrate is ~30–40 nucleotides in length, Rad54p and ySWI/SNF readily bind the substrate, and more extended translocation events take place. The rate of ATP hydrolysis is fairly constant with DNA substrates longer than 60–70 nucleotides, reflecting the possibility that Rad54p and ySWI/SNF have little processivity, and thus they release their substrate after ~60–70 bases regardless of the total length of the DNA molecule. Although the triphasic kinetics of ATPase activity are consistent with a DNA-translocation mechanism, it remains a possibility that the longer single-stranded oligonucleotides exhibit more extended secondary structures that are either more proficient at binding Rad54p (or SWI/SNF) or stimulating its ATPase activity.

Rad54 Is an ATP-dependent Chromatin Remodeling Enzyme—Cairns and colleagues (21) proposed that short-range translocation events may be the key feature of chromatin remodeling enzymes, leading to a "pumping" of DNA across the surface of the histone octamer, which then results in enhanced DNA accessibility and nucleosome movements. To investigate whether Rad54p might also enhance the accessibility of nucleosomal DNA, we used an assay in which nucleosome remodeling activity is coupled to restriction enzyme activity such that remodeling is revealed as an enhancement of restriction-enzyme cleavage rates (12). This assay uses a nucleosomal array substrate in which the central nucleosome of an 11-mer array contains a unique *Sal*I site located at the predicted dyad axis of symmetry (see Fig. 6*A*). In the absence of a remodeling enzyme, the rate of *Sal*I cleavage is very slow (Fig. 6*A*, *solid diamonds*), whereas addition of a remodeling enzyme, such as yeast SWI/SNF, leads to enhanced digestion (Fig. 6*A*, *solid squares*). When Rad54p was added to the remodeling reactions, *Sal*I digestion was also dramatically enhanced (*solid circles*, *triangles*), although a higher concentration of this protein (50 nM) was required to achieve a rate of digestion comparable with that of reactions that contained yeast SWI/SNF (2 nM, *squares*). However, when Rad51p (50 nM) and Rad54p (50 nM) were both present in the reaction, much higher levels of remodeling were attained (*open circles*). Note that Rad51p has no intrinsic chromatin remodeling activity (*open diamonds*). The stimulation of the Rad54p chromatin remodeling activity by Rad51p is congruent with previous studies showing that Rad51p enhances the rate of ATP hydrolysis and DNA supercoiling by Rad54p (19, 25, see Fig. 3). Thus, the above data indicate that Rad54p is sufficient for chromatin remodeling activity but that the combination of Rad51p and Rad54p constitutes a more potent remodeling machine.

Rad54p Does Not Induce Significant Nucleosome Mobilization—A number of chromatin remodeling complexes that contain a Swi2/Snf2-related ATPase (ySWI/SNF, dCHRAC, dNURF, and xMi-2) can use the energy of ATP hydrolysis to move nucleosomes in cis (26–30). To investigate whether Rad54p can also catalyze nucleosome mobilization, ^{32}P-end-labeled nucleosomal arrays were incubated with buffer, ySWI/SNF, or Rad54p, and nucleosome positions were mapped by micrococcal nuclease (Mnase) digestion (Fig. 6*B*). Mnase can only cleave DNA between nucleosomes, which leads to a periodic ladder of digestion products indicative of a positioned 11-mer nucleosomal array (Fig. 6*B*). Consistent with our previous studies, incubation with ySWI/SNF (2 nM) and ATP leads to a complete disruption of the Mnase digestion pattern, indicative of nucleosome sliding (Fig. 6*B*, *left panel*; also see Ref. 28). In contrast, addition of Rad54p (100 nM) and ATP had very little effect on the cleavage periodicity (Fig. 6*B*, *right panel*). Likewise, addition of both Rad51p and Rad54p (100 nM each) to these assays did not change the Mnase digestion profile (data not shown). Importantly, these experiments used concentrations of ySWI/SNF and Rad54p that yielded similar levels of chromatin remodeling in the restriction enzyme accessibility assay (Fig. 6*A*). Thus, although Rad54p can enhance the accessibility of nucleosomal DNA to restriction enzymes, this activity does not appear to reflect large scale rearrangement of nucleosome positions.

DISCUSSION

In eukaryotes, chromatin presents an accessibility dilemma for all DNA-mediated processes, including gene transcription and DNA repair. Although much progress has been made on identifying the enzymes that remodel chromatin structure to facilitate transcription, less is known of how the DNA-repair machinery gains access to damaged DNA within chromatin (reviewed in Ref. 31). In particular, it has not been clear how the recombinational repair machinery can locate short regions of DNA homology when those DNA donor sequences are assembled into chromatin. Here we have shown that the yeast re-

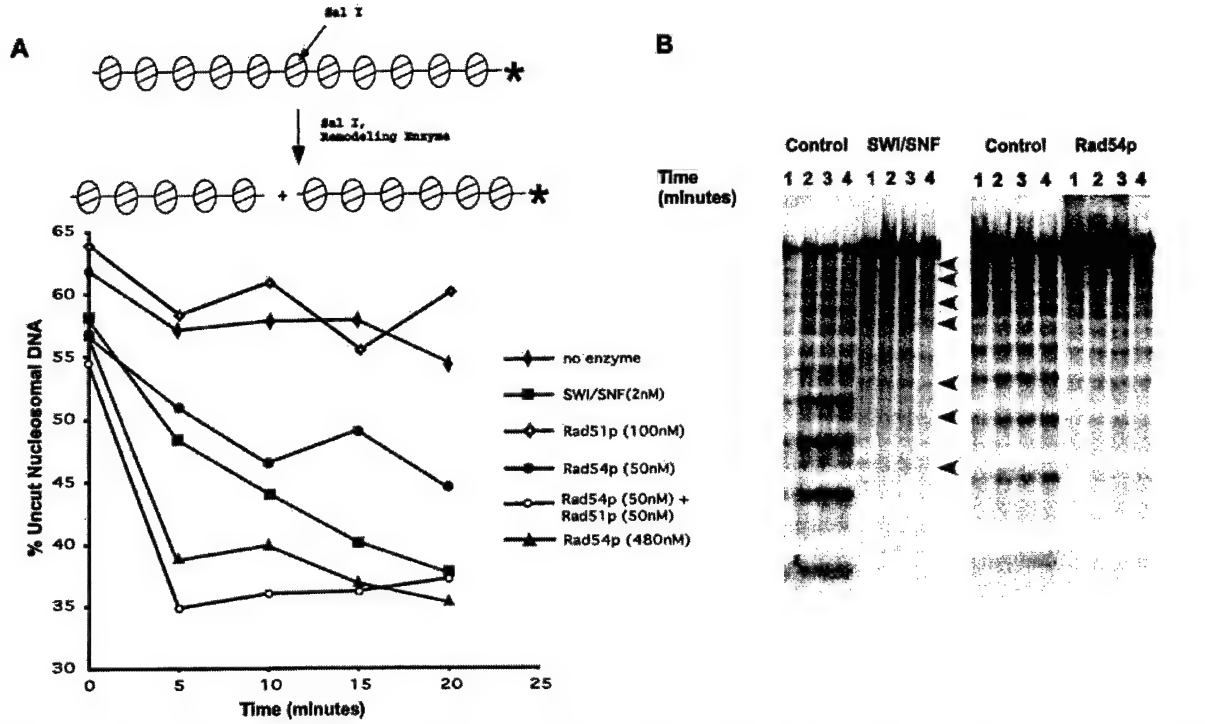

FIG. 6. **Rad54 is an ATP-dependent chromatin remodeling enzyme.** *A*, various concentrations of recombinant Rad54p were tested for chromatin-remodeling activity in a coupled remodeling-restriction enzyme cleavage assay. The nucleosomal substrate was incubated with 50 nM (*closed circles*) or 480 nM Rad54p (*triangles*), 100 nM Rad51p (*open diamonds*), 50 nM Rad54p + 50 nM Rad51p (*open circles*), 2 nM ySWI/SNF (*squares*), or buffer (*closed diamonds*). *B*, 208–11 reconstituted nucleosomal arrays were incubated at 37 °C with 2 nM SWI/SNF, 100 nM Rad54p, or buffer (control lanes). Aliquots were treated with Mnase for the indicated times. The *arrowheads* in the *left panel* indicate the alternate banding pattern as a result of SWI/SNF-induced nucleosome movement.

combination proteins, Rad51p and Rad54p, are sufficient to promote heteroduplex DNA joint formation with chromatin. In contrast, the bacterial recombinase RecA is completely inactive with a chromatin donor. The unique capacity of the eukaryotic machinery to contend with chromatin likely reflects the chromatin-remodeling activity of Rad54p, in which the free energy from ATP hydrolysis enhances the accessibility of nucleosomal DNA. Strand invasion with chromatin may also require a specific interaction between Rad51p and Rad54p because the chromatin remodeling activity of Rad54p does not facilitate RecA-dependent D-loop formation with chromatin (Fig. 1*D*). Recently, Alexiadis and Kadonaga have reported that the *Drosophila* Rad51 and Rad54 proteins can also facilitate strand invasion with chromatin (35).

How Does Rad54p Remodel Chromatin Structure?—Several studies have shown that SWI/SNF-like chromatin remodeling enzymes can perform two separable reactions: 1) they can use the free energy from ATP hydrolysis to enhance the accessibility of nucleosomal DNA and 2) they can use this free energy to mobilize nucleosomes in cis (reviewed in Ref. 32). Recent work from Cairns and colleagues have suggested that both of these activities may be caused by ATP-dependent "pumping" of DNA into the nucleosome (21). In this model, small amounts of DNA translocation might lead to transient exposure of small "loops" of DNA on the surface of the histone octamer, whereas larger quantities of DNA "pumped" into the nucleosome would lead to changes in nucleosome positions. Our data support this model, as we find that both yeast SWI/SNF and Rad54p, like yeast RSC (21), can disrupt a DNA triplex in an ATP-dependent reaction, presumably by translocation of DNA along the surface of the enzyme or by translocation of the enzyme along the DNA. Furthermore, the ATPase activities of ySWI/SNF and Rad54p are sensitive to DNA length, which is diagnostic of DNA-translocating enzymes (21).

Although ySWI/SNF and Rad54p can both enhance the accessibility of nucleosomal DNA, only ySWI/SNF appears to be proficient at changing nucleosome positioning. This result suggests that the precise mechanism of chromatin remodeling by Rad54p may be distinct from that of ySWI/SNF. For instance, Rad54p may only be able to pump small amounts of DNA across the histone octamer surface. Alternatively, Rad54p may translocate along DNA, rather than pumping DNA into the nucleosome. In this model, Rad54p may "pull" the Rad51-ssDNA nucleoprotein filament along the chromatin fiber, leading to changes in nucleosomal DNA topology and DNA accessibility. Such a DNA tracking mechanism might play a key role in facilitating both the search for homology as well as the strand invasion step.

Multiple Roles for Rad54p during Homologous Recombination—Our results suggest that Rad54p is an extremely versatile recombination protein that plays key roles in several steps of homologous recombination. Recently, we found that Rad54p is required for optimal recruitment of Rad51p to a double strand break *in vivo*, and likewise Rad54p can promote formation of the presynaptic filament *in vitro* by helping Rad51p contend with the inhibitory effects of the ssDNA-binding protein replication protein A.[2] Several studies over the past few years have also shown that the ATPase activity of Rad54p plays key roles subsequent to formation of the presynaptic filament. For instance, Rad54p is required for the Rad51p-nucleoprotein filament to form a heteroduplex joint DNA mol-

[2] B. Wolner, S. Van Komen, P. Sung, and C.L. Peterson, submitted for publication.

ecule, even when the homologous donor is naked DNA (Fig. 1*A*; see also Refs. 7, 18, 33). In this case, it has been proposed that Rad54p might use the free energy from ATP hydrolysis to translocate along DNA, which facilitates the homology search process. This DNA-translocation model is fully consistent with our findings that Rad54p can displace a DNA triplex and that the ATPase activity of Rad54p is proportional to DNA length. Rad54p also stimulates heteroduplex DNA extension of established joint molecules (34). Finally, we have shown that Rad54p is required for Rad51p-dependent heteroduplex joint molecule formation with a chromatin donor. In this case, our results suggest that the ATPase activity of Rad54p is used to translocate the enzyme along the nucleosomal fiber, generating superhelical torsion, which leads to enhanced nucleosomal DNA accessibility. It seems likely that this chromatin remodeling activity of Rad54p might also facilitate additional steps after heteroduplex joint formation. Future studies are now poised to reconstitute the complete homologous recombinational repair reaction that fully mimics each step in the repair of chromosomal DNA double strand breaks *in vivo*.

REFERENCES

1. Hiom, K. (2001) *Curr. Biol.* **11,** R278–R280
2. Pâques, F., and Haber, J. E. (1999) *Microbiol. Mol. Biol. Rev.* **63,** 349–404
3. Wood, R. D., Mitchell, M., Sgouros, J., and Lindhal, T. (2001) *Science* **291,** 1284–1289
4. Khanna, K. K., and Jackson, S. P. (2001) *Nat. Genet.* **27,** 247–254
5. Melo, J., and Toczyski, D. (2002) *Curr. Opin. Cell Biol.* **14,** 237–245
6. Kanaar, R., Hoeijmakers, J. H. J., and van Gent, D. C. (1998) *Trends Cell Biol.* **8,** 483–489
7. Petukhova, G., Stratton, S., and Sung, P. (1998) *Nature* **393,** 91–94
8. Eisen, J. A., Sweder, K. S., and Hanawalt, P. C. (1995) *Nucleic Acids Res.* **23,** 2715–2723
9. Jiang, H., Xie, Y., Houston, P., Stemke-Hale, K., Mortensen, U. H., Rothstein, R., and Kodadek, T. (1996) *J. Biol. Chem.* **271,** 33181–33186
10. Clever, B., Interthal, H., Schmuckli-Maurer, J., King, J., Sigrist, M., and Heyer, W. D. (1997) *EMBO J.* **16,** 2535–2544
11. Sambrook, J., Fritsch, E. F., and Maniatis, T. (1989) *Molecular Cloning: A Laboratory Manual*, Cold Spring Harbor Laboratory, Cold Spring Harbor, NY
12. Logie, C., and Peterson, C. L. (1997) *EMBO J.* **16,** 6772–6782
13. Logie, C., and Peterson, C. L. (1999) *Methods Enzymol.* **304,** 726–741
14. Hansen, J. C., Ausio, J., Stanik, V. H., and van Holde, K. E. (1989) *Biochemistry* **28,** 9129–9136
15. Stein, A. (1979) *J. Mol. Biol.* **130,** 103–134
16. Havas, K., Flaus, A., Phelan, M., Kingston, R., Wade, P. A., Lilley, D. M., and Owen-Hughes, T. (2000) *Cell* **103,** 1133–1142
17. Firman, K., and Szczelkun, M. D. (2000) *EMBO J.* **19,** 2094–2102
18. Petukhova, G., Van Komen, S., Vergano, S., Klein, H., and Sung, P. (1999) *J. Biol. Chem.* **274,** 29453–29462
19. Van Komen, S., Petukhova, G., Sigurdsson, S., Stratton, S., and Sung, P. (2000) *Mol. Cell.* **6,** 563–572
20. Ristic, D., Wyman, C., Paulusma, C., and Kanaar, R. (2001) *Proc. Natl. Acad. Sci. U. S. A.* **98,** 8454–8460
21. Saha, A., Wittmeyer, J., and Cairns, B. R. (2002) *Genes Dev.* **16,** 2120–2134
22. Yarranton, G. T., and Gefter, M. L. (1979) *Proc. Natl. Acad. Sci. U. S. A.* **76,** 1658–1662
23. Velankar, S. S., Soultanas, P., Dillingham, M. S., Subramanya, H. S., and Wigley, D. B. (1999) *Cell* **97,** 75–84
24. Dillingham, M. S., Wigley, D. B., and Webb, M. R. (2000) *Biochemistry* **39,** 205–212
25. Mazin, A. V., Zaitseva, E., Sung, P., and Kowalczykowski, S. C. (2000) *EMBO J.* **19,** 1148–1156
26. Guschin, D., Wade, P. A., Kikyo, N., and Wolffe, A. P. (2000) *Biochemistry* **39,** 5238–5245
27. Hamiche, A., Sandaltzopoulos, R., Gdula, D. A., and Wu, C. (1999) *Cell* **97,** 833–842
28. Jaskelioff, M., Gavin, I. M., Peterson, C. L., and Logie, C. (2000) *Mol. Cell. Biol.* **20,** 3058–3068
29. Langst, G., Bonte, E. J., Corona, D. F., and Becker, P. B. (1999) *Cell* **97,** 843–852
30. Whitehouse, I., Flaus, A., Cairns, B. R., White, M. F., Workman, J. L., and Owen-Hughes, T. (1999) *Nature* **400,** 784–787
31. Green, C. M., and Almouzni, G. (2002) *EMBO Rep.* **3,** 28–33
32. Peterson, C. L., and Workman, J. L. (2000) *Curr. Opin. Genet. Dev.* **10,** 187–192
33. Solinger, J. A., Lutz, G., Sugiyama, T., Kowalczykowski, S. C., and Heyer, W. D. (2001) *J. Mol. Biol.* **307,** 1207–1221
34. Solinger, J. A., and Heyer, W. D. (2001) *Proc. Natl. Acad. Sci. U. S. A.* **98,** 8447–8453
35. Alexiadis, V., and Kadonaga, J. T. (2002) *Genes Dev.* **16,** 2767–2771
36. Van Komen, S., Petukhova, G., Sigurdsson, S., and Sung, P. (2002) *J. Biol. Chem.* **277,** 43578–43587

mice with or without the C57Bl/Ka-Ly5.2 recipient bone marrow cells[1]. Reconstitution of donor (Ly5.1) myeloid and lymphoid cells was monitored by staining blood cells with antibodies against Ly5.1, CD3, B220, Mac-1 and Gr-1. The secondary bone marrow transplant was performed with 10^7 whole bone marrow cells from mice reconstituted with *Bmi-1*$^{+/+}$ or *Bmi-1*$^{-/-}$ fetal liver cells.

Retroviral gene transfer of HSCs

Mouse stem cell viruses expressing mouse *p16*^{Ink4a} or *p19*^{Arf} cDNAs together with GFP were produced using Phoenix ecotropic packaging cells[28]. Infection of HSCs was done as described[29] except that three cycles of infections were performed. After 48 h, single GFP-positive cells were sorted into a 96-well plate containing 100 μl HSC medium[29] and grown for 7 days. Each well was scored for the presence of GFP-positive cells by observation with a fluorescence microscope.

Received 10 February; accepted 19 March 2003; doi:10.1038/nature01587.
Published online 20 April 2003.

1. Morrison, S. J. & Weissman, I. L. The long-term repopulating subset of hematopoietic stem cells is deterministic and isolatable by phenotype. *Immunity* **1**, 661–673 (1994).
2. van der Lugt, N. M. *et al.* Posterior transformation, neurological abnormalities, and severe hematopoietic defects in mice with a targeted deletion of the *bmi-1* proto-oncogene. *Genes Dev.* **8**, 757–769 (1994).
3. Ramalho-Santos, M. *et al.* 'Stemness': transcriptional profiling of embryonic and adult stem cells. *Science* **298**, 597–600 (2002).
4. Park, I.-K. *et al.* Molecular cloning and characterization of a novel regulator of G-protein signaling from mouse hematopoietic stem cells. *J. Biol. Chem.* **276**, 915–923 (2001).
5. Park, I. K. *et al.* Differential gene expression profiling of adult murine hematopoietic stem cells. *Blood* **99**, 488–498 (2002).
6. Lessard, J., Baban, S. & Sauvageau, G. Stage-specific expression of Polycomb group genes in human bone marrow cells. *Blood* **91**, 1216–1224 (1999).
7. Kiyono, T. *et al.* Both Rb/p16^{INK4a} inactivation and telomerase activity are required to immortalize human epithelial cells. *Nature* **396**, 84–88 (1998).
8. van der Lugt, N. M. T., Alkema, M., Berns, A. & Deschamps, J. The Polycomb-group homolog Bmi-1 is a regulator of murine Hox gene expression. *Mech. Dev.* **58**, 153–164 (1996).
9. Akashi, K. *et al.* Transcriptional accessibility for genes of multiple tissues and hematopoietic lineages is hierarchically controlled during early hematopoiesis. *Blood* **101**, 383–389 (2003).
10. Morrison, S., Hemmati, H., Wandycz, A. & Weissman, I. The purification and characterization of fetal liver hematopoietic stem cells. *Proc. Natl Acad. Sci. USA* **92**, 10302–10306 (1995).
11. Wright, D. E. *et al.* Hematopoietic stem cells are uniquely selective in their migratory reponse to chemokines. *J. Exp. Med.* **195**, 1145–1154 (2002).
12. Mahmoudi, T. & Verrijzer, C. P. Chromatin silencing and activation by Polycomb and trithorax group proteins. *Oncogene* **20**, 3055–3066 (2001).
13. Weber, J. D. *et al.* Nucleolar Arf sequesters Mdm2 and activates p53. *Nature Cell Biol.* **1**, 20–26 (1999).
14. Jacob, J. *et al.* The oncogene and Polycomb-group gene *bmi-1* regulates cell proliferation and senescence through the *ink4a* locus. *Nature* **397**, 164–168 (1999).
15. Quelle, D. E., Zindy, F., Ashmun, R. A. & Sherr, C. J. Alternative reading frames of the INK4a tumour suppressor gene encode two unrelated proteins capable of inducing cell cycle arrest. *Cell* **84**, 993–1000 (1995).
16. Antonchuk, J., Sauvageau, G. & Humphries, R. K. HOXB4 overexpression mediates very rapid stem cell regeneration and competitive hematopoietic repopulation. *Exp. Hematol.* **29**, 1125–1134 (2002).
17. Lawrence, H. J. *et al.* Mice bearing a targeted interruption of the homeobox gene HOXA9 have defects in myeloid, erythroid, and lymphoid hematopoiesis. *Blood* **89**, 1922–1930 (1997).
18. Christensen, J. L. & Weissman, I. L. Flk-2 is a marker in hematopoietic stem cell differentiation: a simple method to isolate long-term stem cells. *Proc. Natl Acad. Sci. USA* **98**, 14541–14546 (2001).
19. Zhang, Y., Xiong, Y. & Yarbrough, W. G. ARF promotes MDM2 degradation and stabilizes p53: ARF-INK4a locus deletion impairs both the Rb and p53 tumour suppression pathways. *Cell* **92**, 725–734 (1998).
20. Shivdasani, R., Mayer, E. & Orkin, S. Absence of blood formation in mice lacking the T-cell leukaemia oncoprotein tal-1/SCL. *Nature* **373**, 432–434 (1995).
21. Porcher, C. *et al.* The T cell leukemia oncoprotein SCL/tal-1 is essential for development of all hematopoietic lineages. *Cell* **86**, 47–57 (1996).
22. Antonchuk, J., Sauvageau, G. & Humphries, R. K. HOXB4-induced expansion of adult hematopoietic stem cells *ex vivo*. *Cell* **109**, 39–45 (2002).
23. Domen, J., Cheshier, S. H. & Weissman, I. L. The role of apoptosis in the regulation of hematopoietic stem cells: overexpression of BCL-2 increases both their number and repopulation potential. *J. Exp. Med.* **191**, 253–264 (2000).
24. Nichogiannopoulou, A. *et al.* Defects in hemopoietic stem cell activity in Ikaros mutant mice. *J. Exp. Med.* **190**, 1201–1214 (1999).
25. Fisher, R. C., Lovelock, J. D. & Scott, E. W. A critical role for PU.1 in homing and long-term engraftment by hematopoietic stem cells in the bone marrow. *Blood* **94**, 1283–1290 (1999).
26. Cheng, T. *et al.* Hematopoietic stem cell quiescence maintained by p21$^{cip1/waf1}$. *Science* **287**, 1804–1808 (2000).
27. Ohta, H. *et al.* Polycomb group gene *rae28* is required for sustaining activity of hematopoietic stem cells. *J. Exp. Med.* **195**, 759–770 (2002).
28. Pear, W., Nolan, G., Scott, M. & Baltimore, D. Production of high-titer helper-free retroviruses by transient transfection. *Proc. Natl Acad. Sci. U.S.A.* **90**, 8392–8396 (1993).
29. Cotta, C., Swindle, C., Weissman, I. L. & Klug, C. A. *Retroviral Transduction of FACS-Purified Hematopoietic Stem Cells* (eds Klug, C. A. & Jordan, C. T.) 243–252 (Humana Press, Totowa, New Jersey, 2001).
30. Lessard, J. & Sauvageau, G. *Bmi-1* determines the proliferative capacity of normal and leukaemic stem cells. *Nature* advance online publication, 20 April 2003 (doi: 10.1038/nature01572).

Supplementary information accompanies the paper on **www.nature.com/nature**.

Acknowledgements We thank T. Magnuson and C. Klug for providing *Bmi-1*$^{+/-}$ mice and the MSCV plasmid, respectively; and the Flow Cytometry Core and the Microarray Core at the University of Michigan for their work. The Microarray Core is supported in part by a University of Michigan's Cancer Center Support Grant from the NIH. This work is supported by grants from the NIH.

Competing interests statement The authors declare that they have no competing financial interests.

Correspondence and requests for materials should be addressed to M.F.C. (mclarke@umich.edu).

DNA helicase Srs2 disrupts the Rad51 presynaptic filament

Lumir Krejci*†, Stephen Van Komen*†, Ying Li‡, Jana Villemain*, Mothe Sreedhar Reddy*, Hannah Klein§, Thomas Ellenberger‡ & Patrick Sung*

** Institute of Biotechnology and Department of Molecular Medicine, University of Texas Health Science Center at San Antonio, 15355 Lambda Drive, San Antonio, Texas 78245, USA*
‡ Department of Biological Chemistry and Molecular Pharmacology, Harvard Medical School, Boston, Massachusetts 02115, USA
§ Department of Biochemistry, New York University School of Medicine, New York, New York 10016, USA
† These authors contributed equally to the work

Mutations in the *Saccharomyces cerevisiae* gene *SRS2* result in the yeast's sensitivity to genotoxic agents, failure to recover or adapt from DNA damage checkpoint-mediated cell cycle arrest, slow growth, chromosome loss, and hyper-recombination[1,2]. Furthermore, double mutant strains, with mutations in DNA helicase genes *SRS2* and *SGS1*, show low viability that can be overcome by inactivating recombination, implying that untimely recombination is the cause of growth impairment[1,3,4]. Here we clarify the role of *SRS2* in recombination modulation by purifying its encoded product and examining its interactions with the Rad51 recombinase. Srs2 has a robust ATPase activity that is dependent on single-stranded DNA (ssDNA) and binds Rad51, but the addition of a catalytic quantity of Srs2 to Rad51-mediated recombination reactions causes severe inhibition of these reactions. We show that Srs2 acts by dislodging Rad51 from ssDNA. Thus, the attenuation of recombination efficiency by Srs2 stems primarily from its ability to dismantle the Rad51 presynaptic filament efficiently. Our findings have implications for the basis of Bloom's and Werner's syndromes, which are caused by mutations in DNA helicases and are characterized by increased frequencies of recombination and a predisposition to cancers and accelerated ageing[5].

We have been unable to overexpress Srs2 protein significantly in yeast, suggesting that this protein is unstable in, and/or toxic to, yeast cells. We therefore turned to *Escherichia coli* and an inducible T7 promoter as vehicle for Srs2 expression. Srs2 could be revealed by Coomassie Blue staining of *E. coli* extracts and by immunoblotting with antibodies against Srs2 (Fig. 1a). We subjected *E. coli* lysate to precipitation with ammonium sulphate and a five-step chromatographic fractionation scheme to purify Srs2 to near-homogeneity (Fig. 1b). Purified Srs2 has a robust ssDNA-dependent ATPase activity ($k_{cat} \geq 2{,}500\ min^{-1}$) and a DNA helicase activity[6] that is fuelled by ATP hydrolysis (Fig. 1c).

Previous studies have unveiled an anti-recombination function in *SRS2* and a genetic interaction with *RAD51* (refs 7–9). We investigated whether Srs2 protein interacts physically with Rad51 protein, and also tested its effect on the Rad51 recombinase activity[10]. To

examine whether Srs2 associates with Rad51, we coupled the latter to Affi-gel 15 beads and used the resulting matrix to bind Srs2. As shown in Fig. 1d, Srs2 was retained on the Affi-Rad51 beads, but no binding of Srs2 to bovine serum albumin (BSA) immobilized on Affi-beads (Affi-BSA) was detected. An interaction between Rad51 and two carboxy-terminal fragments of Srs2 was seen in the two-hybrid assay in yeast (Fig. 1e). We were unable to detect significant interaction between Rad51 and full-length Srs2 in this assay, which could be the result of low expression of full-length Srs2.

We next tested the effect of Srs2 on the Rad51-mediated homologous pairing and strand exchange reaction that serves to join recombining DNA molecules[10,11]. For this, we employed a commonly used assay in which Rad51 and the heterotrimeric ssDNA-binding factor RPA are incubated with ssDNA and ATP to form a Rad51–ssDNA nucleoprotein filament[11–13]. Such a filament, often called the presynaptic filament[11–13], is then incubated with the homologous linear duplex (Fig. 2Aa). Pairing between the DNA substrates yields a joint molecule, which is further processed by DNA strand exchange to nicked circular duplex (Fig. 2Aa, b). As shown in Fig. 2Ac, d, the addition of a catalytic quantity of Srs2 strongly suppressed the homologous pairing and strand exchange reaction.

To characterize its anti-recombination activity further, Srs2 was added to D-loop reactions in which pairing of a ^{32}P-labelled 90-mer oligonucleotide with a homologous duplex target is mediated by the combination of Rad51 and Rad54 proteins[14,15] (Fig. 2Ba). As reported previously[14–16], efficient D-loop formation was catalysed by Rad51 and Rad54 (Fig. 2Bb, d). As expected, the inclusion of Srs2 decreased the level of D-loop formation (Fig. 2Bb, d). RPA enhanced D-loop formation in the absence of Srs2 (Fig. 2Bc, d), but the inhibitory effect of Srs2 became much more pronounced when RPA was present. We provide an explanation below for this observation.

We considered the possibility that suppression of recombination by Srs2 might result from the dissociation of DNA joints by its helicase activity. To address this, D-loop was formed with Rad51/Rad54 and then Srs2 was added. Srs2 was incapable of dissociating the preformed D-loop, regardless of the presence or absence of RPA (Fig. 3A), suggesting that suppression of the recombination reaction does not stem from the unwinding of DNA by Srs2.

Several approaches were used to test the idea that Srs2 inhibits Rad51 recombinase function by disrupting the presynaptic filament. In doing so, we reasoned that disruption of the presynaptic filament would yield free Rad51 molecules that could be trapped on duplex DNA (dsDNA). The binding of Rad51 to topologically relaxed dsDNA induces lengthening of the DNA[17,18] that can be monitored as a change in the DNA linking number on treatment with topoisomerase I (Fig. 3Ba). The product of this reaction is an underwound species referred to as form U (Fig. 3Bb, lane 4). RPA and Srs2 do not catalyse the formation of form U (Fig. 3Bb, lane 8), and these proteins have no effect on the formation of form U by Rad51 (Fig. 3Bb, compare lanes 6 and 4). The presynaptic filament consisting of Rad51–ssDNA does not make form U (Fig. 3Bc, lane 3). The addition of Srs2 to the Rad51–ssDNA presynaptic filament causes the generation of form U (Fig. 3Bc, lanes 4–6), indicating the transfer of Rad51 from the presynaptic filament to the dsDNA. The addition of RPA further stimulates the Srs2-mediated release of Rad51 from the presynaptic filament and the formation of form U (Fig. 3Bc, lanes 8–10). RPA has high affinity for ssDNA and it can compete with Rad51 for binding to ssDNA[10,19,20]. The enhanced production of form U was therefore probably due to the sequestering of ssDNA by RPA after Srs2 had released Rad51, thereby preventing the renucleation of Rad51 on the ssDNA. This premise was verified by electron microscopy and explains the

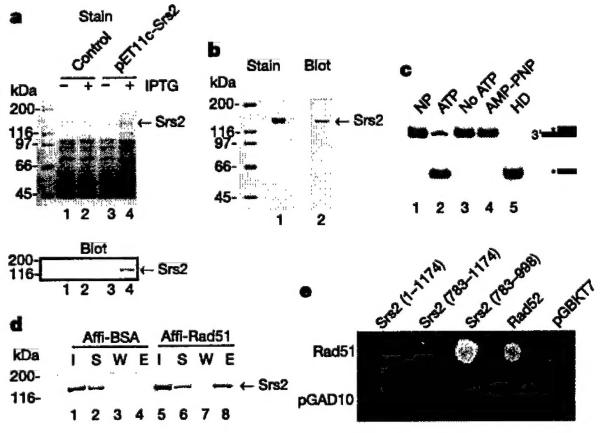

Figure 1 Purification and characterization of Srs2. **a**, Extracts from *E. coli* cells harbouring pET11c::Srs2 and the control vector pET11c grown with or without isopropyl β-D-thiogalactoside (IPTG) were analysed by SDS–PAGE and immunoblotting. **b**, Purified Srs2 was analysed by SDS–PAGE (2 μg) and immunoblotting (20 ng). **c**, DNA unwinding by Srs2 occurs with ATP but not without it or with AMP-PNP. The substrate was also incubated alone (NP) or boiled (HD) for 1 min. **d**, Srs2 was mixed with Affi-Rad51 and Affi-BSA beads. The input (I), supernatant (S), wash (W) and SDS eluate (E) were immunoblotted. **e**, Full-length and truncated versions of Srs2 were tested for two-hybrid interaction with Rad51. Empty vectors and Rad52 were included as controls.

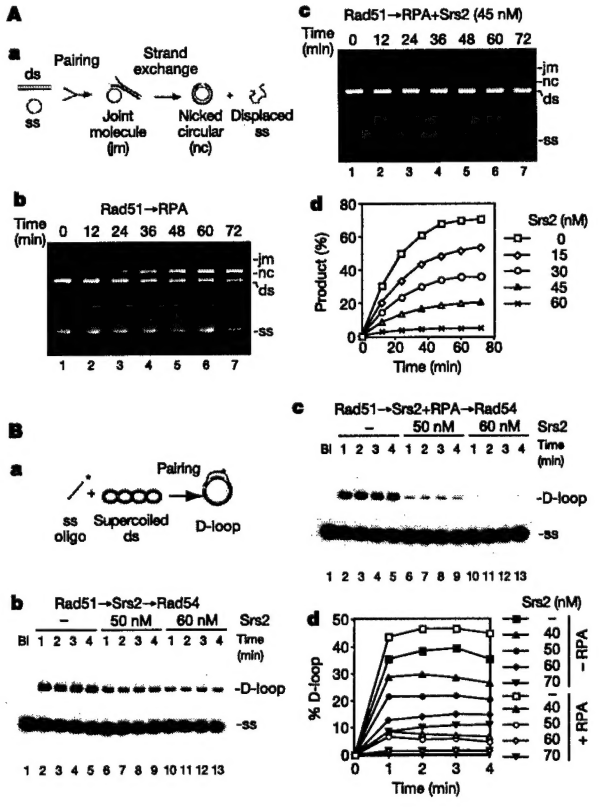

Figure 2 Srs2 inhibits Rad51-mediated DNA pairing and strand exchange. **A**, **a**, The DNA strand exchange scheme. In **b**, the DNA substrates were incubated with Rad51 and RPA. In **c**, Srs2 was also included. The results from **b** and **c** and from reactions with other Srs2 amounts are plotted in **d**. **B**, **a**, The D-loop reaction scheme. In **b**, Rad51, Srs2 and Rad54 were incubated with the DNA substrates. In **c**, RPA was also included. The results from **b** and **c** and from reactions with other Srs2 amounts are plotted in **d**. Filled symbols, reactions without RPA; open symbols, reactions with RPA.

RPA-mediated enhancement of the inhibitory effect of Srs2 in the D-loop reaction (Fig. 2B).

The Srs2-mediated disruption of the Rad51 presynaptic filament was examined by a second approach. Here, Rad51 that had been dissociated from ssDNA by Srs2 was trapped on a DNA duplex bound to magnetic beads through a biotin–streptavidin linkage (Fig. 3Ca). Rad51 was eluted from the bead-bound DNA duplex by treatment with SDS and then analysed in a denaturing polyacrylamide gel. Consistent with results from the topoisomerase I-linked assay (Fig. 3B) was the observation that there was an Srs2-concentration-dependent transfer of Rad51 from the presynaptic filament to the bead-bound DNA duplex (Fig. 3Cb).

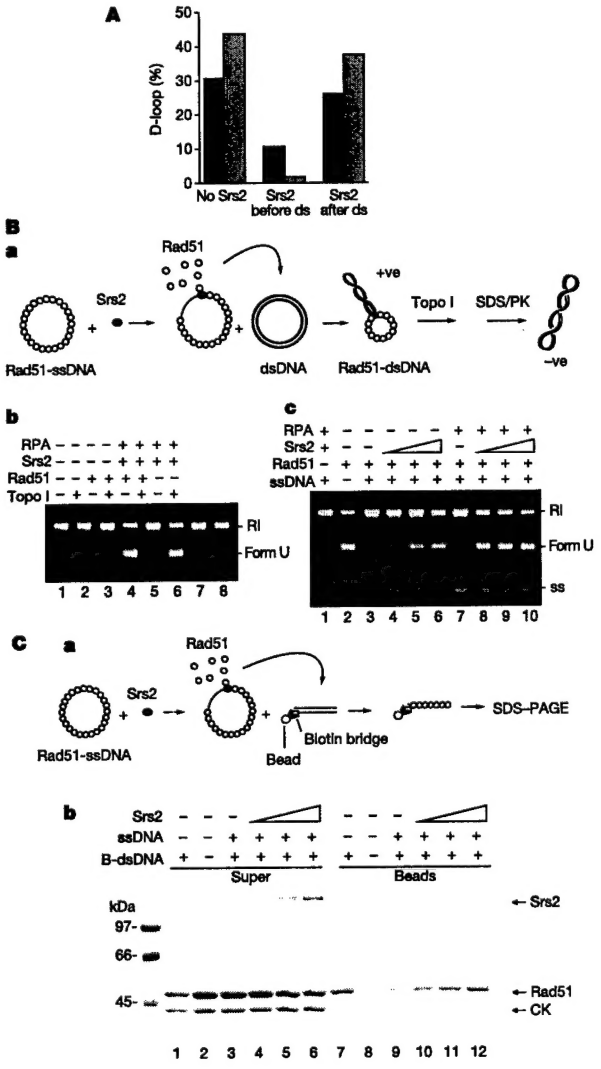

Figure 3 Srs2 disrupts the Rad51 presynaptic filament. **A**, D-loop reactions without and with Srs2 added before or after the duplex substrate were performed. The reactions were repeated with RPA present. Black bars, reactions without RPA; grey bars, reactions with RPA. **B**, **a**, The reaction scheme. PK, proteinase K. **b**, Only Rad51 makes form U. In **c**, Rad51 presynaptic filaments, assembled with or without RPA, were treated with Srs2 and topoisomerase. Lane 2 contained form U marker. RI, relaxed duplex; ss, single-stranded DNA. **C**, **a**, The reaction scheme. In **b**, Rad51 presynaptic filaments were incubated with Srs2 and then with beads containing dsDNA. Rad51 was also incubated with beads containing dsDNA (lanes 1 and 7) and beads without DNA (lanes 2 and 8). The supernatant and bead fractions were analysed. CK, creatine kinase.

Last, we used electron microscopy to characterize the action of Srs2 on the Rad51 presynaptic filament. After incubation of Rad51 with circular ssDNA, abundant presynaptic filaments[17,18] were seen (Fig. 4a). Under the same conditions, RPA formed complexes with ssDNA that appeared as compact structures with distinctive protein bulges (Fig. 4b). Although RPA alone was unable to disrupt the Rad51 presynaptic filaments (Fig. 4c), the addition of Srs2 with RPA to the presynaptic filaments caused a complete loss of the filaments, and the concomitant formation of RPA–ssDNA complexes (Fig. 4d). Previous biochemical experiments had shown transfer of Rad51 from the presynaptic filament to dsDNA promoted by Srs2 (Fig. 3B and C). This Srs2-mediated transfer of Rad51 to dsDNA could be observed directly by electron microscopy (Fig. 4e). The data from the electron microscopic analyses agree with results from the biochemical experiments (Figs 2 and 3), because they show that Srs2 disrupts the Rad51 presynaptic filament.

Even though homologous recombination is important for repairing DNA strand breaks induced by ionizing radiation and endogenous agents, and for restarting delinquent DNA replication forks, it can also generate deleterious genomic rearrangements and create DNA structures that cannot be properly resolved[1]. Cells have therefore evolved mechanisms to avoid untimely recombination[1,5]. Our studies provide evidence that Srs2 does this by disrupting the Rad51 presynaptic filament. The same conclusion has been reached independently[21]. Furthermore, even though RPA can function as a cofactor in the assembly of the Rad51 presynaptic filament[10,20], it might also promote the anti-recombination function of Srs2 by preventing reassembly of the presynaptic filament (Figs 3 and 4). That Srs2 uses the free energy from ATP hydrolysis to dislodge Rad51 from the presynaptic filament has been verified with mutant variants of Srs2 (srs2 K41A and srs2 K41R) defective for ATP hydrolysis. The physical interaction noted between Rad51 and Srs2 further suggests a mechanism for targeting the latter to the presynaptic filament. Taken together, the results presented here indicate that the motor activity of Srs2 driven by ATP hydrolysis is capable of dissociating not only DNA structures[6] but also DNA–protein complexes.

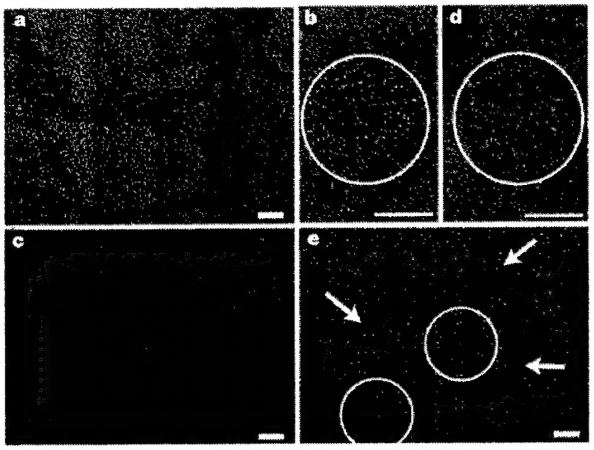

Figure 4 EM analysis of Rad51 filament disruption by Srs2. **a**, **b**, Rad51 (**a**) and RPA (**b**) were each incubated with ssDNA; examples of the nucleoprotein complexes that formed are shown. **c**, RPA was not able to disrupt preformed Rad51 filaments; an example of the Rad51 filaments present is shown. **d**, Incubation of preformed Rad51 filaments with Srs2 and RPA caused the loss of filaments and concomitant formation of RPA–ssDNA complexes, an example of which is shown. **e**, When preformed Rad51–ssDNA filaments were incubated with Srs2, RPA and linear duplex, RPA–ssDNA complexes were formed (circled) and transfer of Rad51 onto the linear duplex was visualized (arrows). Scale bars, 100 nm.

The inhibitory effect of Srs2 on Rad51-mediated DNA strand exchange can be partly overcome by the inclusion of Rad52 protein, a recombination mediator that promotes Rad51 presynaptic filament assembly[11,12]. However, the Rad55–Rad57 complex, which also has recombination mediator activity[11,12], is much less effective in alleviating the inhibitory effect of Srs2. Furthermore, Rad52 and the Rad55–Rad57 complex do not seem to act synergistically. Interestingly, we have found that Srs2 can also dismantle presynaptic filaments of RecA and human Rad51 proteins. It therefore seems that the presynaptic filaments formed by the RecA/Rad51 class of general recombinases share a conserved feature that is recognized by Srs2, making them prone to disruption by the motor activity of Srs2.

The sensitivity of *srs2* mutants to DNA-damaging agents[6,22] is alleviated by deleting *RAD51* (ref. 23), and the inability to remove Rad51 from DNA in the *srs2* mutants most probably accounts for the hyper-recombination phenotype of these mutants[1]. Similarly, the cell cycle checkpoint recovery and adaptation defect in *srs2* mutants might be related to an inability to evict Rad51 from damaged DNA[2]. Cells mutated for *SRS2* grow slowly, exhibit an extended late S and/or G2 phase, and are defective in meiosis[25]. These defects could result from the generation of unresolvable recombination intermediates that trigger checkpoint activation and thereby compromise cell cycle progression. In addition to functioning as an anti-recombinase, Srs2 could conceivably prevent D-loop reversal by removing Rad51 bound to the displaced ssDNA strand. The various activities of Srs2 might be subject to modulation by phosphorylation[24].

Other DNA helicase enzymes are known to suppress recombination in eukaryotic cells, including the *S. cerevisiae* Sgs1 protein and the human BLM and WRN proteins, mutated in Bloom's syndrome and Werner's syndrome, respectively. Untimely and aberrant recombination events in Bloom's syndrome and Werner's syndrome cells could contribute to the genomic instability in these cells[26]. It has been suggested that BLM and WRN proteins control the level of recombination by dissociating recombination intermediates[5,27]. It will be of interest to test whether Sgs1, BLM and WRN proteins affect the integrity of the hRad51 presynaptic filament, as overexpression of Sgs1 protein can partly suppress some of the defects of *srs2* mutants[28]. □

Methods

Antibodies and Srs2 purification

Polyclonal antiserum was raised against residues 177–646 of Srs2 fused to glutathione *S* transferase. Antibodies were purified from the rabbit anti-serum by affinity chromatography on a column containing the antigen crosslinked to cyanogen bromide-activated sepharose 4B matrix (Amersham Biosciences). *SRS2* gene was placed under the T7 promoter in the vector pET11c to yield plasmid pET11c::Srs2, which was introduced into *E. coli* BL21 (DE3). Srs2 expression was induced by isopropyl β-D-thiogalactoside, and extract from 70 l of culture was subjected to precipitation with ammonium sulphate and chromatographic fractionation in columns of Q Sepharose, SP Sepharose, hydroxyapatite and Mono Q. The final Srs2 pool (300 μg at 2 mg ml^{-1}) was nearly homogeneous and stored in small portions at −80 °C.

DNA substrates

The ϕX circular (+) strand was from New England Biolabs. The ϕX replicative form I DNA (Gibco-BRL) was linearized by digestion with *Apa*LI. The pBluescript SK(−) replicative form I DNA was prepared as described[29]. Oligonucleotide D1 has the sequence: 5′-AAATCAATCTAAAGTATATATGAGTAAACTTGGTCTGACAGTTACCAATGCTTAA TCAGTGAGGCACCTATCTCAGCGATCTGTCTATTT-3′, being complementary to positions 1932–2022 of the pBluescript replicative form I DNA. Oligonucleotide H2 has the sequence: 5′-GTAACTGTCAGACCAAGTTTACTCATATATACTTTAGATTGATTT-3′, being complementary to the first 45 residues of oligonucleotide D1. The two oligonucleotides were 5′ end-labelled with [γ-^{32}P]ATP and purified as described[29]. The DNA helicase substrate was obtained by hybridizing D1 to radiolabelled H2, as described[14].

Biotinylated dsDNA coupled to magnetic beads

The ends of a 769-base pair fragment derived from digesting ϕX174 replicative form I DNA with *Apa*LI and *Xho*I were filled in with the Klenow polymerase, using a mixture of dGTP, dTTP, Bio-7-dATP and Bio-11-dCTP (Enzo Diagnostics). The biotinylated DNA fragment was immobilized on streptavidin-coated magnetic beads (Roche Molecular Biochemicals) to give biotinylated DNA at 40 ng μl^{-1} packed volume.

Binding of Srs2 to beads containing Rad51

Rad51 and BSA were coupled to Affi-Gel 15 beads (Bio-Rad) at 5 and 12 mg ml^{-1}, respectively[14]. To examine Srs2 binding, 3 μg Srs2 was mixed with 7 μl Affi-Rad 51 or Affi-BSA beads in 30 μl PBS (10 mM KH_2PO_4 pH 7.2, 150 mM KCl, 1 mM dithiothreitol (DTT) and 0.01% Igepal) at 4 °C for 30 min. The beads were collected by centrifugation; after the supernatant had been decanted off, the beads were washed twice with 100 μl buffer, then treated for 5 min with 30 μl 2% SDS at 37 °C to elute bound Srs2. The various fractions—10 μl each—were analysed by immunoblotting to determine their Srs2 content.

Yeast two-hybrid assay

RAD51 was cloned into pGAD10, which contains the *GAL4* transcription activation domain, and the resulting plasmid was introduced into the haploid yeast strain PJ69-4a (ref. 30). *SRS2* (residues 1–1174), two C-terminal fragments of *SRS2* (residues 783–1174 and residues 738–998), and *RAD52* were cloned into pGBKT7, which contains the *GAL4* DNA-binding domain; the resulting plasmids were introduced into the haploid yeast strain PJ69-4α (ref. 30). Diploid strains obtained by mating plasmid-bearing PJ69-4a and PJ69-4α haploids were grown on synthetic medium lacking tryptophan and leucine. To select for two-hybrid interactions, which would result in the activation of the *ADE2* and *HIS3* reporter genes, diploid cells were replica-plated on synthetic medium lacking tryptophan, leucine and adenine, and also on synthetic medium lacking tryptophan, leucine and histidine[30]. Both platings gave identical results. Only the plating on the tryptophan, leucine and adenine dropout medium is shown in Fig. 1e.

DNA helicase assay

Srs2 (35 nM) was incubated at 30 °C for 10 min with the DNA substrate (300 nM nucleotides) in 10 μl buffer H (25 mM Tris-HCl pH 7.5, 2.5 mM $MgCl_2$, 1 mM DTT, 100 μg ml^{-1} BSA) containing 2 mM ATP or β-γ-imidoadenosine 5′-phosphate (AMP-PNP) and then analysed[14].

Homologous DNA pairing and strand exchange reaction

Buffer R (35 mM Tris-HCl pH 7.4, 2.0 mM ATP, 2.5 mM $MgCl_2$, 50 mM KCl, 1 mM DTT, containing an ATP-regenerating system consisting of 20 mM creatine phosphate and 20 μg ml^{-1} creatine kinase) was used for the reactions, and all the incubation steps were performed at 37 °C. Rad51 (10 μM) was mixed with ϕX circular (+) strand (30 μM nucleotides) in 30 μl for 5 min, followed by the incorporation of RPA (2 μM) in 1.5 μl and a 3 min incubation. The reaction was completed by adding 3 μl 50 mM spermidine hydrochloride and linear ϕX dsDNA (30 μM nucleotides) in 3 μl. Portions (4.5 μl) of the reaction mixtures were taken at the indicated times, deproteinized and resolved in agarose gels followed by ethidium bromide staining of the DNA species, as described previously[18]. Srs2 was added to the reactions in 0.9 μl at the time of RPA incorporation.

D-loop reaction

Buffer R was used for the D-loop reactions. The radiolabelled oligonucleotide D1 (3 μM nucleotides) was incubated with Rad51 (1 μM) in 22 μl for 5 min at 37 °C, followed by the incorporation of Rad54 (150 nM) in 1 μl and a 2-min incubation at 23 °C. The reaction was initiated by adding pBluescript replicative form I DNA (50 μM base pairs) in 2 μl. The reaction mixtures were incubated at 30 °C, and 5-μl aliquots were withdrawn at the indicated times and processed for electrophoresis as described above. The gels were dried and subjected to phosphorimaging analysis. The percentage of D-loop refers to the quantity of the replicative form substrate that had been converted into D-loop. When present, RPA (200 nM) and Srs2 (40–70 nM) were added to the preassembled Rad51 filament, followed by a 4-min incubation at 37 °C before Rad54 was incorporated. In Fig. 3A, Srs2 (45 nM) was added to the D-loop reactions before Rad54 as above, or 1 min after the incorporation of the duplex substrate. The reactions were terminated after 4 min of incubation.

Topoisomerase-I-linked DNA unwinding assay

Buffer R was used for the reactions and all the incubation steps were performed at 37 °C. Rad51 (4 μM) was incubated for 4 min with pBluescript (−) strand (20 μM nucleotides) in 7.8 μl. Srs2 (40, 60 or 80 nM) and RPA (1 μM) were added in 1 μl, followed by a 4-min incubation. Topologically relaxed ϕX174 DNA (12.5 μM nucleotides) in 0.8 μl and 2.5 U calf thymus topoisomerase I (Invitrogen) in 0.4 μl storage buffer were then incorporated to complete the reaction. The reaction mixtures were incubated for 8 min and then stopped by adding SDS to 0.5%. In reactions that did not contain the (−) strand, Rad51, with or without RPA (1 μM) and Srs2 (80 nM), was incubated for 8 min with topologically relaxed ϕX174 DNA and topoisomerase I in a final volume of 10 μl. The reaction mixtures were treated for 10 min with proteinase K (0.5 mg ml^{-1}) before being analysed in 0.9% agarose gels.

Transfer of Rad51 to bead-bound biotinylated dsDNA

M13mp18 circular (+) strand (7.2 μM nucleotides) was incubated for 5 min with Rad51 (2.4 μM) at 37 °C, followed by the addition of Srs2 (30, 60 or 90 nM) in a final volume of 20 μl buffer R containing 50 mM KCl and 0.01% Igepal. After 3 min at 37 °C, 4 μl magnetic beads containing dsDNA were added to the reaction, followed by constant mixing for 5 min at 23 °C. The beads were captured with the Magnetic Particle Separator (Boehringer Mannheim), washed twice with 50 μl buffer, and the bound Rad51 was eluted with 20 μl 1% SDS. The supernatant, which contained unbound Rad51, and the SDS eluate (10 μl each) were analysed by SDS–polyacrylamide-gel electrophoresis (SDS–PAGE).

Electron microscopy

The reactions were performed in buffer R at 37 °C and had a final volume of 12.5 μl. To assemble the Rad51 presynaptic filament, M13mp18 (+) strand (7.2 μM nucleotides) and 1.3 μg Rad51 (2.4 μM) were incubated for 5 min. To test the effects of Srs2 and RPA, these proteins were added to the reaction mixtures containing the preassembled Rad51 presynaptic filament to final concentrations of 60 nM (Srs2) and 350 nM (RPA), followed by a 3-min incubation. In some cases, linear dsDNA (a 5.2-kilobase fragment derived from the pET24 vector) was also added with Srs2 and RPA to 7.2 μM base pairs, followed by a 5-min incubation. For electron microscopy, 3 μl of each reaction mixture was applied to copper grids coated with thin carbon film after glow-discharging the coated grids for 2 min. The grids were washed twice with buffer R and stained for 30 s with 0.75% uranyl formate. After air-drying, the grids were examined with a Philips Tecnai12 electron microscope under low-dose conditions. Images were recorded either with a charge-coupled device camera (Gatan) or on Kodak SO-163 films at × 30,000 magnification and then scanned on a SCAI scanner (Zeiss). The experiments shown in Fig. 4 were each independently repeated three or more times and at least 100 nucleoprotein complexes were examined in each experiment.

Received 3 February; accepted 20 March 2003; doi:10.1038/nature01577.

1. Klein, H. L. A radical solution to death. *Nature Genet.* **25,** 132–134 (2000).
2. Vaze, M. B. *et al.* Recovery from checkpoint-mediated arrest after repair of a double-strand break requires Srs2 helicase. *Mol. Cell* **10,** 373–385 (2002).
3. Lee, S. K., Johnson, R. E., Yu, S. L., Prakash, L. & Prakash, S. Requirement of yeast SGS1 and SRS2 genes for replication and transcription. *Science* **286,** 2339–2342 (1999).
4. Gangloff, S., Soustelle, C. & Fabre, F. Homologous recombination is responsible for cell death in the absence of the Sgs1 and Srs2 helicases. *Nature Genet.* **25,** 192–194 (2000).
5. Oakley, T. J. & Hickson, I. D. Defending genome integrity during S-phase: putative roles for RecQ helicases and topoisomerase III. *DNA Repair* **1,** 175–207 (2002).
6. Rong, L. & Klein, H. L. Purification and characterization of the SRS2 DNA helicase of the yeast *Saccharomyces cerevisiae*. *J. Biol. Chem.* **268,** 1252–1259 (1993).
7. Milne, G. T., Ho, T. & Weaver, D. T. Modulation of *Saccharomyces cerevisiae* DNA double-strand break repair by SRS2 and RAD51. *Genetics* **139,** 1189–1199 (1995).
8. Chanet, R., Heude, M., Adjiri, A., Maloisel, L. & Fabre, F. Semidominant mutations in the yeast Rad51 protein and their relationships with the Srs2 helicase. *Mol. Cell. Biol.* **16,** 4782–4789 (1996).
9. Schild, D. Suppression of a new allele of the yeast RAD52 gene by overexpression of RAD51, mutations in srs2 and ccr4, or mating-type heterozygosity. *Genetics* **140,** 115–127 (1995).
10. Sung, P. Catalysis of ATP-dependent homologous DNA pairing and strand exchange by yeast RAD51 protein. *Science* **265,** 1241–1243 (1994).
11. Sung, P., Trujillo, K. M. & Van Komen, S. Recombination factors of *Saccharomyces cerevisiae*. *Mutat. Res.* **451,** 257–275 (2000).
12. Cox, M. M. Recombinational DNA repair of damaged replication forks in *Escherichia coli*: questions. *Annu. Rev. Genet.* **35,** 53–82 (2001).
13. Bianco, P. R., Tracy, R. B. & Kowalczykowski, S. C. DNA strand exchange proteins: a biochemical and physical comparison. *Front. Biosci.* **3,** 570–603 (1998).
14. Petukhova, G., Stratton, S. & Sung, P. Catalysis of homologous DNA pairing by yeast Rad51 and Rad54 proteins. *Nature* **393,** 91–94 (1998).
15. Mazin, A. V., Zaitseva, E., Sung, P. & Kowalczykowski, S. C. Tailed duplex DNA is the preferred substrate for Rad51 protein-mediated homologous pairing. *EMBO J.* **19,** 1148–1156 (2000).
16. Van Komen, S., Petukhova, G., Sigurdsson, S. & Sung, P. Functional cross-talk among Rad51, Rad54, and replication protein A in heteroduplex DNA joint formation. *J. Biol. Chem.* **277,** 43578–43587 (2002).
17. Ogawa, T., Yu, X., Shinohara, A. & Egelman, E. H. Similarity of the yeast RAD51 filament to the bacterial RecA filament. *Science* **259,** 1896–1899 (1993).
18. Sung, P. & Robberson, D. L. DNA strand exchange mediated by a RAD51-ssDNA nucleoprotein filament with polarity opposite to that of RecA. *Cell* **82,** 453–461 (1995).
19. Sung, P. Yeast Rad55 and Rad57 proteins form a heterodimer that functions with replication protein A to promote DNA strand exchange by Rad51 recombinase. *Genes Dev.* **11,** 1111–1121 (1997).
20. Sugiyama, T., Zaitseva, E. M. & Kowalczykowski, S. C. A single-stranded DNA-binding protein is needed for efficient presynaptic complex formation by the *Saccharomyces cerevisiae* Rad51 protein. *J. Biol. Chem.* **272,** 7940–7945 (1997).
21. Veaute, X. *et al.* The Srs2 helicase prevents recombination by disrupting Rad51 nucleoprotein filaments. *Nature* **423,** 309–312 (2003).
22. Aboussekhra, A. *et al.* RADH, a gene of *Saccharomyces cerevisiae* encoding a putative DNA helicase involved in DNA repair. Characteristics of radH mutants and sequence of the gene. *Nucleic Acids Res.* **17,** 7211–7219 (1989).
23. Aboussekhra, A., Chanet, R., Adjiri, A. & Fabre, F. Semidominant suppressors of Srs2 helicase mutations of *Saccharomyces cerevisiae* map in the RAD51 gene, whose sequence predicts a protein with similarities to procaryotic RecA proteins. *Mol. Cell. Biol.* **12,** 3224–3234 (1992).
24. Liberi, G. *et al.* Srs2 DNA helicase is involved in checkpoint response and its regulation requires a functional Mec1-dependent pathway and Cdk1 activity. *EMBO J.* **19,** 5027–5038 (2000).
25. Palladino, F. & Klein, H. L. Analysis of mitotic and meiotic defects in *Saccharomyces cerevisiae* SRS2 DNA helicase mutants. *Genetics* **132,** 23–37 (1992).
26. Adams, M. D., McVey, M. & Sekelsky, J. J. *Drosophila* BLM in double-strand break repair by synthesis-dependent strand annealing. *Science* **299,** 265–267 (2003).
27. Wu, L., Davies, S. L., Levitt, N. C. & Hickson, I. D. Potential role for the BLM helicase in recombinational repair via a conserved interaction with RAD51. *J. Biol. Chem.* **276,** 19375–19381 (2001).
28. Mankouri, H. W., Craig, T. J. & Morgan, A. SGS1 is a multicopy suppressor of srs2: functional overlap between DNA helicases. *Nucleic Acids Res.* **30,** 1103–1113 (2002).
29. Petukhova, G., Stratton, S. A. & Sung, P. Single strand DNA binding and annealing activities in the yeast recombination factor Rad59. *J. Biol. Chem.* **274,** 33839–33842 (1999).
30. Krejci, L., Damborsky, J., Thomsen, B., Duno, M. & Bendixen, C. Molecular dissection of interactions between Rad51 and members of the recombination-repair group. *Mol. Cell. Biol.* **21,** 966–976 (2001).

Acknowledgements We thank M. Sehorn and K. Trujillo for reading the manuscript. This work was supported by research grants from the NIH (H.K., T.E. and P.S.). S.V.K. was supported in part by a predoctoral fellowship from the US Department of Defense, and Y.L. was supported by a NIH postdoctoral fellowship. The molecular electron microscopy facility at Harvard Medical School was established by a donation from the Giovanni Armeise Harvard Center for Structural Biology, and is maintained through a NIH grant.

Competing interests statement The authors declare that they have no competing financial interests.

Correspondence and requests for materials should be addressed to L.K. (krejci@uthscsa.edu) or P.S. (sung@uthscsa.edu).

The Srs2 helicase prevents recombination by disrupting Rad51 nucleoprotein filaments

Xavier Veaute*, Josette Jeusset†, Christine Soustelle*‡, Stephen C. Kowalczykowski§, Eric Le Cam† & Francis Fabre*

** CEA, DSV, Département de Radiobiologie et Radiopathologie, UMR217 CNRS/CEA, BP6, 92265 Fontenay aux Roses Cedex, France*
† Interactions Moléculaires et Cancer, UMR 81126 CNRS/IGR/UPS, Institut Gustave Roussy, Rue Camille Desmoulins, 94805 Villejuif Cedex, France
§ Sections of Microbiology and of Molecular and Cellular Biology, Center for Genetics and Development, University of California, Davis, California 95616-8665, USA

Homologous recombination is a ubiquitous process with key functions in meiotic and vegetative cells for the repair of DNA breaks. It is initiated by the formation of single-stranded DNA on which recombination proteins bind to form a nucleoprotein filament that is active in searching for homology, in the formation of joint molecules and in the exchange of DNA strands[1]. This process contributes to genome stability but it is also potentially dangerous to cells if intermediates are formed that cannot be processed normally and thus are toxic or generate genomic rearrangements. Cells must therefore have developed strategies to survey recombination and to prevent the occurrence of such deleterious events. In *Saccharomyces cerevisiae*, genetic data have shown that the Srs2 helicase negatively modulates recombination[2,3], and later experiments suggested that it reverses intermediate recombination structures[4–7]. Here we show that DNA strand exchange mediated *in vitro* by Rad51 is inhibited by Srs2, and that Srs2 disrupts Rad51 filaments formed on single-stranded DNA. These data provide an explanation for the anti-recombinogenic role of Srs2 *in vivo* and highlight a previously unknown mechanism for recombination control.

Several phenotypes (discussed below) conferred by the *srs2* deletion are suppressed by mutations that prevent formation of the Rad51 nucleofilaments[8,9]. Two hypotheses could explain this suppression: either Srs2 functions in replication and repair to prevent the formation of toxic recombination structures, or Srs2 disrupts dead-end recombination intermediates, possibly formed after the arrest of the replication fork, to allow repair through alternative pathways. This second proposition led us to ask whether purified Srs2 acts on preformed recombination structures.

Srs2 was expressed from a baculovirus vector in which *SRS2* was cloned in frame with a histidine tag at its amino terminus. We showed that the protein fusion expressed in yeast fully complements the sensitivity of *srs2*-deleted cells to radiation (data not shown).

‡ Present address: UMR2167 CNRS Centre de Génétique Moléculaire, Bâtiment 26, avenue de la Terrasse, 91198 Gif-sur-Yvette Cedex, France.